NOTICE

AVIS

Canada

VIBRONIC SPECTRA AND PHOTOCHEMICAL

TRANSFORMATION OF TERTIARY-BUTYL PHTHALOCYANINE

IN SHPOL'SKII MATRICES

b y

YONGYAN HU

B.Sc, Hangzhou University, 1982

THESIS SUBMITTED IN PARTIAL FULFILLMENT OF

THE REQUIREMENTS FOR THE DEGREE OF

MASTER OF SCIENCE

in the Department

of

Physics

© Yongyan Hu   1991

SIMON FRASER UNIVERSITY

July 1991

Your file   Votre référence

Our file   Notre référence

ISBN 0-315-78191-2

Canada

APPROVAL

NAME: YONGYAN   HU

DEGREE: MASTER OF SCIENCE

TITLE OF THESIS: VIBRONIC SPECTRA AND PHOTOCHEMICAL

TRANSFORMATION OF TERTIARY BUTYL PHTHALOCYANINES IN

SHPOL'SKII MATRICES

EXAMINING COMMITTEE:

Chairman: Dr. J. F. Cochran

Dr. K. E. Rieckhoff ,

Senior Supervisor

Dr. E. M. Voigt

Senior Supervisor

Dr. R. F. Frindt

Dr. E. D. Crozier

Examiner

Professor, Physics Department, SFU

Date Approved   Aug. 15, 1991

PARTIAL COPYRIGHT LICENSE

I hereby grant to Simon Fraser University the right to lend my thesis, project or extended essay (the title of which is shown below) to users of the Simon Fraser University Library, and to make partial or single copies only for such users or in response to a request from the library of any other university, or other educational institution, on its own behalf or for one of its users. I further agree that permission for multiple copying of this work for scholarly purposes may be granted by me or the Dean of Graduate Studies. It is understood that copying or publication of this work for financial gain shall not be allowed without my written permission.

Title of Thesis/Project/Extended Essay

Vibronic Spectra and photochemical Transformation

of Tertiary — Butyl phthalocyanine in Shpol'skii Matrices

Author: _____
(Signature)

Yongyan Hu
(Name)

Aug. 22, 1991
(Date)

ABSTRACT

Electronic spectral properties of tertiary-butyl phthalocyanine (TBH$_2$Pc) in a 4.2K n-hexadecane (C$_{16}$) matrix were investigated. A clear doublet in the 0-0 fluorescence region was recorded, representing a ~20 cm^{-1} Stokes shift due to a different proton geometry (molecular tautomerism) in the centre of the molecule. Well resolved fluorescence and fluorescence excitation spectra were also recorded and assigned. Photochemical interconversion between the tautomers was studied by the intensity variation of fluorescence bands as a function of time. The transformation saturated in several tens to two hundreds of milliseconds under our pumping conditions. Similar investigations of the complex in solid n-nonane (C$_9$), n-tetradecane (C$_{12}$) and n-octadecane (C$_{18}$) were also carried out on a less detailed scale. The results were compared with those for free base phthalocyanine (H$_2$Pc) in a mixed solvent matrix of α-chloronaphthalene (α-CLN) and n-octane (C$_8$).

To my parents and my wife

for their understanding and long time support

ACKNOWLEDGEMENTS

Table of Contents

List of Tables

List of Figures

Chapter 1.   Introduction

In spectroscopic studies of molecular dynamics, some molecular complexes such as the porphyrins and the phthalocyanines have received special attention. The porphyrins are of importance in biology, medicine and bio-chemistry and have been studied extensively[1]. Phthalocyanines (Pc's) are similar in structure to the porphyrins. They are valuable in some commercial applications, e.g. for laser passive Q switching[2], as dyes[3], lubricants[4], photoconductors[5] and for their potential as "organic metals". Besides their commercial application potential, the Pc's are also of interest for more fundamental reasons. In recent years, there has been increasing interest in the study of radiationless processes and intramolecular energy transfer in large molecules with many vibrational degrees of freedom and large densities of vibrational states[6-8]. The high density of states produces dynamical processes which do not occur in small molecules. The porphyrins, phthalocyanines and their related compounds are an interesting series of compounds in which to study large molecule dynamics. The molecular structures for free base porphyrin and free base phthalocyanine molecules are shown in Fig. 1 (a) and (b). The structural similarities are apparent. Many spectroscopic studies have been done on these molecules[9-15] and
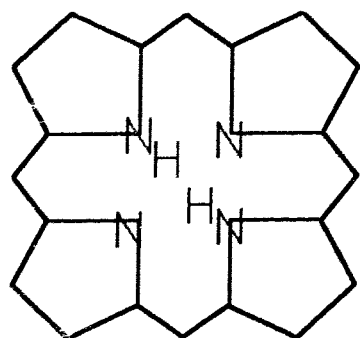
a) Free base porphyrin
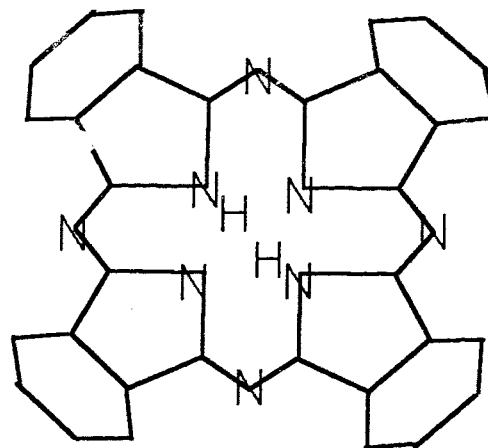
b) Free base phthalocyanine

c) n-octane (C$_8$)
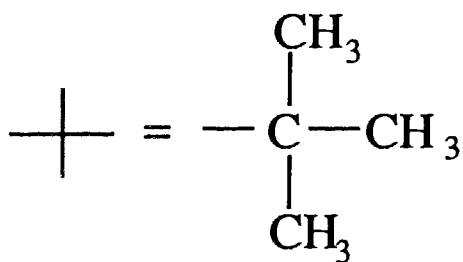
d) Tertiary-butyl group
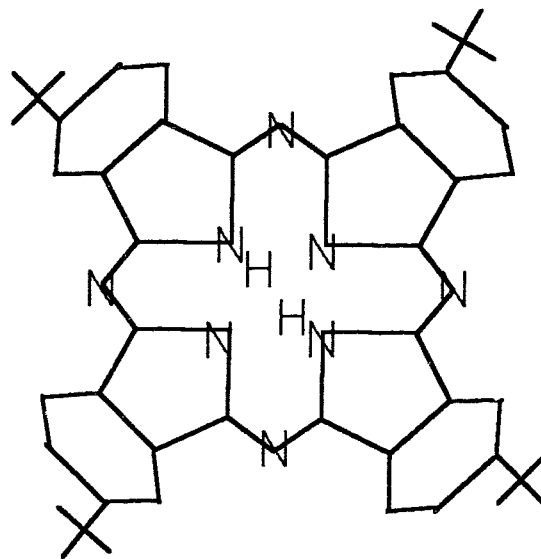
e) Free base tertiary-butyl phthalocyanine

Fig. 1 The Structrues of free base porphyrin, free base phthalocyanine, n-octane, tertiary-butyl group and free base tertiary-butyl phthalocyanine (all the hydrogens at the skeleton of molecules are not shown).

2

their dynamic behaviour has been understood progressively better.

The spectroscopy of porphyrins presents no particular difficulties since absorptions and emissions generally occur in the convenient regions of the visible spectrum, quantum-efficiencies of the fluorescence and/or phosphorescence are sufficiently high for ease of observation, and their solubility is adequate in many solvents to obtain reasonable concentrations. The phthalocyanines (Pc's) present greater difficulties for a number of reasons. Their solubilities are generally very low, particularly in weakly interacting solvents such as alkanes, and -with the exception of the fluorescence of some of them, such as the free base Pc- their quantum yields of luminescence (particularly phosphorescence) are extremely low and occur in a less favorable region for detection, *i.e.* the near infra-red, between 700nm and 1.1μ. The free base tertiary-butyl phthalocyanine (TBH$_2$Pc, see Fig.1 d and e) was synthesized specifically to overcome the low solubility in alkanes and thus to enable researchers to obtain higher concentrations for various spectroscopic studies, but in particular for studies of photochemical hole-burning[16-19]. It was widely expected that this molecule would in other respects such as electronic structure and intra-molecular relaxation processes, behave similarly to the ordinary free-base phthalocyanine (H$_2$Pc). The TBH$_2$Pc has four tertiary-butyl groups appended to the H$_2$Pc skeleton. This raises the question, to which extent its spectroscopic and in particular its dynamic properties are

3

indeed similar to those of the H_2Pc molecule and to which extent there exist significant differences. The study reported here addresses this question experimentally.

The most extensive studies of the vibronic levels of H_2Pc were in Shpol'skii matrices[20] of mixed solvents, i.e. α-chloronaphthalene and n-octane[10,15] (C_8 as in Fig.1c). In such matrices the guest molecule occupies specific well defined sites in an assembly of microcrystals. Also the interaction with the host matrix is sufficiently weak to allow strong 0-0 (the 0 refers the vibrational quantum number of the respective electronic state) lines as well as vibronic levels to be observed in fluorescence and fluorescence excitation. Because of the improved solubility of the TBH_2Pc in pure alkanes, a variety of these alkane solvents were tried and the sample preparation is reported in chapter 2. Detailed fluorescence and fluorescence excitation spectra are presented and discussed in chapter 3.

Of particular interest in the free-base Pc (as well as the porphyrin) is the possibility of phototransformation between isomers. These isomers result from the relative positions of the two central hydrogens in the surrounding ring structure, which has a basic molecular D_{2h} symmetry whether isolated or incorporated into a matrix[21,22]. Depending on the exact nature of the guest matrix, the two isomeric structures differ in absorption, fluorescence and fluorescence excitation spectra by anywhere in the order of tens of wavenumbers. Differences between the spectra of different sites are of the order of wavenumbers and with linewidths in the Shpol'skii matrices of

from 2 to 5 cm^{-1}, different sites and different isomers can be selectively excited. The phototransformation, in which excitation into the vibronic structure of one isomer can result with some probability in the two central hydrogens switching position to the other isomer, can then result in a reduction of the population of the excited species. This is the basis of photochemical hole-burning in H_2Pc and TBH_2Pc [16-19,23-28] where the depletion of one species shows as a "hole" in the absorption spectrum. The exact intramolecular mechanism of this phototransformation is not yet fully understood. But whatever
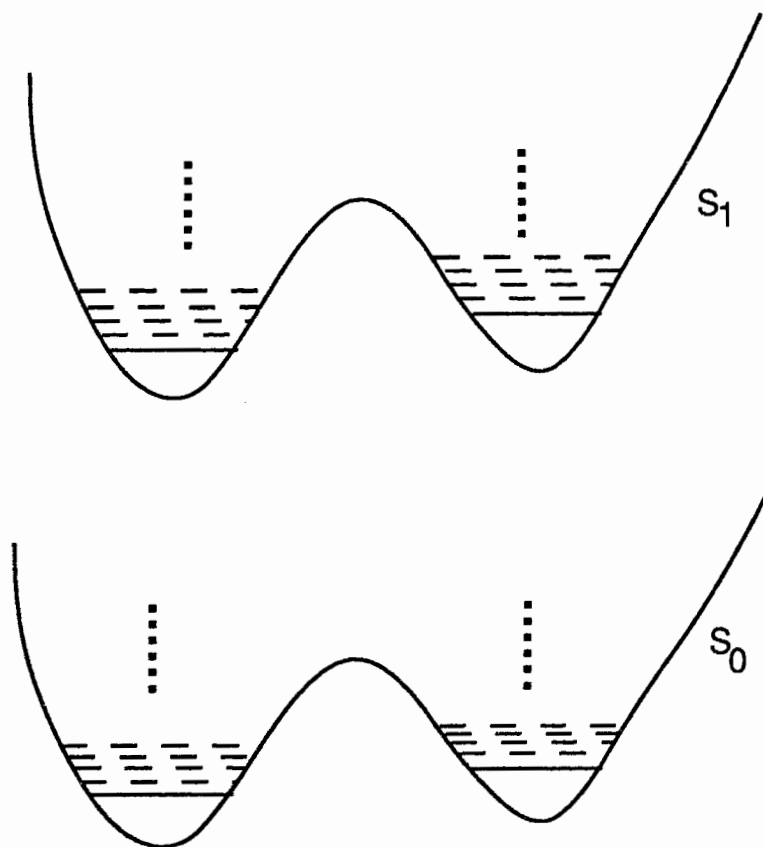
Fig. 2 Potential energy curves in the Pc molecule

the exact nature of the transformation pathway, one usually models the two isomeric states in terms of a double well potential as depicted in Figure 2. This double well potential is caused by the D_{2h} point group symmetry of the molecule in the Shpol'skii matrix referred to earlier. For the metal phthalocyanines, the double well potential is the result of a crystal field stabilized Jahn-Teller effect in the Shpol'skii matrices[29]. For the TBH2Pc molecule, one assumes that it also possesses such a double potential well and this model is used to analyze the data, although detailed knowledge of this double well potential is not available. The experiments described in this thesis on the dynamics of the phototransformation and reported in chapter 3 were performed to assist in providing useful information on this question. Such experiments were done in this laboratory by Chen et al. on H_2Pc[15] and we employed the same technique, in which we follow the fluorescence intensity as a function of time in repeated on-off cycles of excitation. As commented on in the discussion it was found that the dynamics of the phototransformation do behave quite differently in the two molecules.

In summary, the purposes of this thesis were to investigate 1), whether such a large molecule as TBH2Pc can have good Shpol'skii spectra in some alkanes; 2), through a detailed study of electronic and vibrational states to get structural information on the TBH2Pc molecule in Shpol'skii matrices from the electronic and vibronic spectra and to compare the results of TBH2Pc with those of H_2Pc to obtain information on how the

6

outside tertiary-butyl groups affect the electronic and vibronic states; 3), through the studies of the photochemical transformation to get information on energy transfer processes.

The number of normal modes capable of coupling with the observed $a_{1u}(\pi)-e_g(\pi^*)$ electronic transition is enormous, the vibronic spectra and photochemical transformations observed are complicated and hence the analysis of the data is done only qualitatively. However, it is believed that this work will provide a useful basis for further studies of either a theoretical or an experimental nature.

In chapter 2, a detailed description of the experimental setup, apparatus used and how the samples were prepared is presented. In chapter 3, we will present the results of the Shpol'skii effect of TBH$_2$Pc in different alkane solvents. Based on the double well potential and some other models the fluorescence and fluorescence excitation spectra obtained in various good Shpol'skii matrices are assigned and discussed. Comparison of the results of TBH$_2$Pc and those of H$_2$Pc will be made within each section. Finally, the results of photochemical transformation are presented and some simple models to explain the phenomenon are introduced. All the results are summarised in the chapter 4 conclusions.

Chapter 2. Experimental

The basic experimental setup is shown in Fig.3. More detailed descriptions of the component parts are presented in the following sections:

```
┌─────────────┐      ┌──────────────┐      ┌──────────────┐
│   Sample    │◄─────│ Tunable Dye  │◄─────│  Ar⁺ Laser   │
│             │      │ Laser        │      │              │
└─────────────┘      └──────────────┘      └──────────────┘
      │                     ▲
      ▼                     │
┌─────────────┐             │
│ Spectrometer│◄────────────┤
│             │             │
└─────────────┘             │
      │                     │
      ▼                     │
┌─────────────┐             │
│  Photon     │             │
│  Multiplier │             │
└─────────────┘             │
      │                     │
      ▼                     ▼
┌─────────────┐      ┌──────────────┐
│  Photon     │─────►│  Computer    │
│  Counter    │      │ Control System│
└─────────────┘      └──────────────┘
```
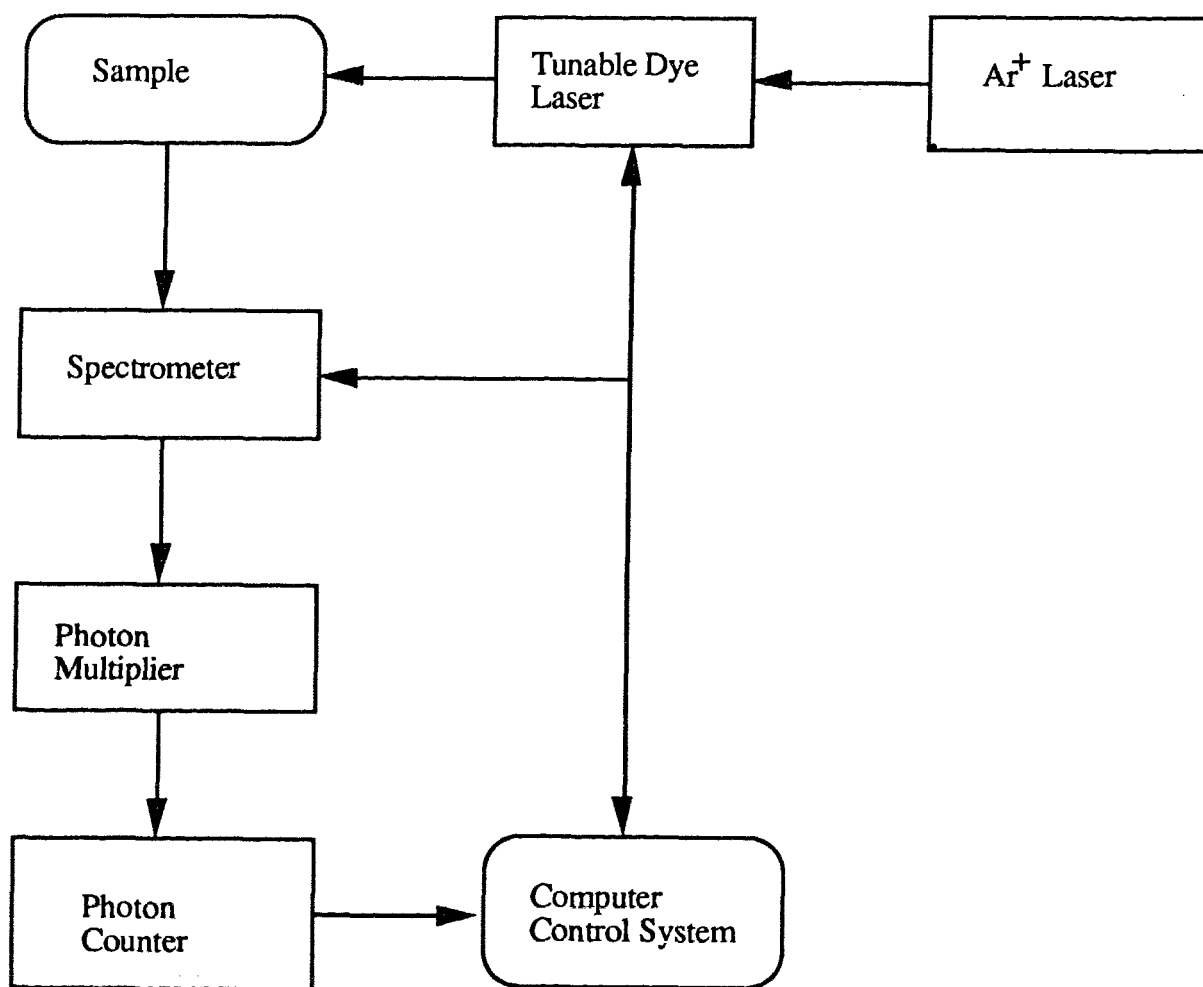
Fig. 3 Experimental setup

2.1 Spectrometer and System Calibration

The spectrometer used was a Spex 1/2 m double grating monochromator. The signal diffracted by the spectrometer was collected by an ITT FW130 (S20) photomultiplier tube cooled to ~-20°C with a dry-ice alcohol mixture. After discrimination and amplification, the output signal was processed by a photon counter (Princeton Applied Research, SS1110). The intensity of the output was digitally stored and could be displayed as photon count rate with the help of a Pc.

There are three slits in the spectrometer to control the the resolution and reduce stray light throughput. The second and third slits were kept at a fixed setting and only the entrance slit width was changed in trade-offs between intensity and resolution. When measuring the laser line, the slit was set to 25μ, and when taking the fluorescence of the sample, the slit was usually set to 200μ. This corresponds to a resolution of 0.5 cm^{-1} and 4 cm^{-1} (to 6328 Å line) respectively.

There are two 5-digit mechanical counters on the spectrometer which permit a setting to 0.1 cm^{-1} precision. We only used the counter which displays absolute wavenumbers. In fact, because the spectrometer had been used for a long time, the wavenumber displayed on the counter had been shifted from the true wavenumber by few of wavenumbers. Hence, we had to calibrate the spectrometer.

The calibration of the spectrometer system which included spectrometer, photomultiplier and photon counter consisted of two parts. One was the calibration of the wavenumber setting, the other was the calibration of the absolute spectral response of the system. We used a neon lamp to calibrate the wavenumber setting with the well known neon emission lines. By comparing the displayed wavenumber with the known true neon line wavenumber, we could get the wavenumber error of the spectrometer. For the wavenumbers between any two known neon lines, we linearly interpolated the error.

To calibrate the spectral response function, we used an EOA L-101 Spectral Irradiance standard lamp which permits accurate calibration of optical sources, detectors and the spectral response of the optical system in the wavelength range from 2500Å to 2.6μ. The spectrometer was moved to the true wavenumber obtained from the neon lamp calibration, and the intensity count on the photon counter was read and compared with the corresponding intensity of the standard lamp obtained from the published operating characteristics of the lamp at the same wavenumber. For the wavenumbers between any two known lines we again used linear interpolation. From this comparison we could obtain the correction factors; if we chose some point as one unit, then we knew the response of the system. Both calibration curves for wavenumber and intensity response for our spectrometer system are shown in Fig.4 and table 1. The maximal error in the position was then within ±2 cm^{-1}.
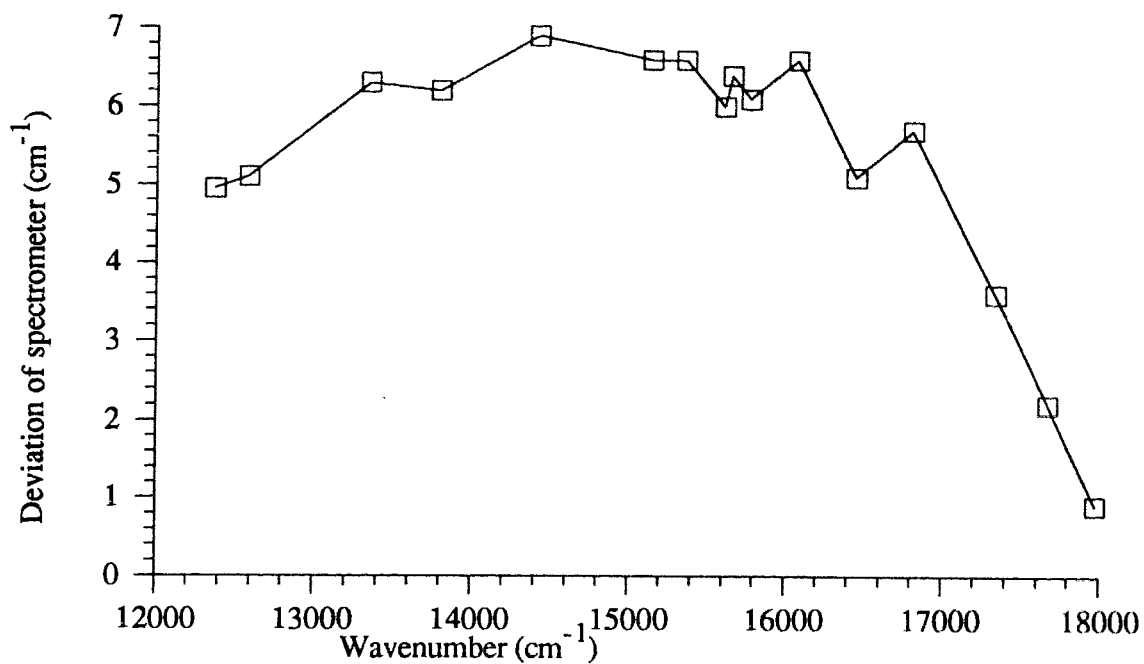
Fig. 4a Spectrometer readout calibration
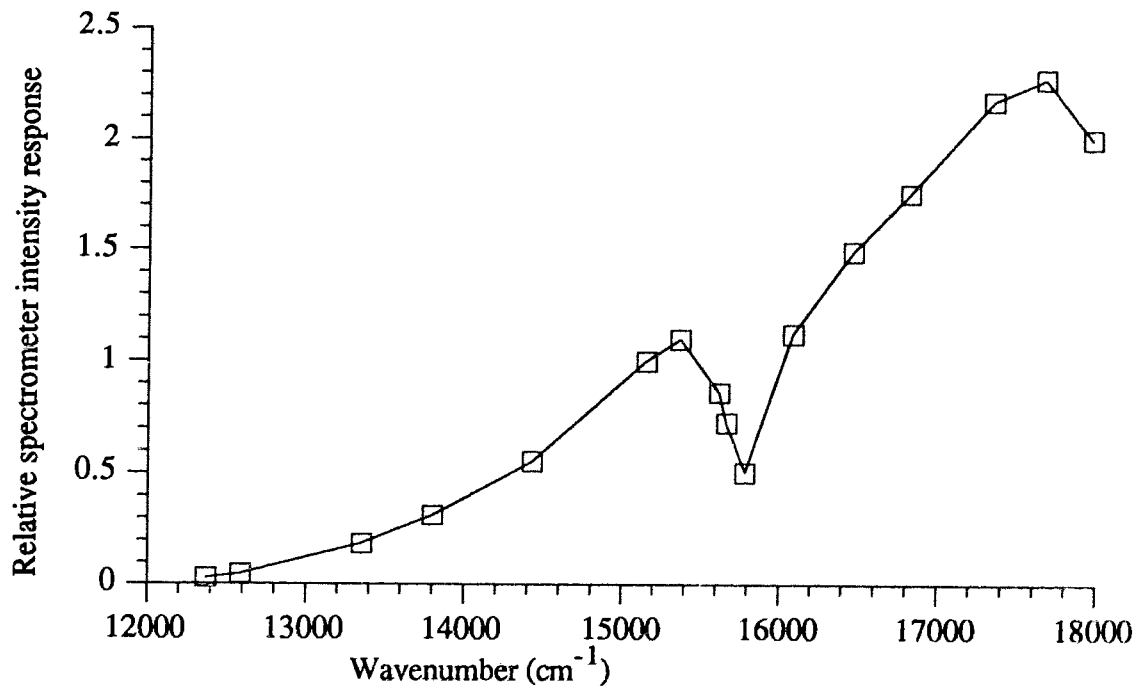
Fig. 4b The spectrometer intensity response calibration.

Table 1   The Calibration of Spectrometer

Standard neon line position (cm^{-1})	Deviation of spectrometer (cm^{-1})	Compensation of intensity
18758.99	-2.0	0.70
17976.67	0.9	0.50
17678.28	2.2	0.44
17347.80	3.6	0.46
16821.33	5.7	0.57
16462.70	5.1	0.67
16084.20	6.6	0.89
15786.75	6.1	1.98
15666.63	6.4	1.38
15619.52	6.0	1.16
15369.18	6.6	0.91
15153.92	6.6	1.00
14431.12	6.9	1.81
13802.30	6.2	3.21
13353.15	6.3	5.47
12589.41	5.1	21.44
12372.47	4.9	35.46

2.2   Excitation

Whereas for fluorescence spectra the sample was excited at a specific wavelength corresponding to an absorption and the light emitted by the sample was focused on the entrance slit of the monochromator, which was then scanned through the spectrum, for the fluorescence excitation spectra the monochromator was set at a fixed specific fluorescence line and the excitation wavelength was scanned while the intensity of the fluorescence line was monitored.

The sample was excited by a multi-mode dye laser (CR599, by Coherent Radiation) which was pumped through an Ar^+ laser (I-S2-4, also by Coherent Radiation). The dye used in the dye laser was DCM (by Exciton Chemical Co.) which could give the desirable power in the wavelength range of interest. The typical DCM dye laser output obtained is shown in Fig.5a. The dye laser output might vary under different operation conditions.

At the beginning of this study, the Ar^+ laser output was around 4W at full power (all lines). Several months later, the Argon laser power was reduced to about 3W which still gave good results. When the power of the Ar^+ laser was about 4W, the dye laser had an output 0-220 mW. After the power of the pumping

Table 2   The Dye Laser Calibration

Micrometer position (mm)	Corresponding wavenumnber (cm^{-1})	Dye laser output (mW)
910	14382.30	15
905	14402.00	20
900	14425.30	35
875	14531.00	55
850	14641.90	55
825	14758.10	70
800	14878.40	100
775	15000.10	110
750	15128.90	115
725	15261.20	130
700	15397.20	130
675	15535.80	130
650	15676.70	130
625	15819.70	130
600	15965.30	130
575	16114.20	130
550	16261.40	100
525	16411.00	20
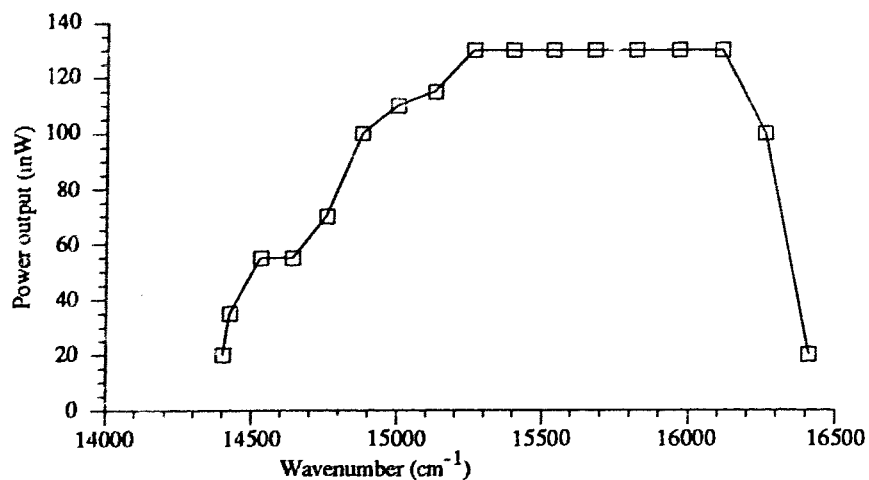
Fig. 5a Dye laser output curve
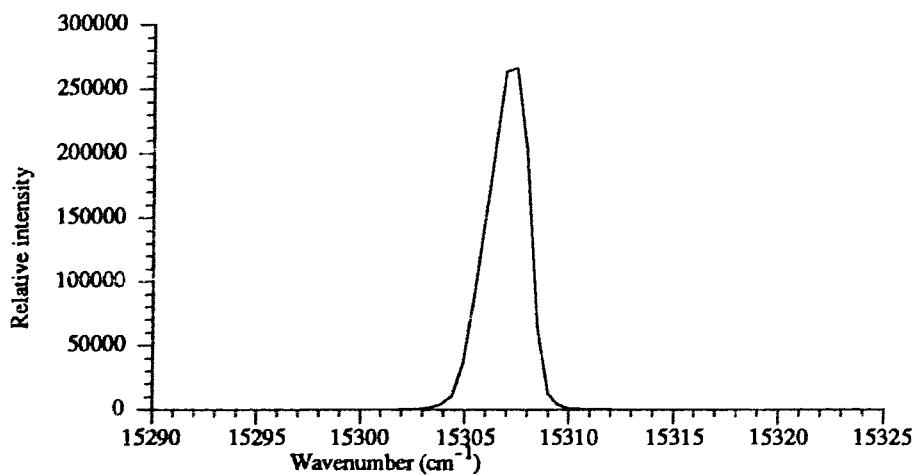
Fig. 5b Example of the laser output shape.
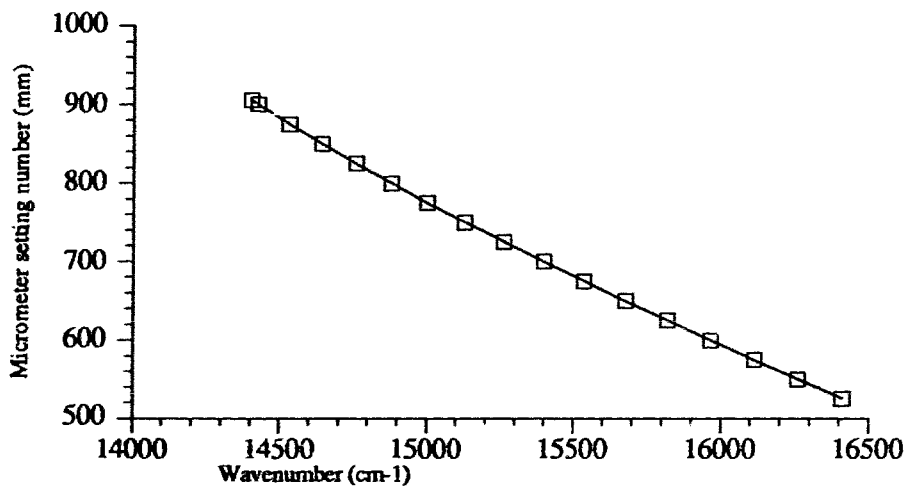
Fig. 5c The relationship between micrometer setting and output wavenumber of dye laser.

14

laser decayed to 3W, the dye laser gave an output of 0-130 mW. In the range of DCM laser output, the laser lines had a width of 2 cm^{-1}. An example of dye laser line shape is given in Fig.5b.

The dye laser wavelength was changed by a low loss crystalline-quartz birefringent filter inserted in the highly stable three-mirror cavity. The filter consisted of plates oriented at Brewster's angle with optical axis in the face of the plate. Rotation of the plates about an axis normal to the surfaces changed the output wavelength. The rotation of the plate was controlled by a micrometer which could be controlled by a stepping motor. To obtained optimal output, the mirrors of the dye laser were frequently adjusted. Thus a specific position of the micrometer did not correspond always to the same wavelength. Once the adjustment was done and the micrometer vs. wavelength obtained, no further changes occurred. Because reading of the numbers on the micrometer was very important for the fluorescence excitation experiments, the calibration of dye laser had to be redone after each excitation experiment to double check the wavelength for each position of the micrometer. Usually we only calibrated some specific points on the micrometer such as at 500, 525, 550, ... 875, 900mm (also see Table 2). For the points in between these settings, we used linear interpolation. One such calibration of the dye laser is shown in Fig.5c.

2.3   Sample and Preparation

All the TBH_2PC sample used in the experiments was kindly donated by Professor D. Haarer (Universität Bayreuth, Institute für Experimental Physik IV, Germany) and was used without any further purification. At room temperature, the TBH_2Pc sample is a greenish-blue powder. The solvents used included n-Octane (C_8), n-Nonane (C_9), n-Decane (C_{10}), n-Tetradecane (C_{14}), Hexadecane (C_{16}), Heptadecane (C_{17}) and Octadecane (C_{18}) by Aldrich Chemical Company, n-Duodecane (C_{12}) by BDH Chemical Ltd and Iso-Octane from Fisher Scientific Company. All these chemical solvents have a purity above 99%. TBH_2Pc was directly dissolved in the solvents usually with concentrations of 10^{-4} to 10^{-5} mol/liter.

The sample was put in to a cleaned and dried glass cell (path length$\leq$1mm). To obtain a good Shopl'skii matrix, the sample was usually cooled very slowly to its final temperature. This would insure optimum equilibration of the TBH_2PC molecules in the Shopl'skii matrix into one dominant site and reduce the inhomogeneous widths of the line spectra and the intensity of the amorphous background. The cooling was done as follows: first, pumping the vacuum of the glass helium dewar that contained the sample to 10^{-5} to 10^{-6} Torr and inserting the sample; second, filling the outer N_2 dewar less than half full; because the liquid nitrogen and sample were thus separated by a vacuum layer, the freezing process was very slow. For example,

it took more than one hour for TBH_2PC in Hexadecane and 2-3 hours in n-Octane to be frozen in this way. After the sample had cooled to liquid nitrogen temperature liquid helium was transferred into the cryostat. The sample cell was directly immersed in liquid helium and this insured that the sample was always at 4.2K for the subsequent measurements. This temperature could be maintained for approximately 4 hours.

2.4   Data Acquisition and Processing

The data acquisition system was controlled and manipulated by an IBM compatible PC/AT computer. The software used was called MONO, it was developed by Dennis Sweatman and Wayne Garret in the Dept. of Chemistry at the University of Queensland, Australia and made available to us by Dr. Peter Milford (now at the Dept. of Astronomy, Stanford University).

The MONO control program was written in Fortran and Assembler languages and compiled with Microsoft Fortran 4.01 and Microsoft Micro Assembler version 4.0. The control program was divided into a main program and a large number of subroutines. The main program handled the command decoding and many of the commands and the subroutines handled individual routines and attempted to isolate all device dependencies.

MONO can manipulate the spectrometer, such as move the monochromater counter to a specific wavenumber by sending pulses to stepper motor which rotates the grating, one step in the

stepper motor equaling 0.02 cm^{-1} etc. More importantly, with the MONO program, the monochromator scans over a range of interested wavenumbers or continuously takes data at some specific wavenumber for a pre-set time which can be set from microseconds to several seconds on the SSR photon counter will be very easy.

The photon counter processed the signal from the photomultiplier. The result was displayed on the counter in units of photons per second. On the other hand, the result was also directly sent to the computer and displayed on the screen of the computer. The "save" command was used to save all our original data of significance.

The MONO program was used mainly for data acquisition. Some further data processing such as calibrating the saved data and changing axis scales was done with the help of programs written by Dr. W. H. Chen (a visiting professor at SFU from the Dept of Electrophysics, National Chiao-Tung University, Taiwan). Because the data saved by MONO was only a single column of numbers which represented the intensity of the signal, these data had to be converted to plots of intensity vs wavenumber or intensity vs time while at the same time incorporating the calibrations of the spectrometer and the dye laser. Then the data could be analyzed. Most of the graphics plotted as well as data manipulation were performed with a commercial spreadsheet software called Quattro Pro by Poland Company. Although it was not designed specifically for use in physics, it performed very adequately.

Chapter 3.   Results and discussion

Before introducing the results of actual measurements, the Shpol'skii effect and its manifestations as they pertain to the free base phthalocyanines are discussed in section 3.1 as is the nature of the states of the H_2Pc (and TBH_2Pc) molecule in a Shpol'skii matrix. In section 3.2 Shpol'skii spectra of TBH_2Pc in a variety of alkanes are shown and their characteristics are commented upon. A very detailed presentation and discussion of the Shpol'skii fluorescence and fluorescence excitation spectra of TBH_2Pc in C_9, C_{12}, C_{16} and C_{18}, with particular emphasis on C_{16}, is given in sections 3.3 and 3.4. Section 3.5, finally, deals with the phototransformation of TBH_2Pc in C_{16} and C_{18} matrices (schematically shown in Fig.26). This transformation has some unusual aspects that are discussed. Comparison of the results of fluorescence, fluorescence excitation, photochemical transformation and other results pertaining to TBH_2Pc with those of H_2Pc are made within each of the appropriate sections of this chapter.

3.1   Shpol'skii Effect and the Electronic States of TBH_2Pc

The Shpol'skii effect arises when guest molecule species dissolved in a host solvent solidify in such a way that a significant fraction of the guest molecules find themselves in

well defined sites inside the largely crystalline host matrix. In such a situation, when the host-guest interaction is sufficiently weak, the guest molecules associated with a specific local environment will, at sufficiently low temperatures, exhibit sharp line spectra in absorption and, if applicable, in emissions. The lines corresponding to specific vibronic and electronic transitions characterize the guest molecule in the specific micro-environment, the so-called "cage". To obtain Shpol'skii spectra then, two conditions have to be met: the guest must have a reasonable fit into vacancies of the host-crystal, and the coupling between the phonons in the host matrix and the guest molecules must be weak. For the latter condition to be met, it is necessary, but not sufficient, to operate at low temperatures. Hence, good Shpol'skii spectra are usually obtained at liquid helium temperatures. Alkanes, with their low polarizability compared with aromatic solvents and a well defined crystal structure at low temperatures have been favoured solvents for obtaining Shpol'skii spectra of porphyrins as well as phthalocyanines[10,25]. Their disadvantage, in particular for use with phthalocyanines, lies in the fact, that the Pc's usually do not dissolve sufficiently well in alkanes to obtain the concentrations necessary for spectra with reasonable signal to noise ratios. The technique developed in this laboratory to obtain useable Shpol'skii spectra with Pc's has been to use mixed solvents[15] of α-chloronaphthalene (α-ClN) with alkanes. In this method the Pc of interest is first dissolved in α-ClN, which is one of the best solvents for Pc's,

and then the solution is diluted with the appropriate alkane by a factor of between 3 and 10. Good Shpol'skii spectra were thus obtained and it was proved that the presence of the α-ClN did not affect the spectra[13].

As mentioned in the introduction TBH$_2$Pc was developed to overcome the solubility problem of the normal H$_2$Pc in pure alkanes and it was commonly assumed that its electronic properties and the dynamics of the phototransformation between its two isomers (relative position of the central two protons with respect to the D_{2h} symmetry axes of the "caged" molecule as in Fig. 1) would be unaffected by the addition of the tertiary butyl groups on the outside of the Pc ring structure.

In general, if one wishes to use Shpol'skii spectra to obtain information on electronic and vibronic states either in absorption or emission, one likes to have samples in which there is only one dominant site for the guest molecule, so as to avoid confusion between spectra belonging to different sites, typical site differences being in the range of 1 to 10 cm^{-1}. Such multiple site spectra can be sorted out and identified best in luminescence excitation, where a particular emission line (often the strongest 0-0 transitions in fluorescence or phosphorescence) is monitored and a narrow line (≤ 2cm^{-1}) from a tunable laser is scanned through the absorption.

Often one can minimize the formation of multiple sites by slow cooling of the sample through the freezing point, thereby favouring the guest setting into configurations that are thermodynamically favoured. Still, even with clearly

21

identifiable dominant sites one usually finds a broad background absorption (and emission) corresponding to a, for practical purpose, continuous rather than discrete distribution of sites characteristic of an amorphous matrix. Also, even the discrete sites are still inhomogeneously broadened (presumably as a result of differences on the next to nearest neighbour distribution of the host molecules forming the "cage"). Moreover, the line spectra are also subject to a temperature dependent homogeneous line broadening arising from the interaction with the phonon spectrum of the host matrix. It is apparent from this brief description of the Shpol'skii effect, that spectra resulting from it are neither easy to obtain nor easy to interpret and understand.

In the special case of interest for this study, some general statements regarding the electronic structure of H_2Pc are desired. The free molecule structure is considered to have D_{2h} symmetry which is perturbed in the "cage" formed by the host crystal and has two lowest excited electronic singlet states: the lower usually referred to as the Q_x or, in this work, the S_1 state, the higher as the Q_y or the S_2 state. Their separation is typically of the order 900 cm^{-1}. A further splitting in the spectra is obtained that results from the two tautomeric species, labelled in this work by superscripts $S^{(1)}$ and $S^{(2)}$ and differing in the positions of the central protons. The 0-0 transitions of these tautomers differ by several 10s of cm^{-1} depending on the particular host and site. We are thus dealing in our spectra with four pure electronic transitions

$S_0{}^{(1)} \leftrightarrow S_1{}^{(1)}$, $S_0{}^{(1)} \leftrightarrow S_2{}^{(1)}$ and $S_0{}^{(2)} \leftrightarrow S_1{}^{(2)}$, $S_0{}^{(2)} \leftrightarrow S_2{}^{(2)}$, two belonging to each of the two tautomeric species.

We are not concerned in this study with any higher electronic states (the "Soret-band") that occur at much higher energies. Since the triplet state has so far not been observed in the free-base Pc, it does not enter explicitly either in this study. However, the vibrational structure of the ground state (observed in fluorescence spectra) as well as the first and second excited electronic states (observed in fluorescence excitation) have been investigated.

The phototransformation between the tautomers, which is one of the major motivations for this study, arises when a molecule in the $S_0{}^{(1)}$ or $S_0{}^{(2)}$ state is excited but does not relax to its original state but ends in the ground state of the other tautomer, i.e. in $S_0{}^{(2)}$ or $S_0{}^{(1)}$ respectively. It should be kept in mind that this transformation involves a repositioning of the two central protons and will have an effect on the relative population in the ground state of these tautomers. It should be stated here, that prior to this study no definite information existed as to whether or not there was a significant difference in the ground state energies of the two tautomers.

In Fig. 6 we show the two 0-0 fluorescences of H_2Pc in a Shpol'skii matrix of C_8. The tautomeric splitting is seen to be 60 cm^{-1} and the (inhomogeneous) linewidth is 3-4 cm^{-1}.
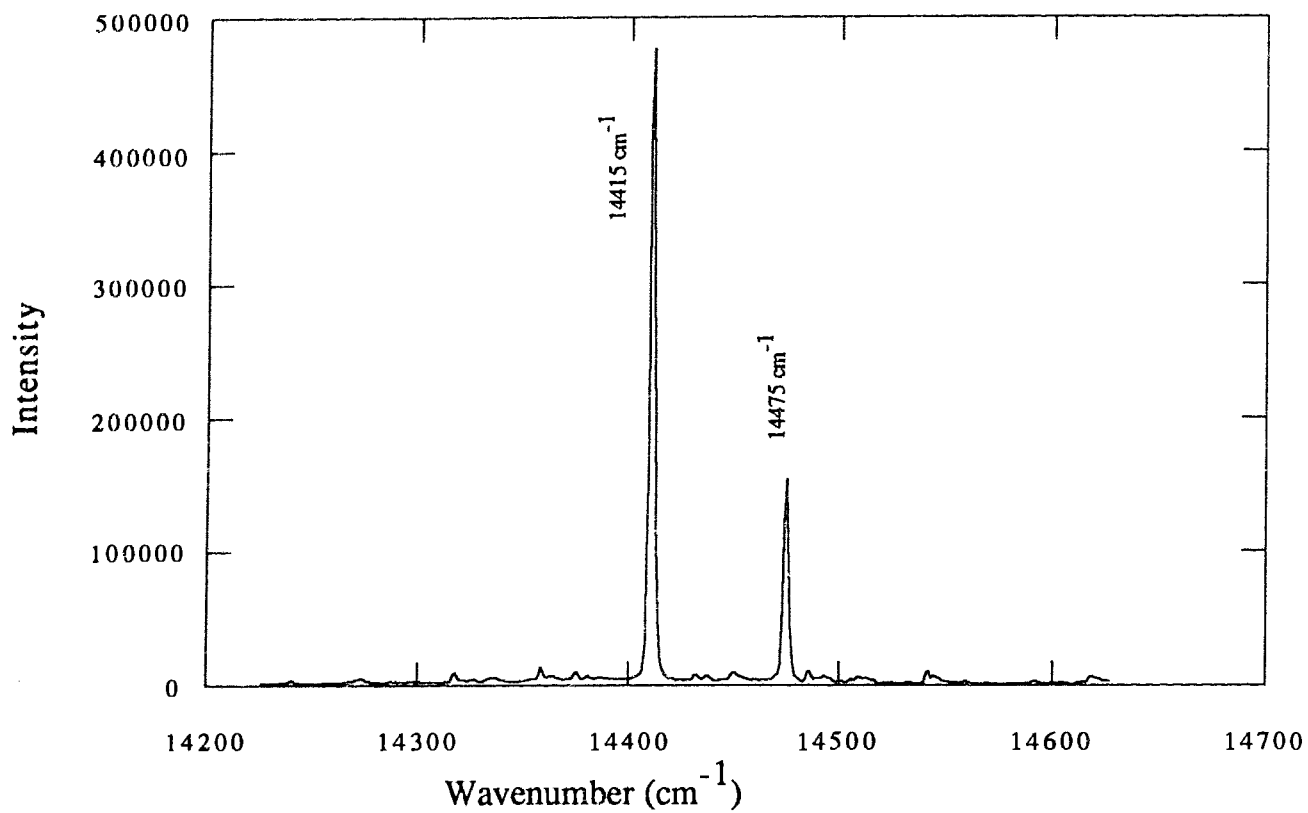
Fig. 6 The doublet (0-0 transition) of H_2Pc in C_8 and αClN matrix under excitation of $\upsilon_{exc}=15653$ cm^{-1}. It represents a good Shpol'skii effect.

3.2 Shpol'skii Spectra of TBH$_2$Pc

In this section luminescence spectra of TBH$_2$Pc in a variety of alkanes are presented. C_8, C_9, C_{10}, C_{12}, C_{14}, C_{16}, C_{17} and C_{18} were used as host solvents in an attempt to identify those alkanes best suited for further study and comparison with H$_2$Pc.

In Fig. 7 the various typical spectra obtained with single frequency excitation at 4.2K are shown. The excitation energies were chosen to optimize a dominant site and the associated 0-0 fluorescence. Both amorphous background and number of sites observed under single frequency excitation varied widely. The best Shpol'skii effect with a dominant site was observed with C_{16}, next came C_{12}, C_{18} and C_9. C_{17} turned out to show practically no Shpol'skii effect at all, which may surprise in view of the good results obtained with C_{16} and C_{18}. TBH$_2$Pc seems to have a good Shpol'skii effect in C_8 and C_{10}. It is found that the high peaks 14476 cm^{-1}, 14412 cm^{-1} in C_8 and 14307 cm^{-1}, 14282 cm^{-1} in C_{10} belong to different sites. The two peaks of 14417 cm^{-1} and 14409 cm^{-1} in C_{14} are from the same site, but the background from other sites is really strong. The 14447 cm^{-1} and 14321 cm^{-1} peaks in C_9, the 14429 cm^{-1} and 14417 cm^{-1} transitions in C_{12}, the 14436 cm^{-1} and 14415 cm^{-1} peaks in C_{16} and 14437 cm^{-1} and 14337 cm^{-1} in C_{18} are found to be from the same site respectively. Although there are other sites in the spectra, these are the dominant positions. One can say that TBH$_2$Pc has a good Shpol'skii effect in C_9, C_{12}, C_{16} and C_{18}. The
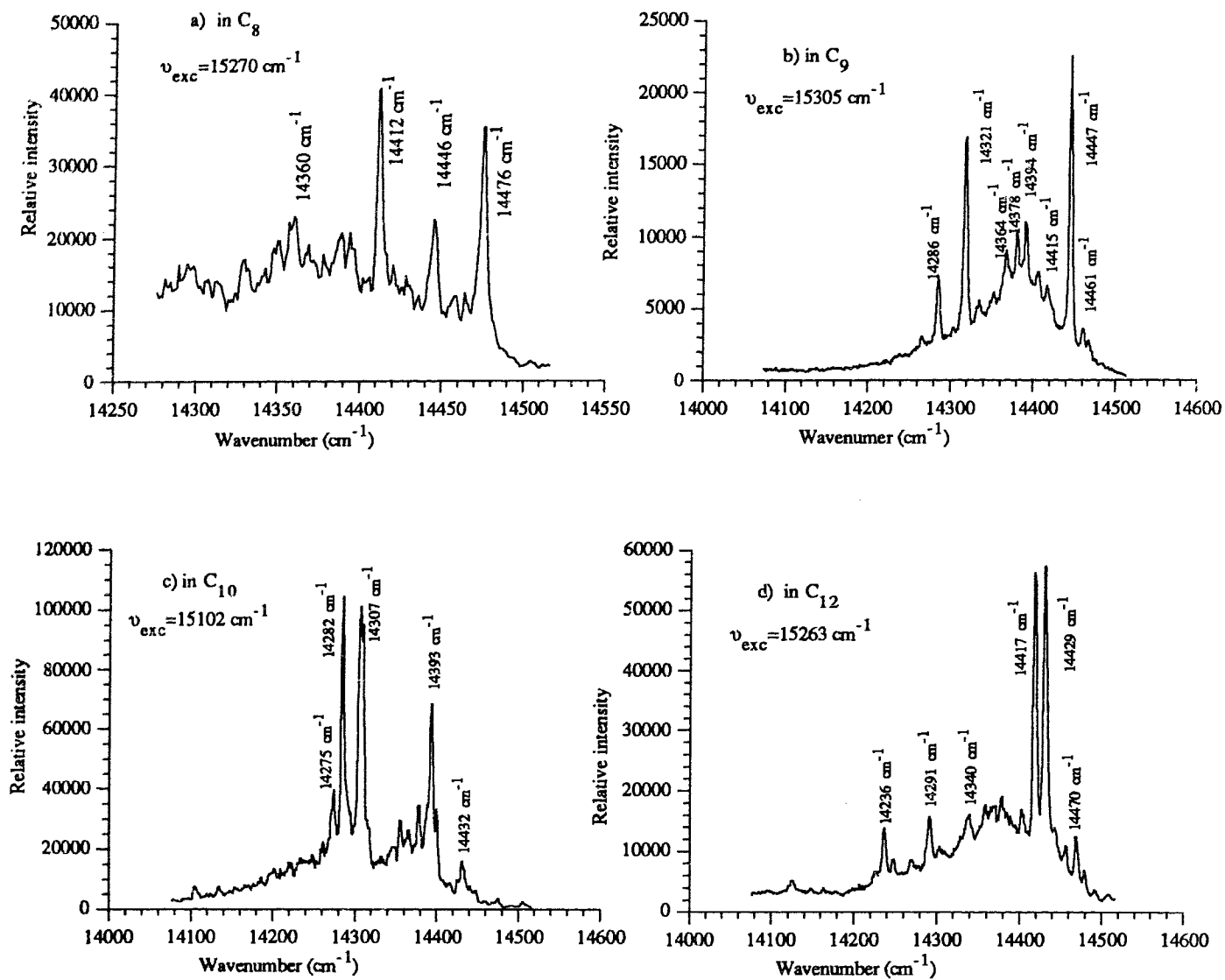
Fig. 7   0-0 transitions of TBH_2Pc in different Shpol'skii matrices.
All of the recognizable peaks are labeled on each figure.

26
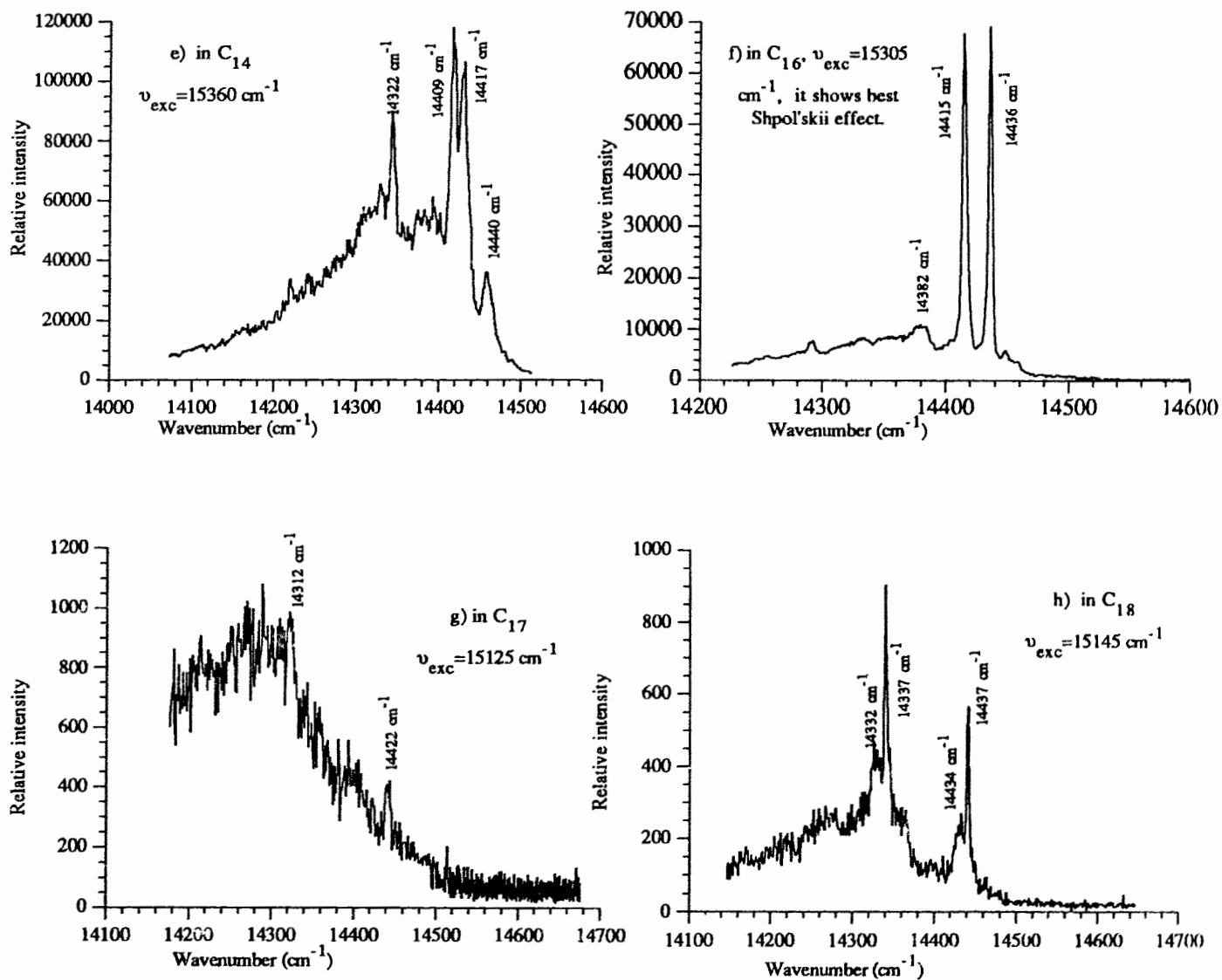
Fig. 7 (continued) 0-0 transitions of TBH_2Pc in different Shpol'skii matrices. All of the recognizable peaks are labeled on each figure.

exact reason for the different behaviour of the TBH$_2$Pc molecule in the various alkane matrices would be an interesting study in its own right that could lead to a better prediction of good Shpol'skii hosts for specific guest species. Clearly it must be related to crystal structure of host, size of guest, and nature of their interaction. Such investigations are beyond the scope of this study.

In Fig. 8 the effect of fast cooling on the Shpol'skii spectra in C$_9$, C$_{12}$ and C$_{16}$ is shown. Appearance of multiple sites in C$_9$ and a significant broadening in spectra of C$_{12}$ and C$_{16}$ are evident pointing toward a less uniform crystallization process.

The broadening effect at higher temperatures mentioned in the previous section is shown in Fig. 9 which compares the 0-0 fluorescences obtained in C$_{16}$ at 4.2K and 77K respectively.

Details of the Shpol'skii spectra of TBH$_2$Pc in C$_9$, C$_{12}$, C$_{16}$ and C$_{18}$ with special emphasis on C$_{16}$ for comparison with H$_2$Pc are given in the following sections.

3.2.1 Electronic Transitions of TBH$_2$Pc in C$_{16}$

TBH$_2$Pc in C$_{16}$ shows the best Shpol'skii effect among all the solvents tried (see Fig.7; a to h). After excitation with selected laser frequencies (such as 15305 cm^{-1}), minor sites were actually suppressed. The two 0-0 fluorescences of TBH$_2$Pc in C$_{16}$ were measured at 14436 and 14415 cm^{-1} respectively for S$_1$$^{(1)}$ and S$_1$$^{(2)}$ with a 21 cm^{-1} splitting. The full widths at
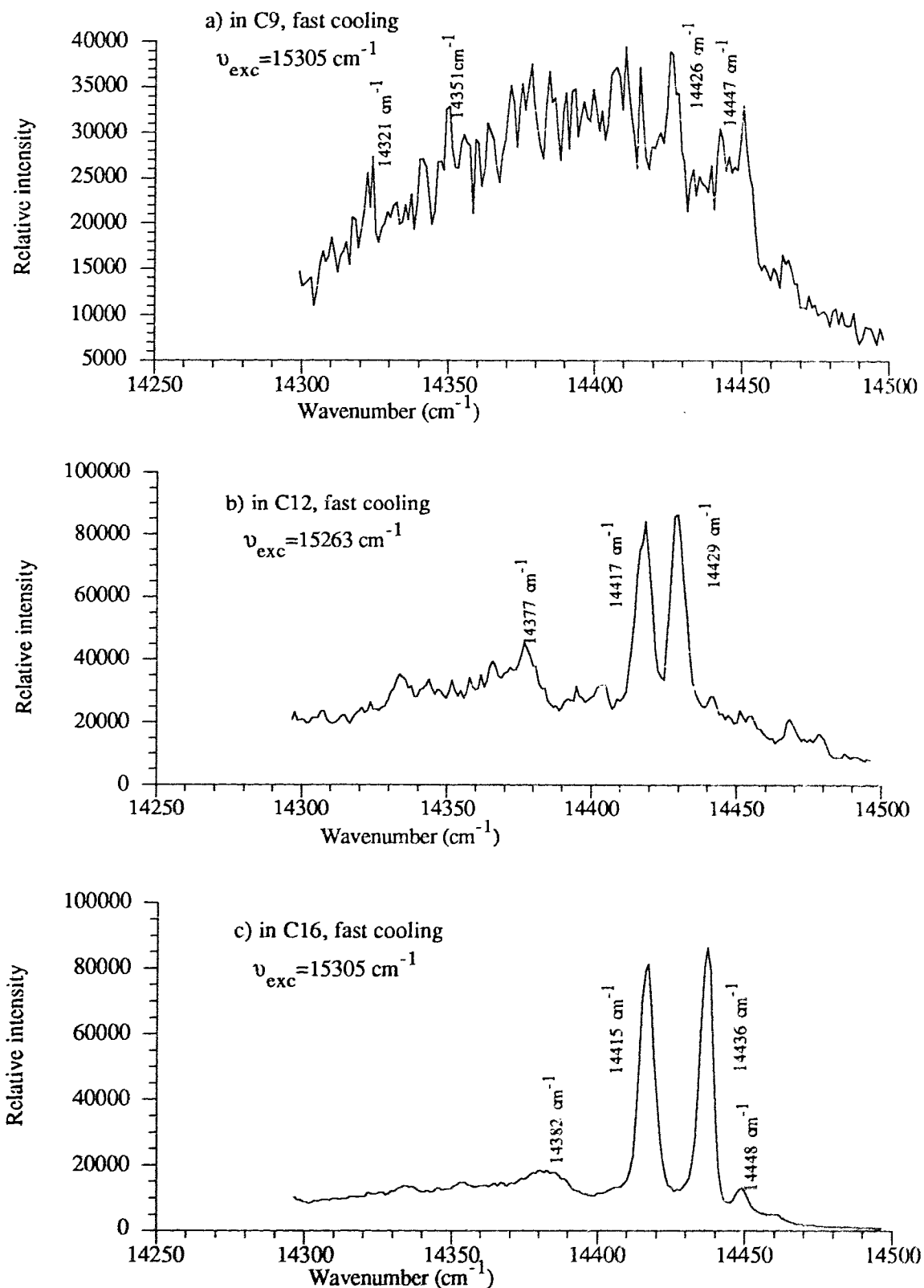
Fig. 8 The dependence of Shpol'skii effect with the cooling rate. A fast cooling causes a bad Shpol'skii effect.
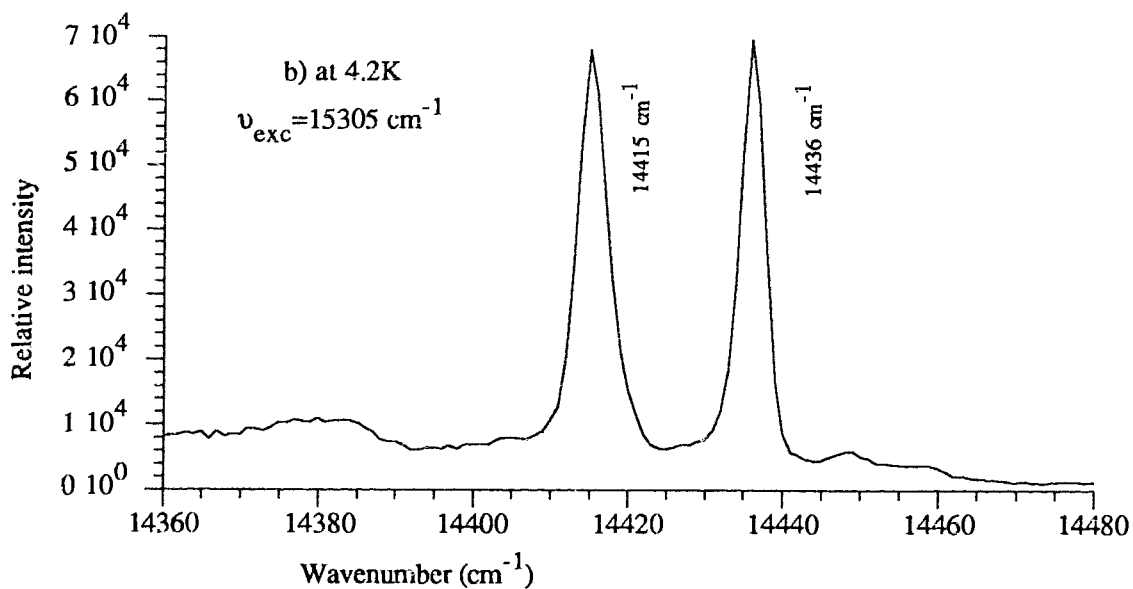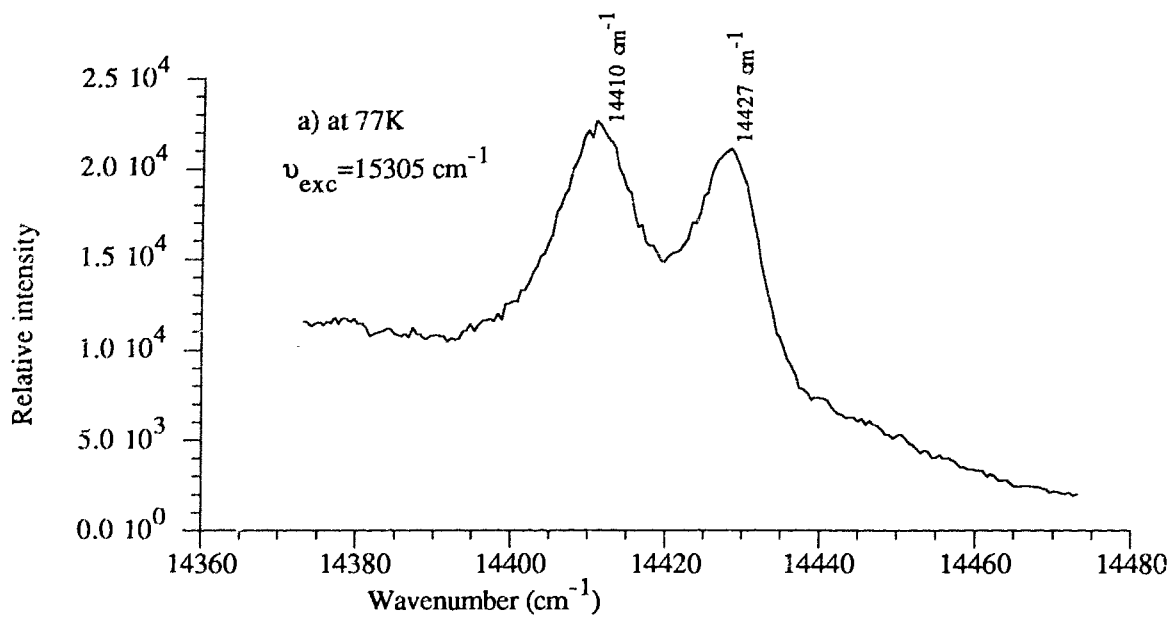
Fig. 9 The Shpol'skii effect also strongly depends on the temperature. TBH$_2$Pc in C$_{16}$: a) at 77K; b) at 4.2K under the same other conditions.

half maximum (fwhm) of the doublet are about 5 and 4 cm^{-1} and their shapes are Gaussian.

The 14436 cm^{-1} and 14415 cm^{-1} fluorescences derive from the two lowest excited electronic states which are shown as follows: First, these two transitions are much stronger than the rest of the observed fluorescences which agrees with the generally known fact that 0-0 transitions are much stronger than 0-1 bands. Second, approximately the same spectral positions of $S_1^{(1)}$ and $S_1^{(2)}$ were obtained from fluorescence excitation spectra (see sec. 3.4) which confirmed that the origins are genuine. The fluorescence excitation spectrum in Fig. 10a observed at 13729 cm^{-1} ($S_1^{(2)} \rightarrow S_0^{(2)}$+686 cm^{-1}) shows two peaks at 14436 cm^{-1} and 14418 cm^{-1} (shifted $S_1^{(2)}$), whereas Fig. 10b monitored at 13750 cm^{-1} ($S_1^{(1)} \rightarrow S_0^{(1)}$+686 cm^{-1}) reveals only one peak at 14436 cm^{-1} ($S_1^{(1)}$). This shows that $S_1^{(1)}$ is higher than $S_1^{(2)}$ in energy and there is no cross 0-1 transition between the two species. This result was verified by observation of the fluorescences after direct excitation into 14436 cm^{-1} and 14415 cm^{-1} respectively, which are shown in Fig. 11. After excitation by 14436 cm^{-1} ($S_1^{(1)}$), two fluorescences at 14435 cm^{-1} and 14415 cm^{-1} were observed although the 14415 cm^{-1} peak was very weak. But if excited at 14415 cm^{-1} ($S_1^{(2)}$), only the 14415 cm^{-1} fluorescence was observed, this time relatively strong. This indicates that $S_1^{(1)}$ is higher than $S_1^{(2)}$ in energy and the transfer rate from $S_1^{(1)}$ to $S_1^{(2)}$ is very slow.

The relative intensity of the 0-0 fluorescence emissions of TBH_2Pc in C_{16} as a function of the excitation frequency is
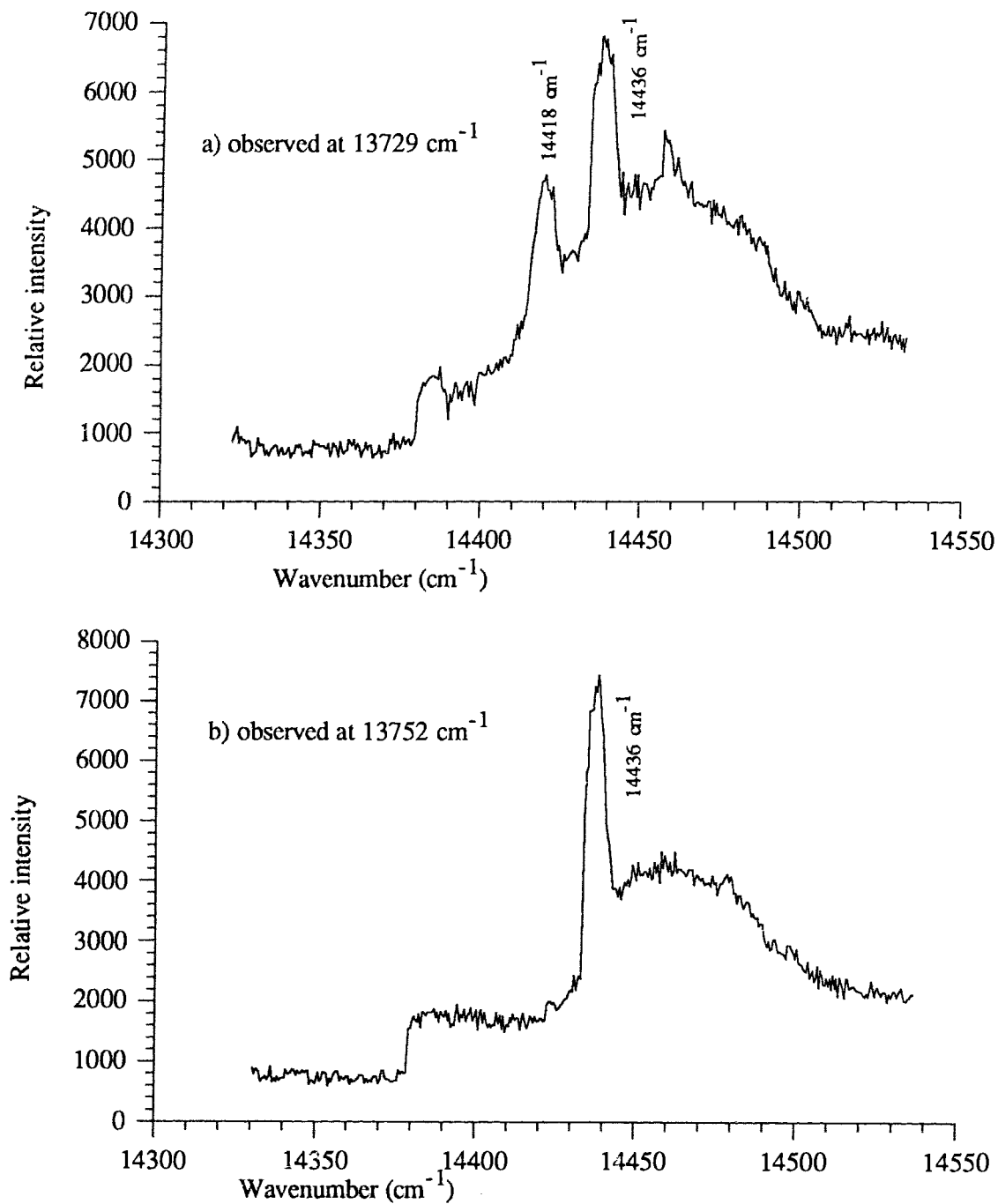
Fig. 10 Fluorescence excitation spectra monitored at a) 13729 cm^{-1}; b) 13752 cm^{-1}.

Their difference indicates $S_1^{(1)}$ is higher than $S_1^{(2)}$ in energy.
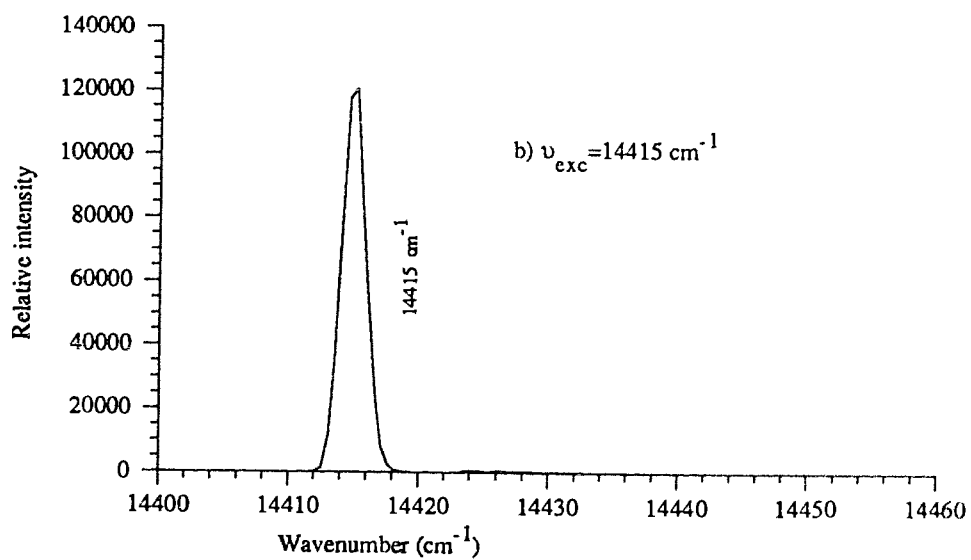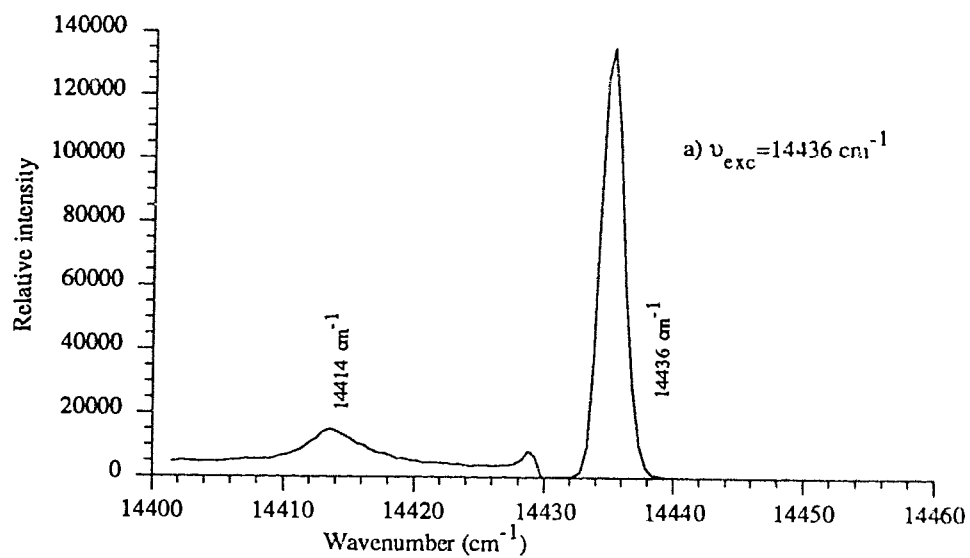
Fig. 11 Fluorescence excitation spectra at a) 14436 cm^{-1} or b) 14415 cm^{-1}. They also show that $S_1^{(1)}$ is higher than $S_1^{(2)}$ in energy.

shown in Fig.12. It is found that the peak intensity of the higher energy component of the 0-0 double fluorescences relative to that of the lower energy component can't be accounted for by a Boltzmann factor. This implies that the transformation between $S_1^{(1)}$ and $S_1^{(2)}$ is slow at 4.2K. Such a slow transformation indicates the existence of a substantial potential barrier between the $S_1^{(1)}$ and $S_1^{(2)}$ orientations in analogy with the situation in H_2Pc. Because of this potential barrier between $S_1^{(1)}$ and $S_1^{(2)}$, when the normal vibrations of $S_1^{(1)}$ or $S_1^{(2)}$ were excited, we observed the stronger $S_1^{(1)}$ or $S_1^{(2)}$ fluorescence, relative to that of $S_1^{(2)}$ or $S_1^{(1)}$. For example, when TBH_2Pc in C_{16} was excited by 14647 cm^{-1} wavelength, fluorescence spectra of $S_1^{(1)}$ and $S_1^{(2)}$ observed were obtained as shown in Fig.12b, and obviously the emission of $S_1^{(1)}$ is stronger than that of $S_1^{(2)}$. In section 3.4, it will be shown that the $\upsilon_{exc}=14647$ cm^{-1} is the vibronic level $S_1^{(1)}+211$ cm^{-1}. When TBH_2Pc was excited by 14590 cm^{-1}, the 0-0 fluorescence observed is shown in Fig.12c where the fluorescence from $S_1^{(2)}$ is stronger than from $S_1^{(1)}$. In fact, the wavelength 14590 cm^{-1} is just one of the vibronic levels of the $S_1^{(2)}$ progression ($S_1^{(2)}+175$ cm^{-1}). This accounts for the relative intensity changes of the $S_1^{(1)}$ and $S_1^{(2)}$ doublet as a function of excitation wavelength, and it also provides a valuable method to determine whether a vibronic level above $S_1^{(1)}$ or $S_1^{(2)}$ belongs to a given tautomer. It is to be noted that when TBH_2Pc is excited by 15305 cm^{-1} or 15264 cm^{-1} the resultant 0-0 fluorescences are always two very strong peaks of almost equal

34
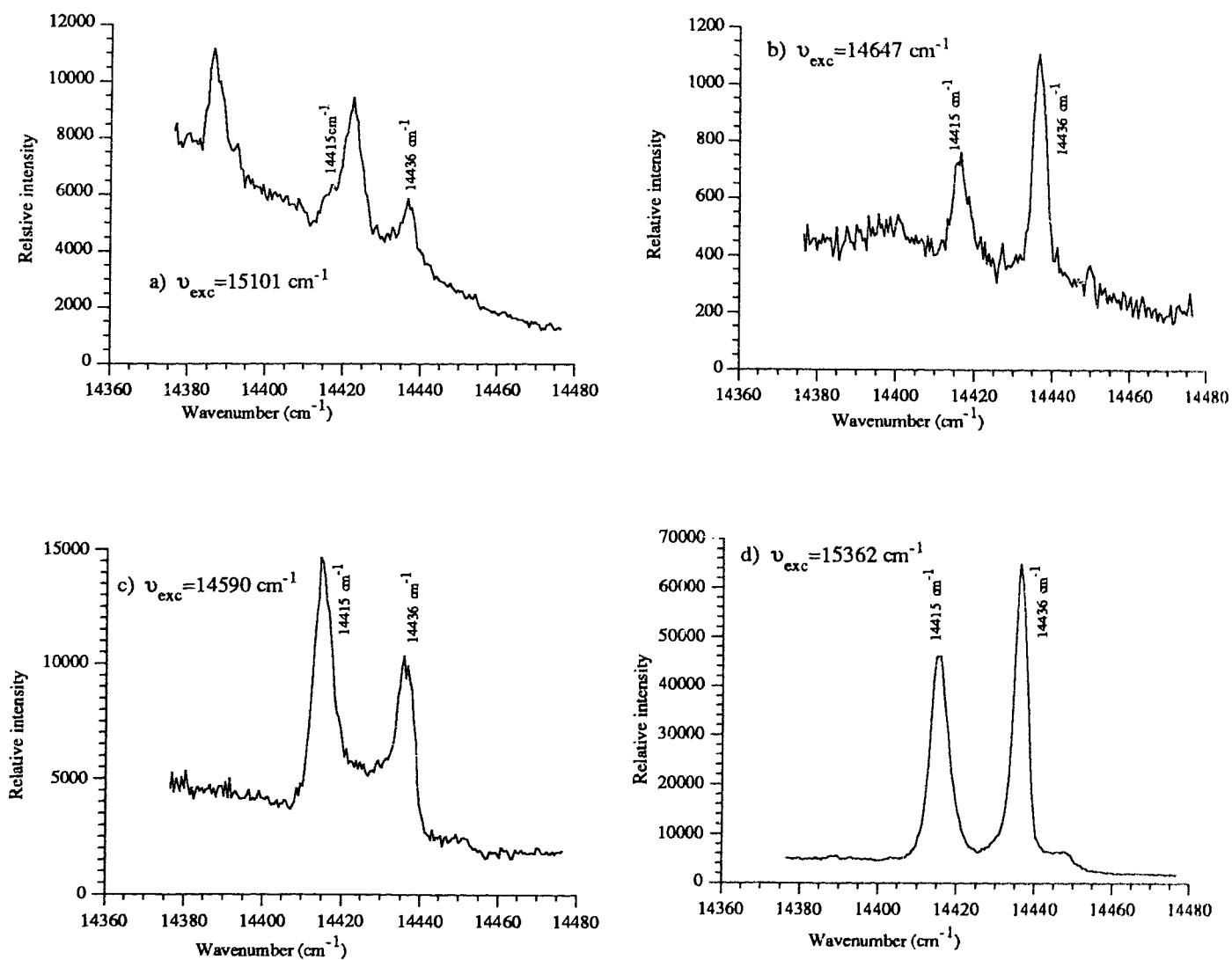
Fig. 12 The data show that 0-0 transitions are dependent on the laser excitation wavelength. a)-d) illustrated with different excitations of 0-0 transitions of TBH_2Pc in C_{16}.

intensity (Fig.7f). The reason is 15305 cm^{-1} and 15264 cm^{-1} are excitations into the two higher electronic states $S_2^{(1)}$ and $S_2^{(2)}$ belonging to Q_y. This will be discussed in detail below.

It is interesting to note that when TBH$_2$Pc is excited by 15362 cm^{-1} ($S_1^{(1)}$+926 cm^{-1}) the relative intensity of the fluorescence of $S_1^{(1)}$ is apparently stronger than that from $S_1^{(2)}$ as in Fig.12d. This suggests that the potential barrier between $S_1^{(1)}$ and the lower lying $S_1^{(2)}$ in TBH$_2$Pc is more than 4.2K (or 6 cm^{-1}) above the fundamental level of the 926 cm^{-1} vibration in $S_1^{(1)}$. This is similar to what was observed for H$_2$Pc [10].

Two very strong fluorescence-excitation bands were found in the vibronic progressions of $S_1^{(1)}$ and $S_1^{(2)}$ at 15305 cm^{-1} and 15264 cm^{-1} in C$_{16}$ (see Fig.21;(2), these two peaks are explicitly labeled.). They are above $S_1^{(1)}$ and $S_1^{(2)}$ 869 cm^{-1} and 849 cm^{-1} respectively. We assign these two bands to $S_2^{(1)}$ and $S_2^{(2)}$ based on the following considerations:

1. TBH$_2$Pc in a C$_{16}$ matrix shows no corresponding spectrum of $S_1^{(1)}$+869 cm^{-1} in the vibronic progression of $S_1^{(2)}$ and neither does the $S_1^{(2)}$+849 cm^{-1} band show a vibronic level in the $S_1^{(1)}$ progression. In general, if level $S_1^{(1)}$+869 cm^{-1} or $S_1^{(2)}$+849 cm^{-1} is one of the vibronic levels in a given vibronic progression, one expects to observe a corresponding vibronic level around $S_1^{(2)}$+869 cm^{-1} or $S_1^{(1)}$+849 cm^{-1} with comparable intensity, but we did not find any such corresponding transitions.

2. Further, no corresponding vibronic bands of $S_1^{(1)}$+869 cm^{-1} and $S_1^{(2)}$+849 cm^{-1} were observed in the vibronic progressions of $S_0^{(1)}$ and $S_0^{(2)}$ in fluorescence. In general, if $S_1^{(1)}$+869 cm^{-1} and $S_1^{(2)}$+849 cm^{-1} are vibronic levels of the first excited electronic states, one expects corresponding vibronic levels to appear in $S_0^{(1)}$ and $S_0^{(2)}$ vibronic progressions with suitable intensity; but again, no such peaks were observed in the fluorescence spectra.

3. Direct transition bands from around 15302 cm^{-1} (shifted 15305 cm^{-1} due to weakness and large uncertainty) and from 15264 cm^{-1} to the ground states were seen as weak fluorescences when excited with υ_{exc}=15987 cm^{-1}. They are shown in Fig.13, and their intensities are estimated to be at least 3 to 4 orders of magnitude weaker than those of $S_1^{(1)}$ and $S_1^{(2)}$.

4. For H_2Pc in αClN+C_8 the $S_2^{(1)}$ and $S_2^{(2)}$ states were measured at $S_1^{(1)}$+864 cm^{-1} and $S_1^{(2)}$+857 cm^{-1}[10]. Comparing these states to TBH_2Pc in C_{16} we believe that assigning 15305 cm^{-1} ($S_1^{(1)}$+869 cm^{-1}) and 15264 cm^{-1} ($S_1^{(2)}$+849 cm^{-1}) to the two S_2 tautomeric electronic states is reasonable.

5. It is plausible to denote 15305 cm^{-1} and 15264cm^{-1} as $S_2^{(1)}$ and $S_2^{(2)}$ respectively. When TBH_2Pc is excited into either of these, the $S_1^{(1)}$ and $S_1^{(2)}$ fluorescences are much stronger than those by any other excitation wavelengths which have been tried in excitation-fluorescence (see Figs.21, 23-25) and will be discussed later in section 3.4. The relative intensity of the doublet is almost the same and does not depend on the laser power, which indicates that the fluorescences from $S_1^{(1)}$ and
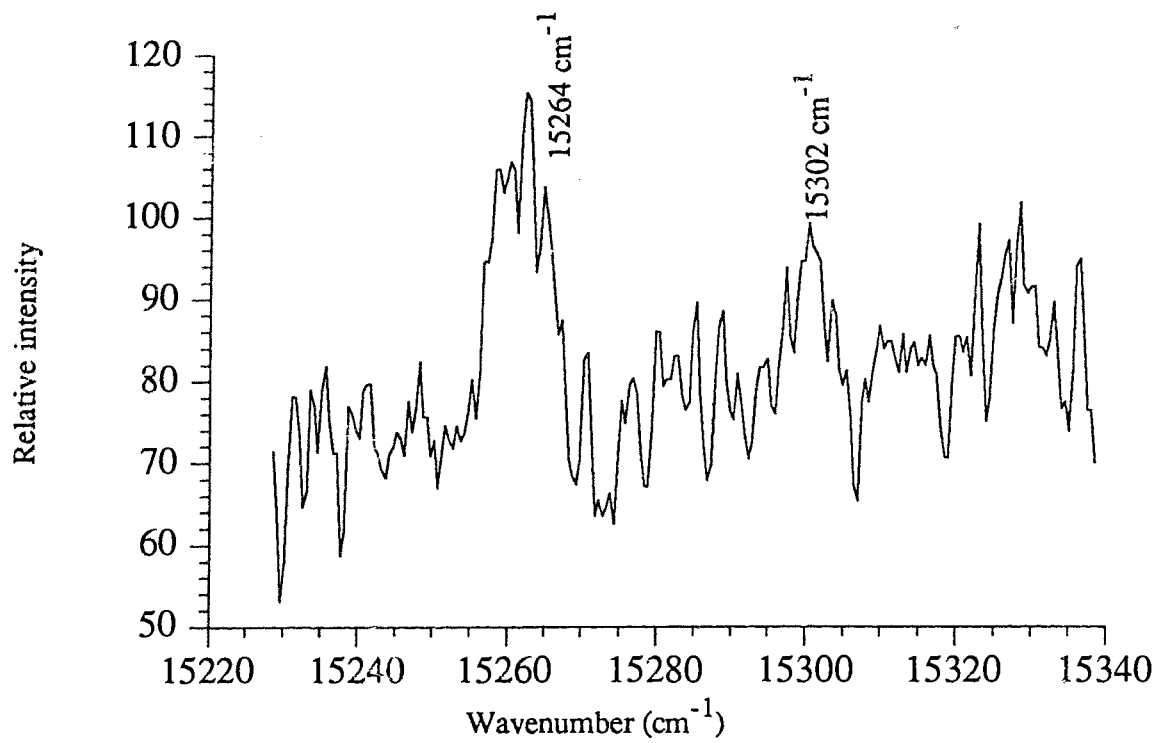
Fig. 13 Direct observation of S_2-S_0 transitions with excitation of υ_{exc}=15987 cm^{-1}.

$S_1^{(2)}$ are relaxed from $S_2^{(1)}$ or $S_2^{(2)}$ after excitation by 15305 cm^{-1} or 15264 cm^{-1}, respectively. In this case vibronic relaxation from $S_2^{(1)}$ or $S_2^{(2)}$ to $S_1^{(1)}$ and $S_1^{(2)}$ procedes easily and without interference by the potential barrier between $S_1^{(1)}$ and $S_1^{(2)}$. Their equal fluorescence intensity and independence of excitation power suggest also that the transformations either from $S_1^{(1)}$ to $S_1^{(2)}$ or from $S_0^{(1)}$ to $S_0^{(2)}$ were very slow.

In summary, we conclude that for TBH$_2$Pc in a C$_{16}$ Shpol'skii matrix, the two lowest excited singlet electronic states with respect to their ground states are:

$B_{3u}(Q_x)$	$B_{2u}(Q_y)$
$S_1^{(1)}$: 14436 cm^{-1}	$S_2^{(1)}$: 15305 cm^{-1}
$S_1^{(2)}$: 14415 cm^{-1}	$S_2^{(2)}$: 15264 cm^{-1}

Clearly, the split caused by the internal crystal field effect (869 cm^{-1} and 849 cm^{-1}) is much larger than the split from tautomerism (21 cm^{-1} and 41 cm^{-1}, respectively).

To compare the spectra of TBH$_2$Pc and H$_2$Pc, we cite previous results obtained in this laboratory for H$_2$Pc in Shpol'skii matrices of α–ClN and C$_8$ which showed the doublet occuring at 14475 and 14411 cm^{-1} for $S_1^{(1)}$ and $S_1^{(2)}$ respectively[10, 15]. The fwhm of the doublet are 3.3 cm^{-1} for $S_1^{(1)}$ and 2.4 cm^{-1} for $S_1^{(2)}$. Our results for TBH$_2$Pc in C$_{16}$ show the doublet is at 14436 and 14415 cm^{-1} with fwhm 4 cm^{-1} for $S_1^{(1)}$ and 5 cm^{-1} for $S_1^{(2)}$. This implies for TBH$_2$Pc in C$_{16}$ a

greater inhomogeneity than H_2Pc has in an α-ClN and C_8 matrix. This can be checked also in the 0-0 doublet fluorescence spectra of TBH_2Pc and H_2Pc. With TBH_2Pc in C_{16} the 0-0 fluorescences always have some broad background (see Fig.7f), but for H_2Pc in mixed matrices of α-ClN and C_8 the 0-0 doublet fluorescences have only a very small background (see Fig.6). The main reason for the broad spectral background stems from the structure of the TBH_2Pc molecule which fits into the C_{16} Shpol'skii matrix only with difficulty. As can been seen from Fig.1, TBH_2Pc is derived from H_2Pc by attaching four tertiary-butyl groups symmetrically at the four corners of the H_2Pc molecule. These four protruding tertiary-butyl groups increase the interaction between the TBH_2Pc and the matrix environment making a good "Shpol'skii fit" difficult. Another contributing factor to the background and inhomogeneity of the spectra might be the cooling rate of TBH_2Pc. This rate is always important to obtain good Shpol'skii matrices. For instance, for TBH_2Pc in C_9, fast cooling made the doublet disappear into the background as in Fig.8a. Although we did not know exact freezing rates in cooling TBH_2Pc or H_2Pc matrices to 4.2K, we prepared both samples (H_2Pc and TBH_2Pc) in the same way. Thus a controlled, very slow freezing rate would yield better Shpol'skii matrices of TBH_2Pc in C_{16}.

A further difference between the doublet emissions of TBH_2Pc and H_2Pc is that the intensity of H_2Pc in mixtures of α-ClN and C_8 is much larger than that of TBH_2Pc in C_{16}. This weak fluorescence will be discussed again later in section 3.3.

However, we suggest the following explanations for the observed intensity difference:

First, the larger TBH_2Pc molecule has more difficulty adjusting itself to the cage of C_{16} molecules than H_2Pc in the mixture of $\alpha-ClN$ and C_8 molecules. The relatively stronger background is due to emission from randomly situated molecules which weaken the Shpol'skii emission of the dominant site. Second, there may be a tighter guest-host (electron-phonon) coupling in the TBH_2Pc and C_{16} system than that in the H_2Pc with $\alpha-ClN$ and C_8 system. Phonon wings of prominent fluorescence bands appear at the lower energy side of this transition but are masked by emissions from other sites and other 0-1 transitions. Third and most importantly, we expect the vibrational relaxation and internal conversion rates in TBH_2Pc to be greater than those in H_2Pc.

Other differences between the doublet of TBH_2Pc and H_2Pc exist, such as for H_2Pc in $\alpha-ClN + C_8$ the $S_1^{(1)}$ peak is wider than $S_1^{(2)}$ (3.3 cm^{-1} to 2.4 cm^{-1}), but the $S_1^{(1)}$ peak is narrower than $S_1^{(2)}$ (4 to 5 cm^{-1}) for TBH_2Pc in C_{16}; and also, comparing Fig.6 with Fig.7f, the higher energy emission is usually less populated in H_2Pc, but the doublet emissions are almost equally populated in TBH_2Pc. These differences are caused mainly by the different exciting laser wavelengths and by the more complex vibrational level structures in the TBH_2Pc molecule.

3.2.2   0-0 Transitions of TBH_2Pc in C_{12}, C_9 and C_{18}

TBH_2Pc formed good Shpol'skii matrices with C_9, C_{12} and C_{18} as well [see Fig.7; b), d) and h)]. The results for TBH_2Pc in C_{12} have some similarities with those in C_{16}. The doublet emissions of TBH_2Pc occur at 14429 and 14417 cm^{-1} as $S_1^{(1)}$ and $S_1^{(2)}$ respectively, with a split of 12 cm^{-1} (compared to 21 cm^{-1} in C_{16}). The fwhm of the doublet are 5.5 cm^{-1} and 5 cm^{-1} individually. Two very strong excitation-fluorescence bands were also found at 15295 cm^{-1} and 15263 cm^{-1}. Using our previous arguments, we assign them as $S_2^{(1)}$ and $S_2^{(2)}$. Like TBH_2Pc in C_{16}, the doublet in C_{12} is relatively stable and the cooling rate has little effect on the doublet(see Fig.8b). The fluorescence intensity of TBH_2Pc in C_{12} is weaker than that in C_{16} and there are somewhat larger background emissions. This means greater phonon-electron interaction and a worse Shpol'skii matrix in C_{12} than that in C_{16}. The characteristics of TBH_2Pc in C_{12} were not studied in as much detail as TBH_2Pc in C_{16}.

On the other hand, TBH_2Pc in C_{18} was studied in as much detail as in C_{16}. The 0-0 doublet of the $S_1^{(1)}$ and $S_1^{(2)}$ emissions is located at 14437 cm^{-1} and 14337 cm^{-1}. However the data of TBH_2Pc in C_{18} show some differences with those in C_{16}. The 0-0 doublet fluorescence (position and intensity) is very sensitive to sample preparation and mostly depends on the freezing rate as well as on the solute concentration. With different sample preparations, the position of the doublet has ± 5 cm^{-1} uncertainty and sometimes the doublet is totally

undistinguishable (-that problem may have arisen from the difficulty of controlling the cooling process because C_{18} is a solid at room temperature. Immersion of the sample cell in a hot water bath and cooling slowly would improve the result-). The doublet shown in Fig.7h is among the best we obtained. The doublet here is 100 cm^{-1} apart which is almost 5 times the split in C_{16} and shows clearly the difference between the Shpol'skii matrix formation of TBH_2Pc in C_{16} and in C_{18}. The intensity of the $S_1^{(1)}$ and $S_1^{(2)}$ doublet emission in C_{18} is much weaker than in C_{16}. As a result the fluorescence of TBH_2Pc in C_{18} was more difficult to detect. The two higher electronic states $S_2^{(1)}$ and $S_2^{(2)}$ occurred in C_{18} at 15296 and 15231 cm^{-1}, $i.e.$ $S_1^{(1)}+859$ cm^{-1} and $S_1^{(2)}+894$ cm^{-1}, with a split of 65 cm^{-1}.

TBH$_2$Pc in C_9 also shows a clear Shpol'skii effect with a 0-0 fluorescence as depicted in Fig.7b. As in C_{18}, the 0-0 doublet is very sensitive to sample preparation, especially to the freezing rate and other minor sites appear as well. The dominant 0-0 fluorescences were observed at 14447 cm^{-1} and 14321 cm^{-1}, with a split of 126 cm^{-1}. The two other higher electronic states $S_2^{(1)}$ and $S_2^{(2)}$ occur at 15304 and 15235 cm^{-1} with a split of 69 cm^{-1}. The results obtained for C_9 and C_{18} show some similarities such as their $S_1^{(1)}$ and $S_1^{(2)}$, $S_2^{(1)}$ and $S_2^{(2)}$ positions, splits etc. The reason may be that the chain length of C_9 is just half of that C_{18}. However, the fluorescence intensity of TBH_2Pc in C_9 is stronger than that in C_{18}. It is interesting to note that TBH_2Pc in C_8 doesn't show a good Shpol'skii effect as the chain length of C_8 is half that of C_{16}.

In summary, the two lowest electronic states of TBH_2Pc in four different Shpol'skii matrices are given in Table 3:

Table 3: Positions of lowest excited electronic states of TBH_2Pc in different Shpol'skii matrices

| | First excited electronic state ($S_1 = Q_x$) | | Second excited electronic state ($S_2 = Q_y$) | |
	$S_1{}^{(1)}$ cm^{-1}	$S_1{}^{(2)}$ cm^{-1}	$S_2{}^{(1)}$ cm^{-1}	$S_2{}^{(2)}$ cm^{-1}
C_9	14447	14321	15304	15235
C_{12}	14429	14417	15295	15263
C_{16}	14436	14415	15305	15264
C_{18}	14437	14337	15296	15231

3.3 Vibronic Transitions in Fluorescence Spectra

The fluorescence spectra of TBH_2Pc for a single site in the four different Shpol'skii solvents are shown in this section. They are characterized by very short vibronic progressions each of which consists of large number of 0-1 transitions and their intensities are much weaker than the corresponding 0-0 transitions (one order of magnitude smaller at least). This is further support that two electronic states are involved in the fluorescences observed. The two origins of the vibronic progressions are specially indicated in the fluorescence spectra. Because the overall fluorescence of TBH_2Pc is much weaker than that of H_2Pc, all fluorescences observed for

TBH$_2$Pc were assigned to 0-1 transitions and combinations and overtones were excluded.

TBH$_2$Pc in Shpol'skii matrices can generally be considered as systems of weak electron-phonon interaction. The vibronic spectra of such a system are characterized by a very strong 0-0, weak 0-1 and very weak 0-2 bands (if detectable). This agrees with our observation of short vibronic progressions as is evident in Figs.15, 18-20. Because of the very weak guest/host interaction in Shpol'skii matrices, the vibronic spectra of the TBH$_2$Pc guest molecules are characterized by sharp 0-0, 0-1 and 0-2 bands associated with the intramolecular transitions. The electronic and vibronic excitations in this case are localized.

The appearance of the fundamental vibrations in the fluorescence spectra at 4.2K can be analyzed via the following equation for the electric dipole transition between the ground state |K] |k> and the excited state |R] |r>[30].

$$M = m_{KR}(Q_0) <k \mid r> + \sum_{T \neq R} \sum_{v} m^{KT}(Q_0) h_{RT}(Q_0) <k \mid Q_v \mid r> \qquad (1)$$

where

$$m_{KR}(Q_0) = [K^{(0)} \mid er \mid R^{(0)}] \qquad (2)$$

is the electronic transition moment evaluated at the equilibrium position of the vth normal coordinate and

$$h_{RT}(Q_0) = \frac{[R^{(0)} \mid \{\partial H_{ev}/\partial Q_v\}_0 \mid T^{(0)}]}{E_{\mid T^{(0)} \mid \mid 0>} - E_{\mid R^{(0)} \mid \mid 0>}} \qquad (3)$$

45

In equations (1)-(3), H_{ev} stands for the interaction Hamiltonian between the electronic and vibrational motions, Q_v for the normal coordinate of the vth mode, and Q_0 for the equilibrium value of the normal coordinate. $|r>$ is defined as $|0,0,0,r_v,0,0,......>$ in which the vth normal mode of $|R(0)]$ is excited to the rth level, whereas all the other modes are unexcited. Furthermore, the factor $|h_{RT}(Q_0)]<k|Q_v|r>$ in Eqn.(1) determines the extent of the vibronic mixing between the zeroth order electronic state $|T(0)]|0>$ and $|R(0)]|0>$.

Vibrational relaxation of TBH$_2$Pc is fast because the Shpol'skii matrices act as heat sinks and it can be assumed therefore that at 4.2K most of the excited state population relaxes down to the vibrationless level $|R]|0>$ before fluorescence takes place, where $|0>=|0,0,0,.....>$ denotes the state in which none of the normal modes are excited. The intensity for the 0-0 transition is then derived mostly from the first term in Eqn.(1) when k=0. It is very large for the Pc's, including TBH$_2$Pc because the first term in Eqn.(1) is strongly electric dipole allowed and because $<0|0> >> <k|0>$ where k = 1, 2, 3, ... Note that $|R(0)]$ in Eqn.(2) stands for the electronic states which are S$_1$ (^{1}B$_{3u}$) and S$_2$ (^{1}B$_{2u}$) in TBH$_2$Pc. The vibronic intensities observed in our fluorescence spectra for the cases where k=1, 2,... and r=0 in Eqn. (1) arise from constributions, the nonvanishing Franck-Condon integrals $<k|r>$ in the first term. If one assumes for simplicity that molecular symmetry in the ground and the first excited states are identical, then the Franck-Condon integrals can be nonzero if

$\langle k|$ is totally symmetric as $|0\rangle$ is. While a detailed analysis of every fundamental's symmetry and their specific vibronic intensities are quite beyond the scope of this thesis, we wish to point out that it is generally accepted that the strongest transitions belongs to totally symmetric vibrations $a_g (D_{2h})$.

Because of the very fast inter- and intramolecular relaxation processes in our systems it is possible to use a very simple model to describe their excitation and subsequent deexcitations as sketched in Fig.14a, where the jagged arrow denotes radiationless decay. We will now discuss some of the details of the fluorescence spectra of TBH$_2$Pc in the Shpol'skii matrices studied.

3.3.1. Fluorescence of TBH$_2$Pc in C$_{16}$

The fluorescence spectrum of TBH$_2$Pc in C$_{16}$ at 4.2K is shown in Fig.15 (excitation at $15305cm^{-1}$) and all recognizable vibrations of the ground states are labeled and also given in table 4. We see that the vibronic spectra are well resolved. Fig.16 depicts the same fluorescence spectrum at 77K. It is clear that most spectral details obtained at 4.2K in Fig.15 have now disappeared or can not be distinguished at 77K which implies much randomisation has occurred in the matrix sites. The data show fundamental progressions of both tautomeric ground states. Identifiable vibrations are individually labeled: those associated with $S^{(1)}$ are begun with a '*' sign and those with $S^{(2)}$ are not. Only 21 fundamentals are found in contrast to the

47

a)

S$_1$

Pumping

Spectrometer
Scanning

Vibrational levels
of ground electronic state

S$_0$

b)

Laser
scanning

Vibrational levels in the
first excited
electronic state.

S$_1$

Monitoring

S$_0$
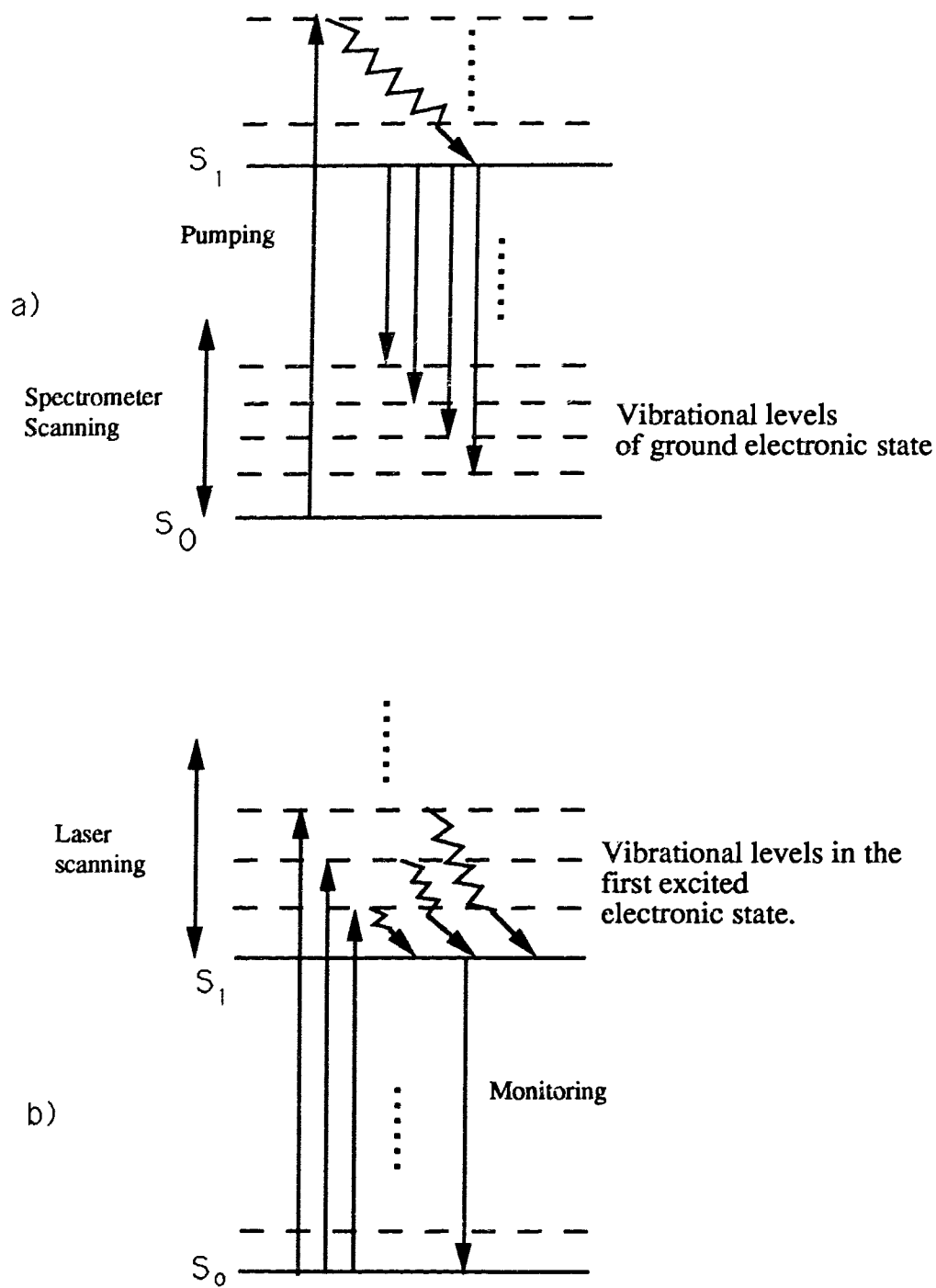
Fig.14 Basic level schemes for a) fluorescence spectra;
b) for fluorescence excitation spectra.

Fig. 15 Fluorescence spectra of TBH$_2$Pc in C$_{16}$ at 4.2K (x 5 means the data are multiplied by 5). The two origins are at 14436 cm^{-1} (S$_1^{(1)}$) and 14415 cm^{-1} (S$_1^{(2)}$).
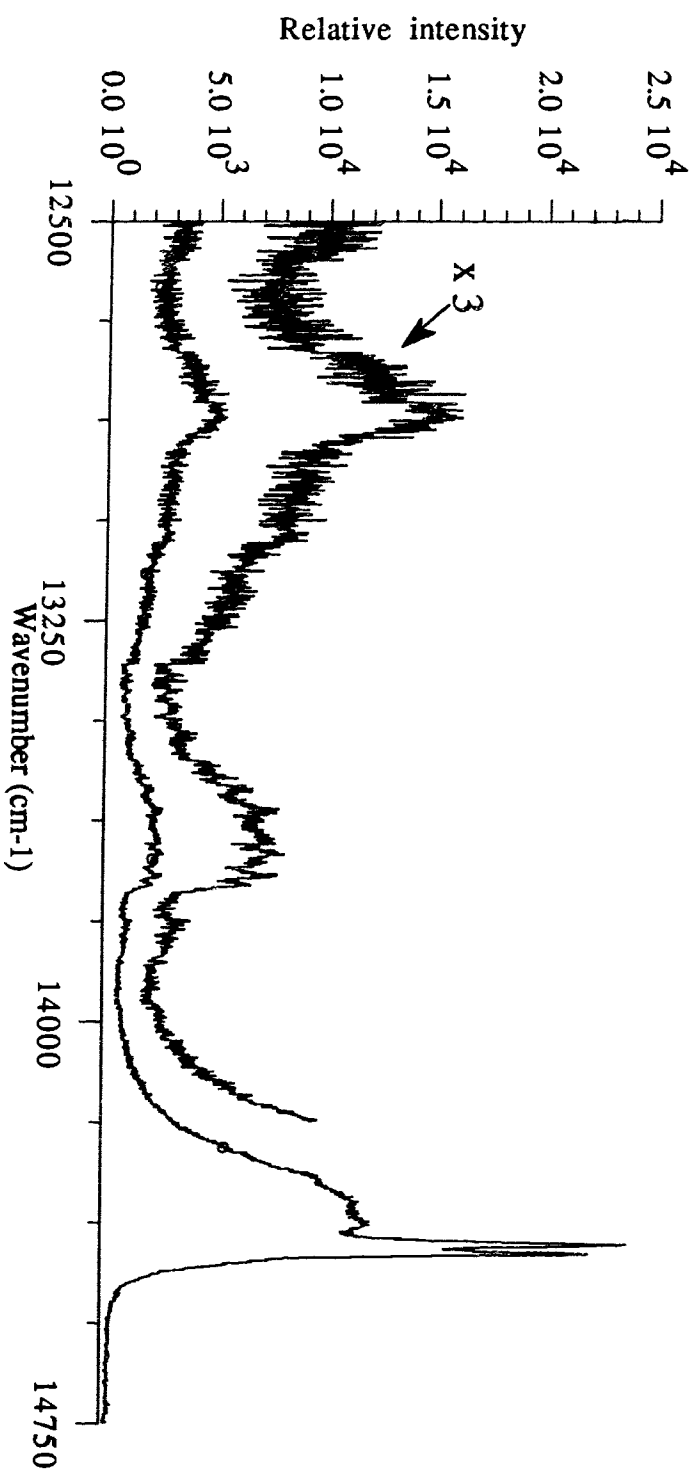
Fig. 1c Fluorescence of TBH_2Pc in C_{16}, ν_{exc} =15305 cm^{-1}, at 77K. Note, most of the 0-1 transitions are indistinguishable. x 3 means the data is amplified 3 times.

55 fundamentals observed in H_2Pc[10]. The reasons why the fluorescence intensity of TBH_2Pc is much weaker than that of H_2Pc have been discussed in section 3.2.1. Fluorescence excited by other frequencies, i.e. $\upsilon_{exc}=15264$ cm^{-1}, $\upsilon_{exc}=14436$ cm^{-1} etc. were also recorded; they gave the same results except that the spectra were not as good as that by excitation with 15305 cm^{-1}.

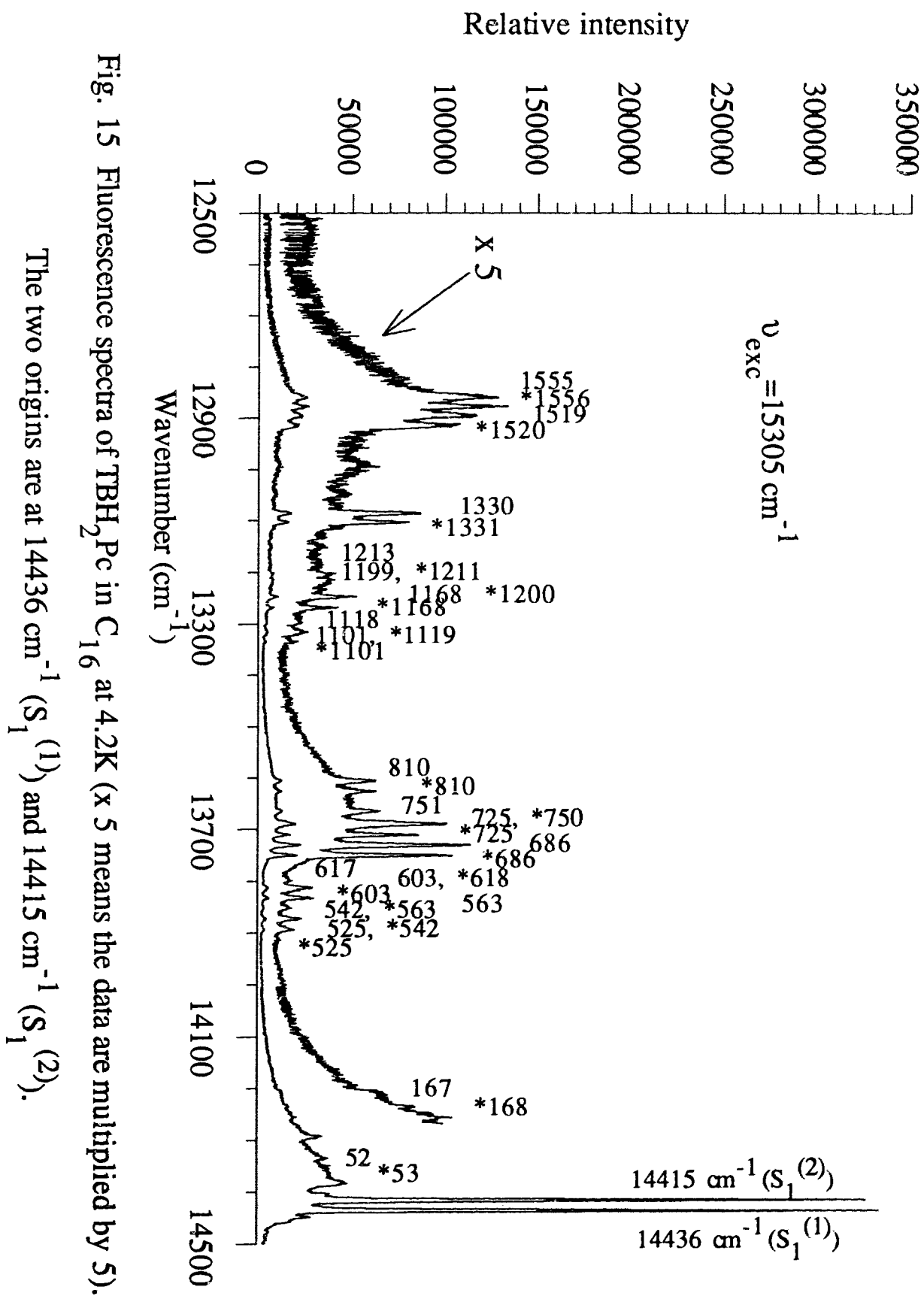The assignment of the fluorescence spectra are done as follows: Because excitation with 15305 cm^{-1} goes into the $S_2^{(1)}$ state, both $S_1^{(1)}$ and $S_1^{(2)}$ are pumped. When the spectrometer scans the region below S_1 states the fluorescence spectra should contain the vibronic bands of both tautomers. They appear in pairs with a separation of $S_1^{(1)}-S_1^{(2)}=21$ cm^{-1} and each pair shown has approximately equal intensity when the excitation is into high electronic states. Using this as a guideline we can eliminate some of the peaks originating elsewhere (such as impurities).

We searched also for 0-1 fluorescence from the origins of $S_2^{(1)}$ and $S_2^{(2)}$ on excitation by 15305 cm^{-1}. A number of very weak vibronic bands were found which corresponded to transitions ending at 686(#10 (number in Table 4)), 725(#11), 751(#12) and 810(#13) fundamentals of $S_0^{(1)}$. Similar results were obtained for excitation with 15264 cm^{-1}. These vibronic bands were independently observed for the origins of S_1 as the strongest in the entire 0-1 fluorescence region (Fig.17b). Fig.17a shows three of the very weak 0-1 fluorescences resulting from $S_2^{(2)}$ excitation. Fig 17b displays the equivalent region where S_1

Table 4 Vibrational energies (cm^{-1}) in the ground states of TBH_2Pc

In C_{16} / In C_{18}

#	14436 cm^{-1}	14415 cm^{-1}	14437 cm^{-1}	14337 cm^{-1}
1	54 sm	53 m		
2	82 sm	83 sm		
3	104 sm	106 sm		
4	168 w	167 w		
5	525 m	525 sm		
6	541 m	543 m		
7	562 m	563 m		
8	602 m	604 m		
9	616 m	617 w		
10	686 s	686 s	687 sm	687 m
11	725 s	725 s	725 sm	726 m
12	750 s	751 m		
13	810 m	811 m		
14	1101 w	1101 sm		
15	1118 sm	1119 sm		
16	1168 m	1169 m		
17	1198 sm	1200 w		
18	1211 sm	1213 sm		
19	1331 s	1231 s	1332 m	1334 m
20	1520 s	1519 s	1519 m	1521 m
21	1555 s	1556 s	1557 m	1555 s

In C_{12} / In C_9

#	14429 cm^{-1}	14417 cm^{-1}	14447 cm^{-1}	14321 cm^{-1}
1	60 s	58 s	53 s	53 m
2	172 sm	171 m		
3	593 w	593 w	603 vw	600 sm
4	629 w	628 sm		
5	668 w	667 sm		
6	688 m	689 s	687 m	687 m
7	701 s	703 sm		
8	715 sm	715 m		
9	727 m	726 sm	727 sm	726 m
10			750 sm	760 w
11	813 vw?	812 vw?	814 m	809 w
12	870 vw?	869 vw?		
13			998 w	1003 vw
14	1097 vw?	1099 vw?		

15	1174 w	1175 sm	1170 vw?	1175 vw?
16	1330 w	1331 m	1333 sm	1334 w
17	1343 m	1345 sm		
18	1554 s	1552 s	1553 sm	1555 vw

Note: s=strong, m=medium, sm=small, w=weak and vw=very weak
      ?=not sure

states end at some vibrations of S_0. Spectra like that of Fig.17a) should have the same information about the ground fundamentals as those presented in Fig.17b) have. However, due to their weakness, far fewer vibronic bands were observed. Nevertheless, Fig.17a is important to identify $S_2^{(2)}$ ($15264 cm^{-1}$) as the origin of the next higher excited electronic state.

Comparing the fluorescence spectra of TBH_2Pc in C_{16} with H_2Pc in C_8, it is found the number of vibronic bands in TBH_2Pc is much less than that appeared in H_2Pc and basically the position and intensity of vibrational bands of the two molecules differ from each other. However, four of the most strongest 0-1 fluorescence of H_2Pc in C_8 coincide with those of TBH_2Pc in C_{16} both in vibrational shift and intensity. They are 686 (#10), 725 (#11), 1520 (#20) and 1555 (#21) for $S^{(1)}$; and 686 (#10), 725 (#11), 1519 (#20) and 1556 (#21) for $S^{(2)}$, respectively. These indicate that in TBH_2Pc the tertiary butyl groups perturb the π-electron system and modify the vibrational modes of the molecule. Only a few strongest bands in H_2Pc which are totally symmetric transitions are not affected.

$\upsilon_{exc}=15264 \text{ cm}^{-1}$

749

724

685

Relative intensity

Wavenumber (cm^{-1})
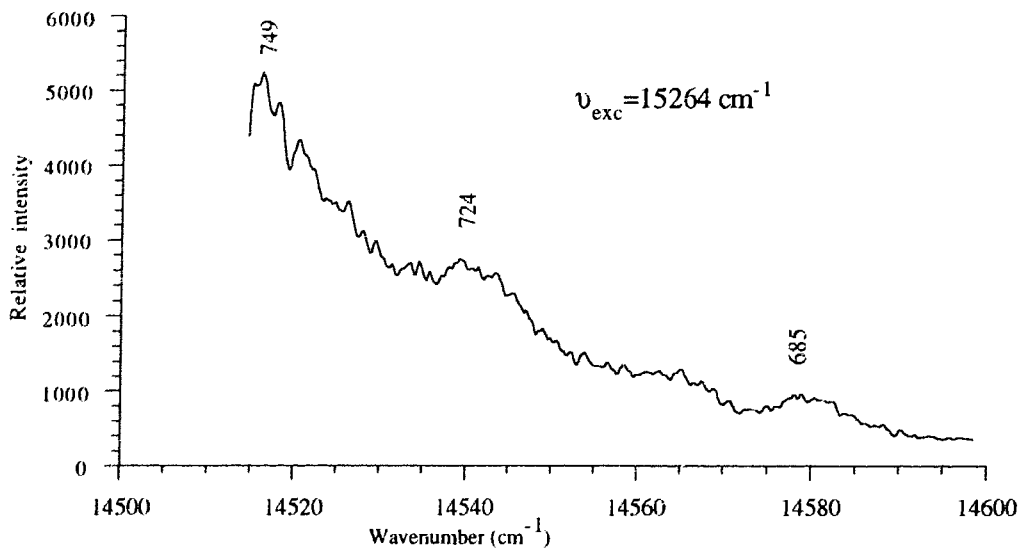
Fig. 17, (a) Direct fluorescence from $S_2^{(2)}$.

810

*810

751

*750, 725

*725

686

*686

$\upsilon_{exc}=15264 \text{ cm}^{-1}$

Relative intensity

Wavenumber (cm^{-1})
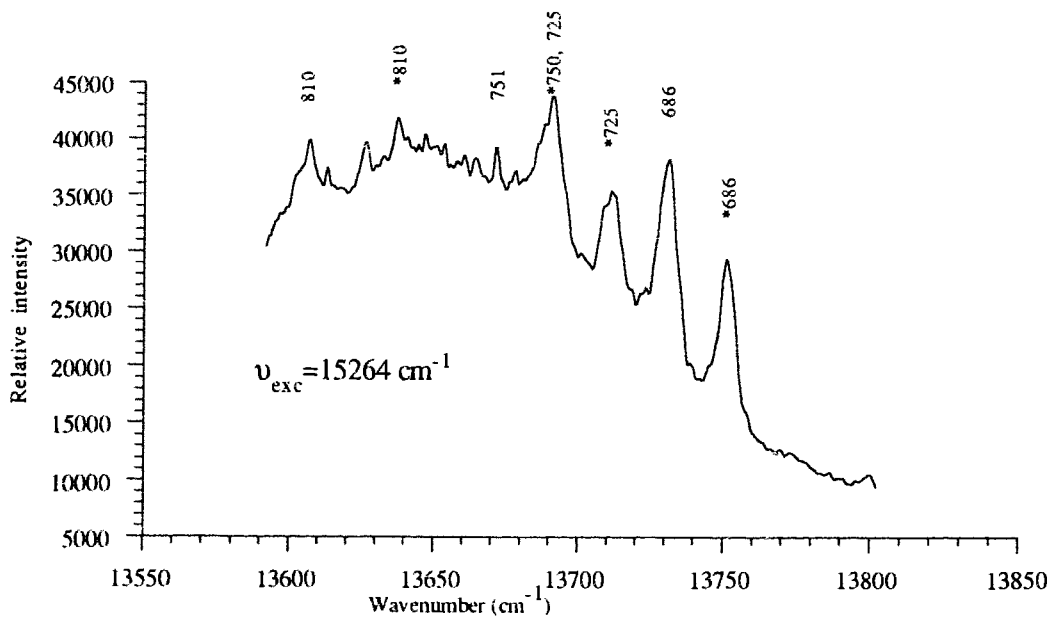
Fig. 17, (b) Fluorescence from $S_1^{(2)}$.

3.3.2. Fluorescences of TBH$_2$Pc in C$_9$, C$_{12}$ and C$_{18}$

The fluorescence spectra of TBH$_2$Pc in C$_9$, C$_{12}$ and C$_{18}$ are given in Figs.18-20, which had excitation of 15305 cm^{-1}, 15300 cm^{-1} and 15143 cm^{-1} respectively. The recognizable peaks are assigned and presented in Table 4. Because the fluorescence intensities are further reduced (worse Shpol'skii effects) the number of recognizable vibronic bands are fewer than in C$_{16}$. We can see that most of the bands' positions and intensities observed in C$_9$, C$_{12}$ and C$_{18}$ are consistent with what was discussed for C$_{16}$ matrices which comfirms the accuracy of the positions for the vibronic transitions observed. On the other hand, their peak resolution is worse than that in C$_{16}$.

3.4 Fluorescence-Excitation Spectra

Fluorescence-excitation spectra provide equivalent information to absorption spectra. A explanation diagram of fluorescence-excitation spectra is shown in Fig.14b. In fact, these transitions measure the vibronic bands belonging to the first excited electronic state. After electronic excitation into a higher vibronic level of S$_1$ the molecule relaxes rapidly into the vibrationless level of that state and may return to the ground state by fluorescence. If one monitors the intensity of this S$_1$-S$_0$ (0-0) fluorescence while scanning the laser over the region of the vibronic levels of the first excited electronic
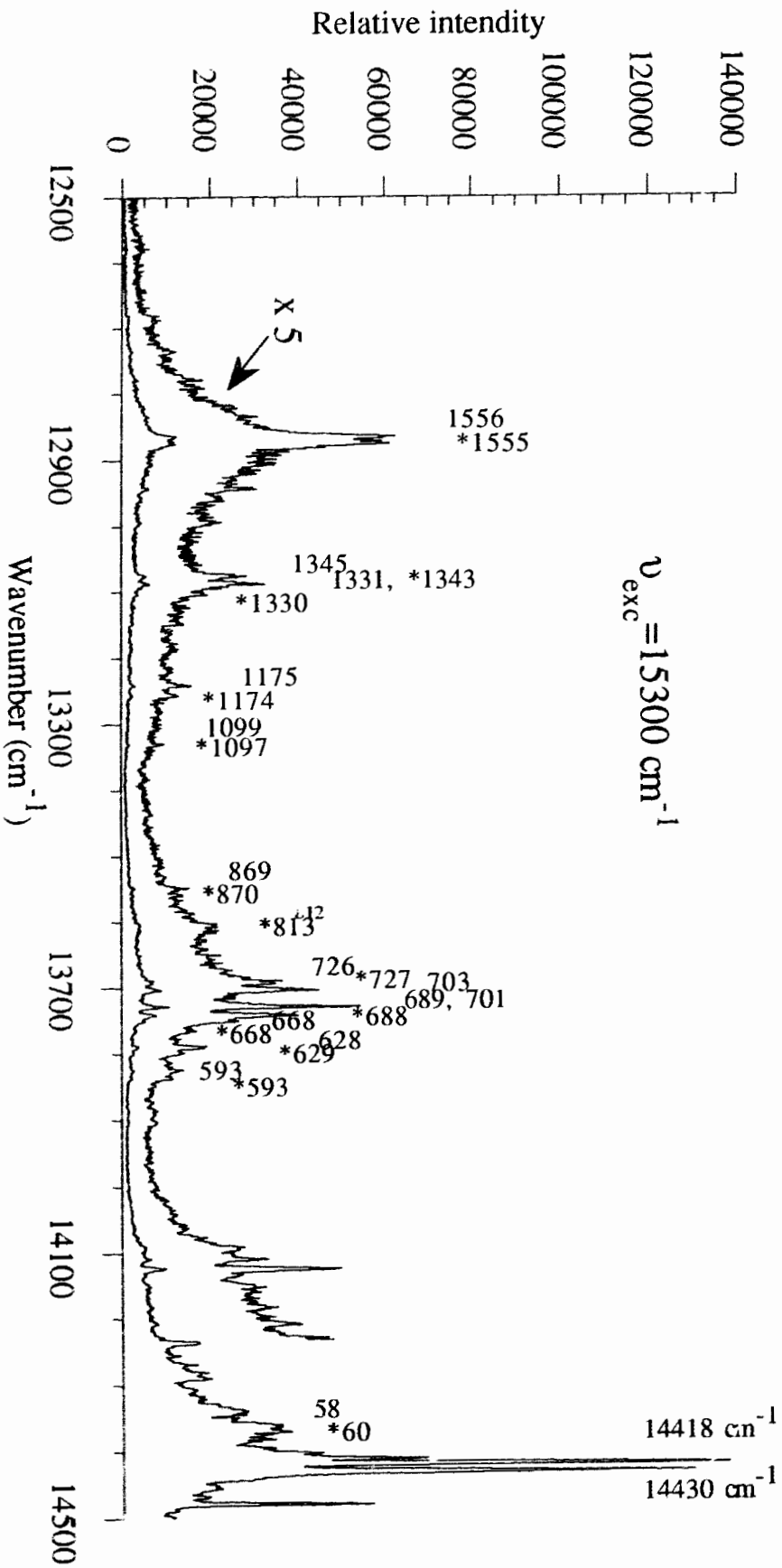
Fig. 18 Fluorescence spectra of TBH$_2$Pc in C$_{12}$ at 4.2K. The graph with label x 5 is enlarged by 5. Two origins are at 14430 cm^{-1} and 14418 cm^{-1}.
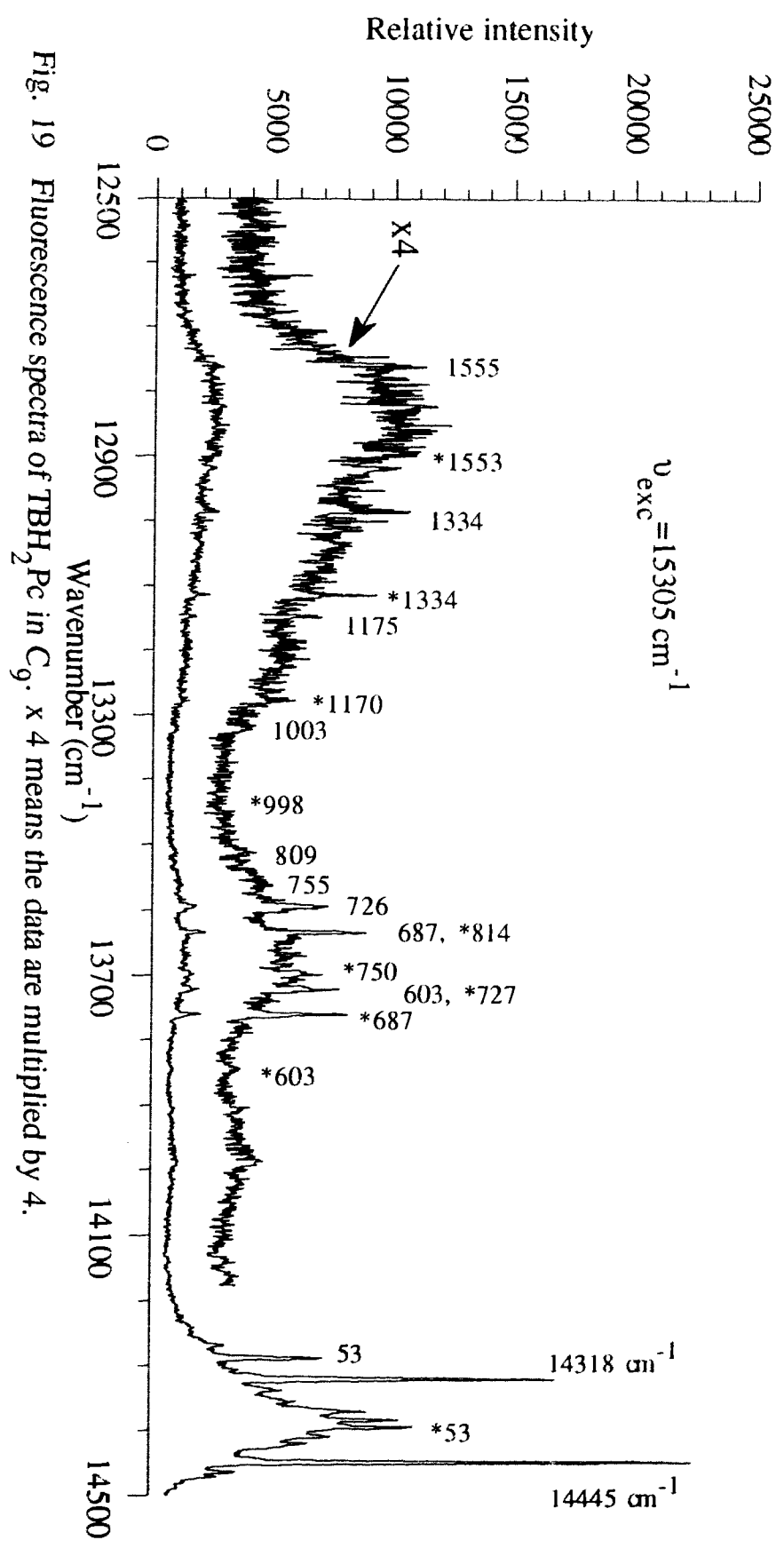
56

Fig. 19 Fluorescence spectra of TBH$_2$Pc in C$_9$. x 4 means the data are multiplied by 4.

Two origins are at 14445 cm^{-1} and 14318 cm^{-1}.
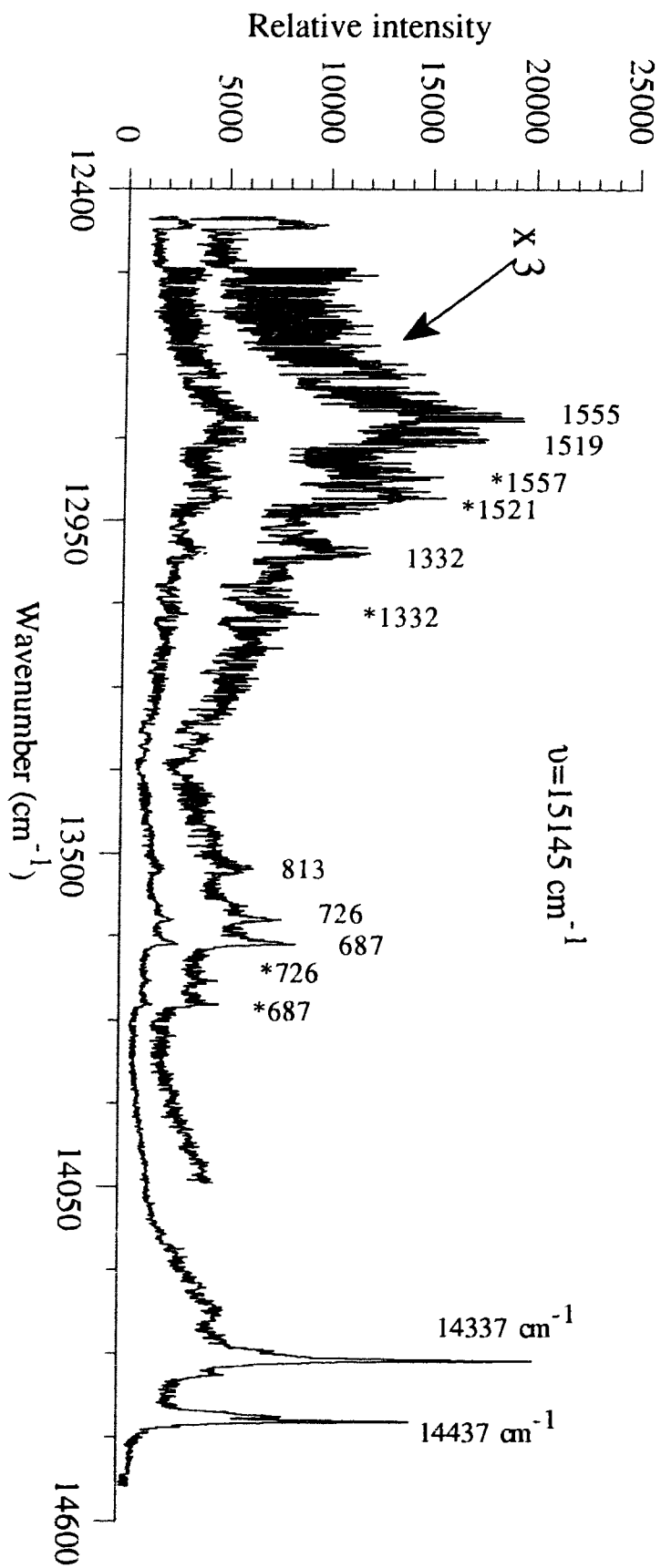
Fig. 20 Fluorescence of TBH$_2$Pc in C$_{18}$ with excitation of υ=15145 cm^{-1}. x 3 indicates the data are multiplied by 3. Two origins are at 14437 cm^{-1} and 14337 cm^{-1}.

x 3

υ=15145 cm^{-1}

1555
1519
*1557
*1521
1332
*1332
813
726
687
*726
*687

14337 cm^{-1}
14437 cm^{-1}

Relative intensity

25000
20000
15000
10000
5000
0

Wavenumber (cm^{-1})

12400
12950
13500
14050
14600

state and measuring the laser wavelength at the same time, one obtains the fluorescence-excitation spectrum. The fluorescence intensity at the peak positions corresponds to the intensity of the vibronic bands. Two assumptions are involved in this simple model. One, that always the same number of electrons are pumped and two, that always the same ratio of electrons excited to this level will relax rapidly to the zero level of the first excited electronic state.

The fluorescence-excitation spectra of TBH$_2$Pc in several good Shpol'skii matrices are presented in this section. Generally we found that in comparison with the fluorescence spectra discussed in the last section the fluorescence excitation spectra are richer in structure and higher in intensity. As well, there is no mirror symmetry between them. The asymmetries between fluorescence and fluorescence-excitation can be attributed to interference between two intensity contributing factors in the transition moment of Eq.(1): the Franck-Condon and Herzberg-Teller integrals. For non-totally symmetric vibronic transitions the intensities of excitation and fluorescence appear to be comparable as the Herzberg-Teller integral usually dominates (due to a vanishing or very small Franck-Condon term) and there is no serious interference between the two factors. On the other hand, for totally symmetric vibronics the Franck-Condon term is non-vanishing and interferes with the Herzberg-Teller term in the transition moment. The observed stronger 0-1 absorptions result from constructive interferences, whereas weaker fluorescences are attributed to

destructive interference. Although this non-Condon effect accounts for the general asymmetric character in the 0-1 transitions of excitation and fluorescence, some other factors such as the Duschinskii effect[31] and Fermi resonance[34] may also play a role.

The fluorescence-excitation spectra obtained deviate markedly from the mirror images of their fluorescences and show greatly increased peak numbers which appear formidable to assign. However, analysis gives basically two short vibronic progressions along with a number of possible transition bands. Assignment of a specific transition to the appropriate progression is facilitated by the observation that many vibronic bands of $S_1^{(1)}$ show up stronger than those of $S_1^{(2)}$ when fluorescence from the vibrationless level of $S_1^{(1)}$ is monitored and vice-versa. We found this a valuable tool to assist us in our assignments.

It is obvious from the observation of two vibronic progressions in the fluorescence-excitation spectra that fluorescence can arise from the vibrationless levels of the higher lying states as the vibronic levels of the lower lying ones are excited. Relaxation between the two vibrationless (fluorescing) levels, separated by several tens of cm^{-1}, is expected to be slow at 4.2K and we conclude therefore that the population of the initially prepared vibronic state does not relax solely down to the vibrationless level of the same state, but instead ends up to some extent on the vibrationless level of the tautomeric state.

The fluorescence-excitation spectra of TBH_2Pc shown in this section are further complicated by the existence of two higher tautomeric electronic states $S_2^{(1)}$ and $S_2^{(2)}$. These two higher electronic states together with their vibronic levels interact with the vibronic levels belonging to $S_1^{(1)}$ and $S_1^{(2)}$, which complicated the assignment of spectra even further.

The method used to assign the fluorescence-excitation spectra is as follows. First, the position of each peak relative to $S_1^{(1)}$ (or $S_1^{(2)}$) was calculated from the spectra monitored at $S_1^{(1)}$ (or $S_1^{(2)}$). Then the peak positions of another progression monitored at $S_1^{(2)}$ (or $S_1^{(1)}$) were found. Second, the positions of the two progressions were compared with each other and the positions of same or almost same pairs from two progressions were picked out. These pairs were assigned as basic vibronic bands belonging to $S_1^{(1)}$ or $S_1^{(2)}$ because, in general, the vibrational levels of $S_1^{(1)}$ should agree with those of $S_1^{(2)}$ except for some relative intensity differences (peak heights). So that if we move the vibronic progression of $S_1^{(2)}$ to the $S_1^{(1)}$, the two vibronic progressions should coincide. On the other hand, such coincidence of the two vibronic progressions confirms the validity of our interpretation of the spectra. Third, as regards the assignment of the remaining transitions, all additional information known about the spectral behavior of our system had to be considered. We shall now describe in some detail the assignment of the vibronic bands of TBH_2Pc in the different solvent matrices studied.

3.4.1. Fluorescence-Excitation Spectra of TBH2Pc in C16

The fluorescence-excitation spectra in C_{16} were obtained by monitoring the intensities of 14436 cm^{-1} ($S_1^{(1)}$) (Fig.21a; 1 to 3) and 14415 cm^{-1} ($S_1^{(2)}$) (Fig. 21b; 1 to 3). It is evident that these spectra are much richer in structure and higher in intensities when compared to the fluorescence spectra. The spectra show the assigned vibronic bands and their intensities are listed in table 5. All spectra shown have been corrected for instrument response and laser power difference; their position uncertainty is ±2 cm^{-1}. Spectra obtained from the $S_1^{(1)}$ origin were all assigned to vibronic bands of $S_1^{(1)}$. But the spectra obtained from the $S_1^{(2)}$ origin were assigned to either vibronic bands of $S_1^{(2)}$ or those of $S_1^{(1)}$ because some of the vibronic bands in $S_1^{(1)}$ may also appear in this series through tunneling or vibronic coupling. Note that the spectra from the vibronic bands of $S_1^{(1)}$ are labeled with a star *. Some of the vibronics which appeared with the $S_1^{(1)}$ origin, *i.e.* #55, 1626, #56, 1650 *etc.* do not appear in the $S_1^{(2)}$ progression, but are included in table 5.

In fact, Fig.21; 1 to 3 show not only the progressions of $S_1^{(1)}$ and $S_1^{(2)}$ but also those of $S_2^{(1)}$ and $S_2^{(2)}$. Since the S_2 states observed in TBH2Pc are much stronger than most fundamentals of S_1 (this is not the case for H2Pc in C_8, see [10]), the fundamentals of S_2 are observable and have intensities comparable to those of S_1's. This causes many instances of band coalescence and structure masking as well as broadening in the
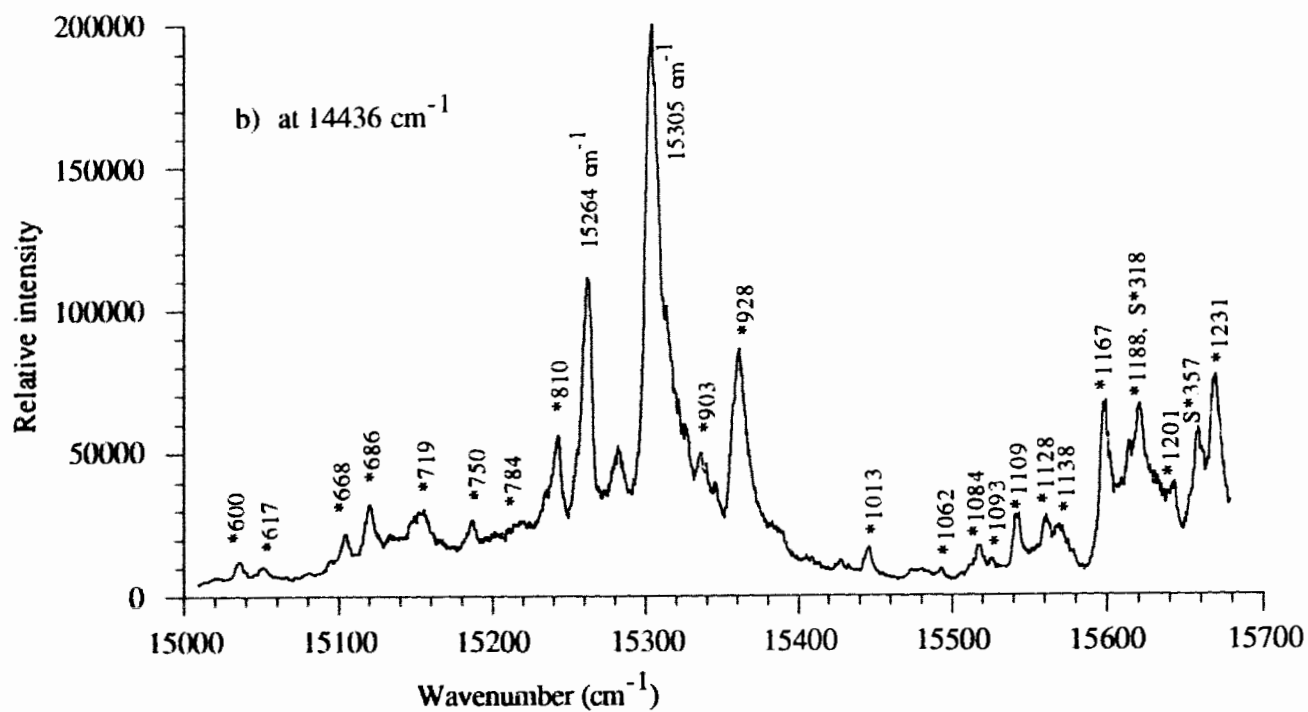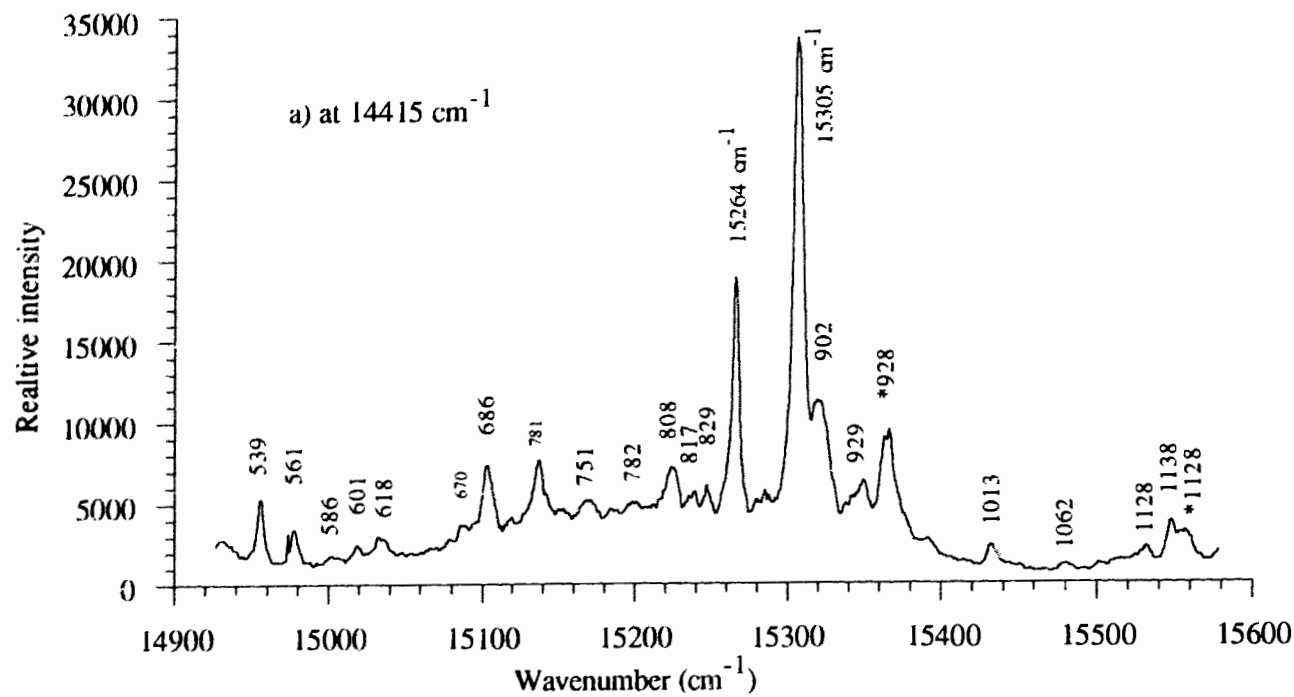
Fig. 21, (1) Fluorescence excitation spectra of TBH$_2$Pc in C$_{16}$; a) observed at 14415 cm^{-1}, b) at 14436 cm^{-1}. Note the label difference among levels of S$_1$ and S$_2$.

Fig. 21. (2) Fluorescence excitaton spectra of TBH$_2$Pc in C$_{16}$; a) observed at 14415 cm^{-1}, b) at 14436 cm^{-1}.

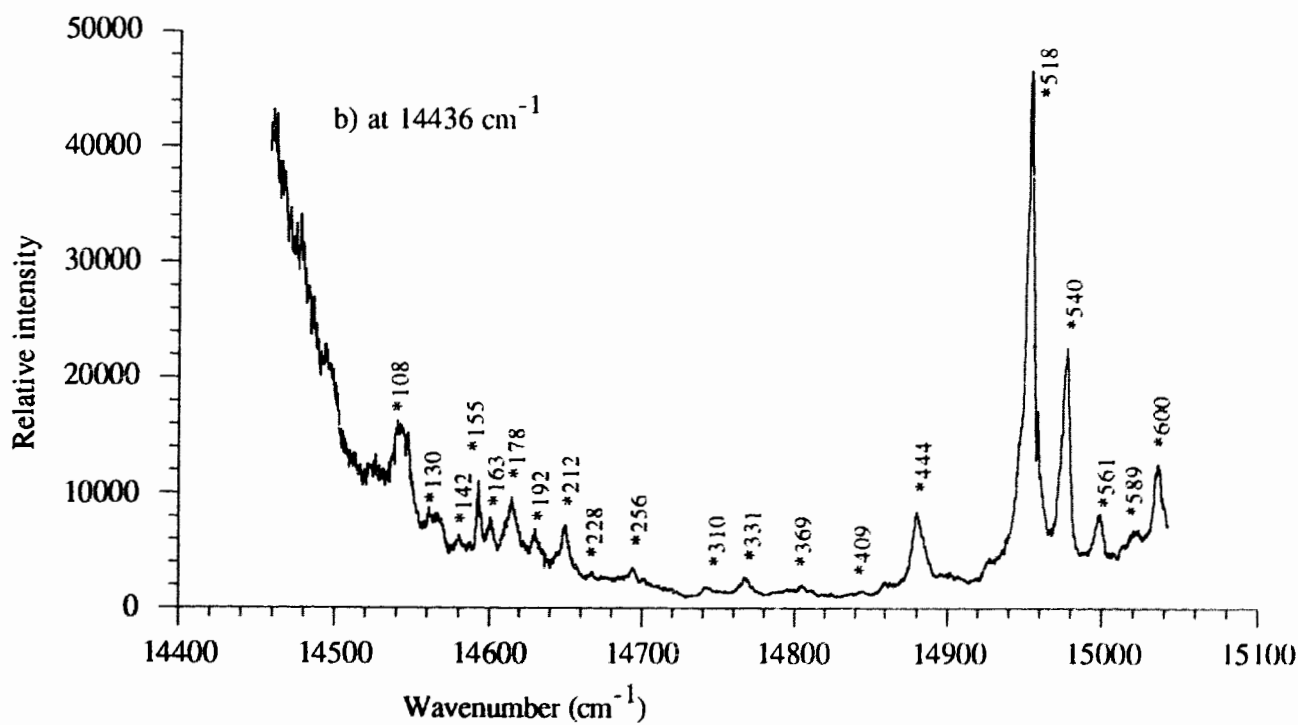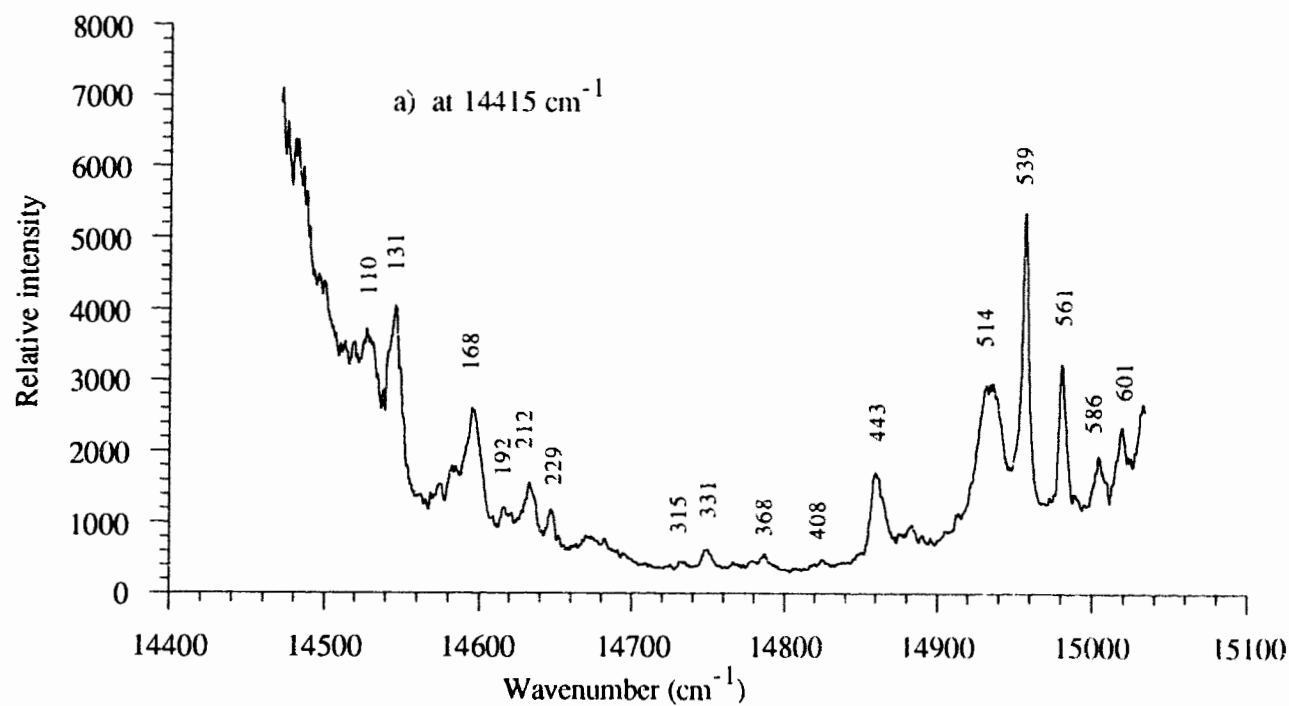The two S$_n$ states are at 15305 cm^{-1} and 15264 cm^{-1}.

64

Fig. 21, (3) Fluorescence excitation spectra of TBH$_2$Pc in C$_{16}$; a) observed at 14415 cm^{-1}, b) at 14436 cm^{-1}.

65

Table 5 Vibrational energies of the first excited states of TBH$_2$Pc in C$_{16}$, C$_{18}$, C$_{12}$ and C$_9$

	In C$_{16}$		In C$_{18}$	
	14436 cm^{-1}	14415 cm^{-1}	14437 cm^{-1}	14337 cm^{-1}
1	108 m	110 sm	111 w	111 sm
2	130 sm	131 m	127 w	128 m
3	142 w	143 vw		141 w
4	155 sm	155 vw		156 w
5	163 w	168 sm		
6	178 sm	178 sm	178 w	178 sm
7	192 w	195 w		
8	212 sm	212 sm		211 sm
9	228 vw	229 w		228 sm
10	256 w	256 w		248 w
11	310 w	315 vw		311 vw
12	331 w	331 w		334 vw
13	369 w	368 w	368 vw	368 w
14	409 vw	409 vw		
15	444 m	443 sm	445 sm	444 sm
16	518 s	514 m	516 m	516 sm
17	540 m	539 s	539 m	537 sm
18	561 sm	561 m	563 sm	562 sm
19	589 sm	586 sm		586 sm
20	600 sm	601 sm	600 sm	604 sm
21	617 w	618 sm	617 m	617 sm
22	669 sm	670 w		
23	685 m	686 s	685 m	685 sm
24	719 sm	718 s		718 sm
25	750 sm	751 sm	749 s	748 sm
26	784 w	782 w		780 sm
27	810 s	808 s	811 s	806 s
28	828 s	829 m	836 s	835 m
29	903 m	902 s	898 m	
30	928 s	929 s	923 m	931 m
31	1013 sm	1013 m	1011 m	1011 sm
32	1062 sm	1062 sm	1058 sm	1058 w
33	1084 sm	1084 w	1084 sm	1084 sm
34	1093 sm	1094 w	1093 w	1094 sm
35	1109 m	1110 w	1108 m	1112 sm
36	1128 m	1128 sm		1122 sh
37	1138 m	1138 m	1135 s	1137 sm
38	1167 s	1167 m	1165 s	1165 sm
39	1188 s	1188 sm	1181 m	1184 m
40	1201 sm	1201 sm	1191 m	1192 m
41	1231 s	1231 m	1231 m	1233 m
42	1258 m	1258 sm	1264 w	1262 m

43	1281 m	1281 m	1281 w	1279 m
44	1303 m	1303 w	1303 sm	1298 m
45	1334 m	1334 m	1335 s	1335 sm
46	1343 m	1345 m		1341 w
47	1366 sm	1366 m	1365 w	1365 vw
48	1403 m	1403 w		
49	1415 s	1415 m		
50	1436 s	1437 m	1434 s	1436 sm
51	1468 m	1469 m		1467 vw
52	1533 s	1535 sm	1535 m	1531 m
53	1557 m	1557 m		
54	1591 sm	1591 sm	1592 sm	1591 w
55	1626 sm			
56	1650 m			
57	1670 w			
58	1709 sm			
59	1728 sm			
60	1804 sm			
61	1823 sm	1823 w		
62	1851 sm	1851 w		

	In C_9		In C_{12}	
	14447 cm^{-1}	14321 cm^{-1}	14429 cm^{-1}	14417 cm^{-1}
1	129 w			
2	164 w			166 sm
3	182 w		172 sm	174 w
4	195 w		199 sm	187 vw
5			212 sm	212 sm
6	226 w		222 vw	228 vw
7		247 w		
8		256 w	257 vw	259 vw
9	309 w	309 w	309 w	314 w
10	324 w		332 w	330 w
11	370 sm	363 vw	372 w	
12	409 sm		401 w	403 w
13	443 sm	444 w	449 sm	444 sm
14		461 w		
15	518 sm	515 sm	514 m	515 m
16	539 sm	536 w	540 sm	534 sm
17	559 sm	560 sm	564 w	561 w
18	586 sm	584 sm	589 sm	592 sm
19	600 sm	600 w	603 vw	
20	618 sm	612 sm	616 sm	615 sm
21	669 w	670 sm	676 sm	670 sm
22	686 m	682 m	685 m	686 m
23	717 sm	719 sm	724 m	723 m
24	752 sm	748 sm	758 w	757 sm
25		788 s	784 sm	781 sm
26	808 s	807 sm	810 sm	805 s
27	827 s	824 m		820 sm

28	897	m	895	m	901	s	907	m
29	930	m	925	sm	928	s	931	m
30	1013	m	1016	sm	1014	m	1015	m
31	1059	sm			1057	vw	1064	sm
32	1092	sm	1093	w	1084	vw	1084	w
33	1110	m	1109	sm	1113	sm	1114	m
34	1128	m	1129	sh	1129	m	1132	m
35	1137	s	1136	m	1143	m	1143	m
36	1165	s	1163	m	1168	sm	1169	sm
37	1191	m	1191	w	1187	m	1187	sm
38	1200	m	1197	m	1199	m	1199	m
39	1232	m	1235	m	1231	m	1232	sm
40	1240	s			1250	m	1246	m
41					1258	m	1265	m
42	1279	m	1286	w	1290	m	1283	sm
43	1300	s	1308	m	1306	m	1301	s
44	1334	s	1340	sm	1339	m	1334	sm
45							1343	s
46	1341	s	1350	sm	1353	sm	1353	m
47	1364	s	1363	sm	1367	sm	1368	s
48	1389	m	1394	sm	1400	sh	1406	sh
49	1415	m	1415	m	1421	s	1420	s
50	1433	m	1436	s	1435	s	1432	s
51	1467	sm	1471	s	1464	sm	1465	sm
52	1531	w	1530	s	1537	s	1530	m
53	1557	vw	1556	s	1562	m	1552	sm
54			1572	s				
55	1587	w	1591	m	1593	m	1588	vw
56	1608	w	1612	m			1611	w
57	1621	vw	1628	sm	1627	w	1636	w
58	1658	vw	1651	s	1654	w		
59			1670	w				
60			1709	sm				
61			1738	sm				

Note: s=strong, m=medium, sm=small, w=weak, vw=very weak

energy region of 900 cm^{-1} above the S_1 states. Fig. 21 (1 to 3) show clearly that for excitation energy greater than 15600 cm^{-1} the peaks appear more diffuse and noisier. Since these spectra were reproducible we could conclude that the congestion was due to intramolecular state coupling between the vibronics belonging to the S_1 and S_2 states.

Direct observation of fluorescence excitations of $S_2^{(1)}$ and $S_2^{(2)}$ are also tried. One region of interest is shown in

Fig.22, while the remaining spectral region is flat with some fluctuations. The small humps in Fig.22 consists of the extremely weak 15989 cm^{-1} ($S_2^{(1)}$+684 cm^{-1}) and 15952 cm^{-1} ($S_2^{(2)}$+688 cm^{-1}) 0-1 transitions. Both are detected in S_1 as two of the strongest vibronics. This shows clearly that excited vibronic bands of S_2 will relax very rapidly to lowest states such as S_1 or other vibrational states. Thus in the region >900 cm^{-1} of the S_1 states in fluorescence-excitation, one can also obtain some information about the vibronics of the S_2 states and our results are listed in Table 6. The assignment method used was the same as discussed before. Note also that the notation in Fig.21-1 for transitions from $S_2^{(2)}$ start with 'S' and those from $S_2^{(1)}$ with 'S*'.

Table 6   Vibrational energies of the second excited electronic states of TBH$_2$Pc

	15305 cm^{-1} ($S_2^{(1)}$)		15264 cm^{-1} ($S_2^{(2)}$)	
1	319	m	319	m
2	342	m	340	m
3	357	m	356	m
4	412	s	412	s
5	498	w	500	w
6	547	m	549	w
7	682	m	683	m
8	695	m	694	m
9	723	w	723	w
10	759	w	758	w
11	781	m	782	m
12	841	w	840	w
13	1095	w	1094	w

Note: S=strong, m=medium, w=weak
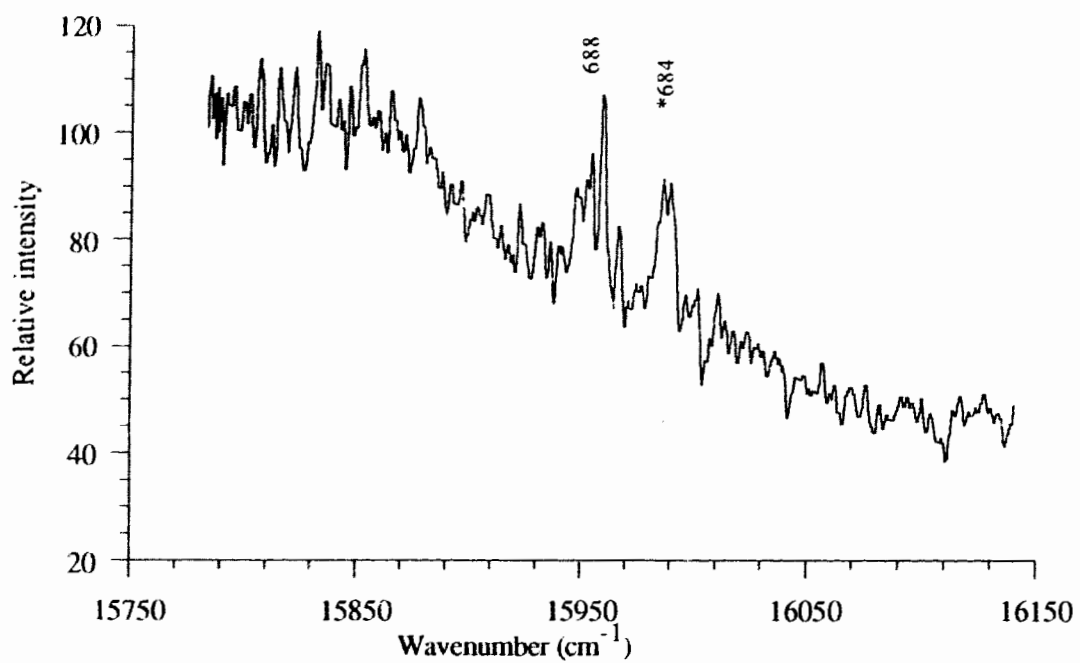
Fig. 22 Fluorescence excitation spectra from S_2 by monitoring at 15264 cm^{-1}.

3.4.2. Fluorescence-Excitation Spectra of TBH_2Pc in C_9, C_{12}, and C_{18}

The fluorescence-excitation spectra of TBH_2Pc in C_9, C_{12} and C_{18} are given in Figs.23-25. They were monitored at 14321 and 14447 cm^{-1} (for C_9), 14417 and 14429 cm^{-1} (for C_{12}), 14347 and 14437 cm^{-1} (for C_{18}) respectively. As was found for the spectra in C_{16}, when the fluorescence spectra are compared with the fluorescence-excitation spectra the latter are richer in structure, higher in intensity and do not possess mirror symmetry to their respective fluorescences. The assignments of the vibronic bands were done in the same way as discussed for C_{16} and are shown on the spectra as well as summarized in Table 5. In general we found fluorescence-excitation intensities in C_{18} weaker than those in C_{16}. We attribute this to less well-defined Shpol'skii matrices in C_{18} than in C_{16}, which also caused a diminished number of vibronics in C_{18} as compared to C_{16}. The results we got from fluorescence excitation spectra of TBH_2Pc in the C_{12} and C_9 matrices are in general consistent with those in C_{16} in position and intensity except for some small or weak peaks for which the vibronic band assignments are shown on the spectra and listed in Table 5.

Comparing the fluorescence excitation spectra of TBH_2Pc in C_{16} and H_2Pc in $\alpha-C1N+C_8$, we found that the vibrational levels of the first excited electronic states in the two
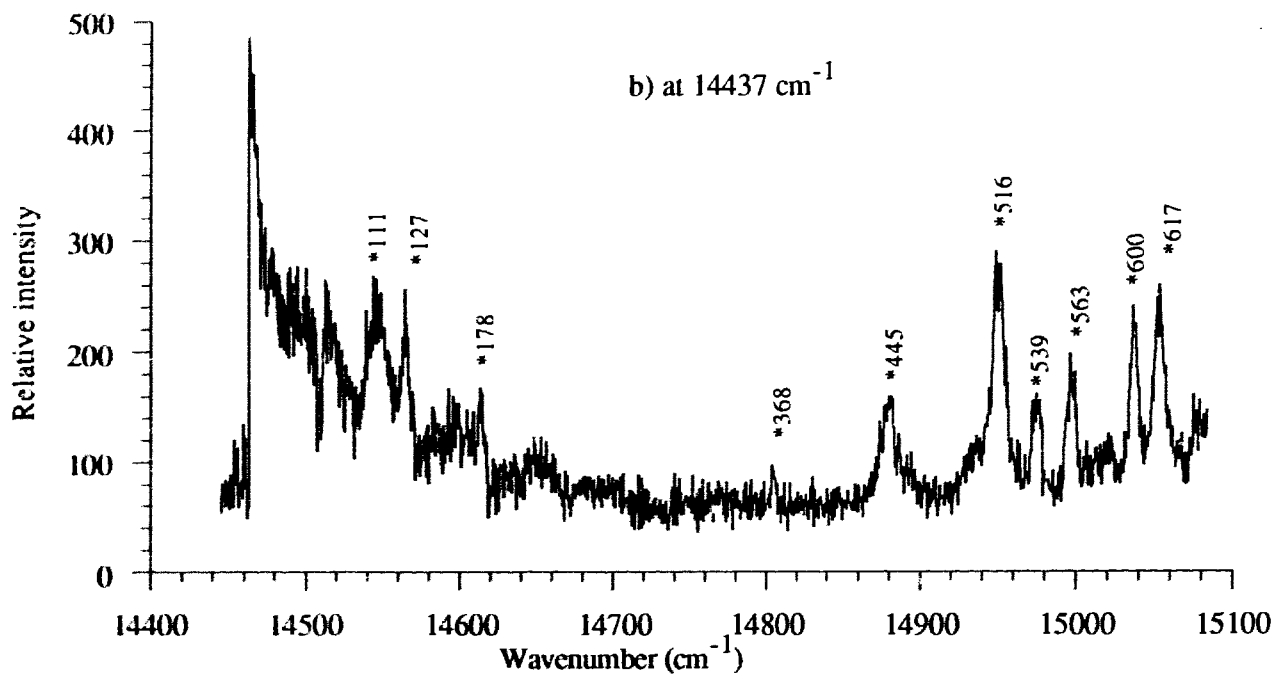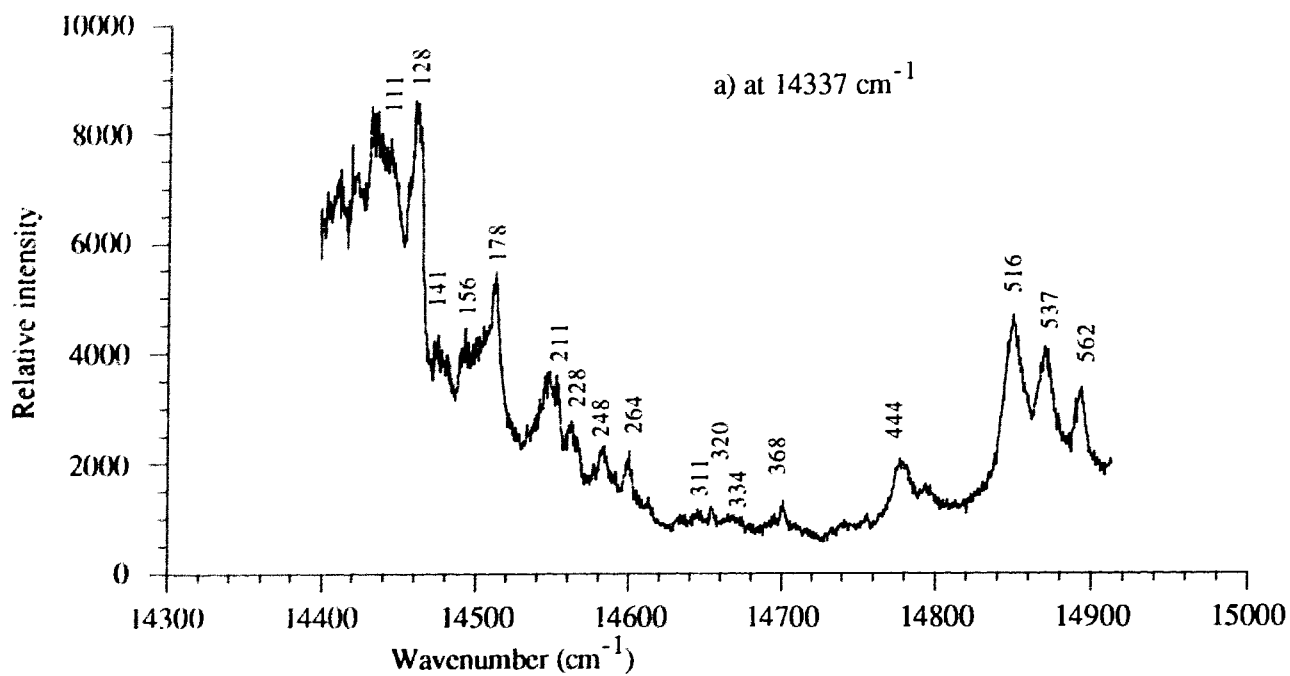
Fig. 23. (1) Fluorescence excitation of TBH$_2$Pc in C$_{18}$: a) monitored at 14337 cm^{-1}, b) at 14437 cm^{-1}.
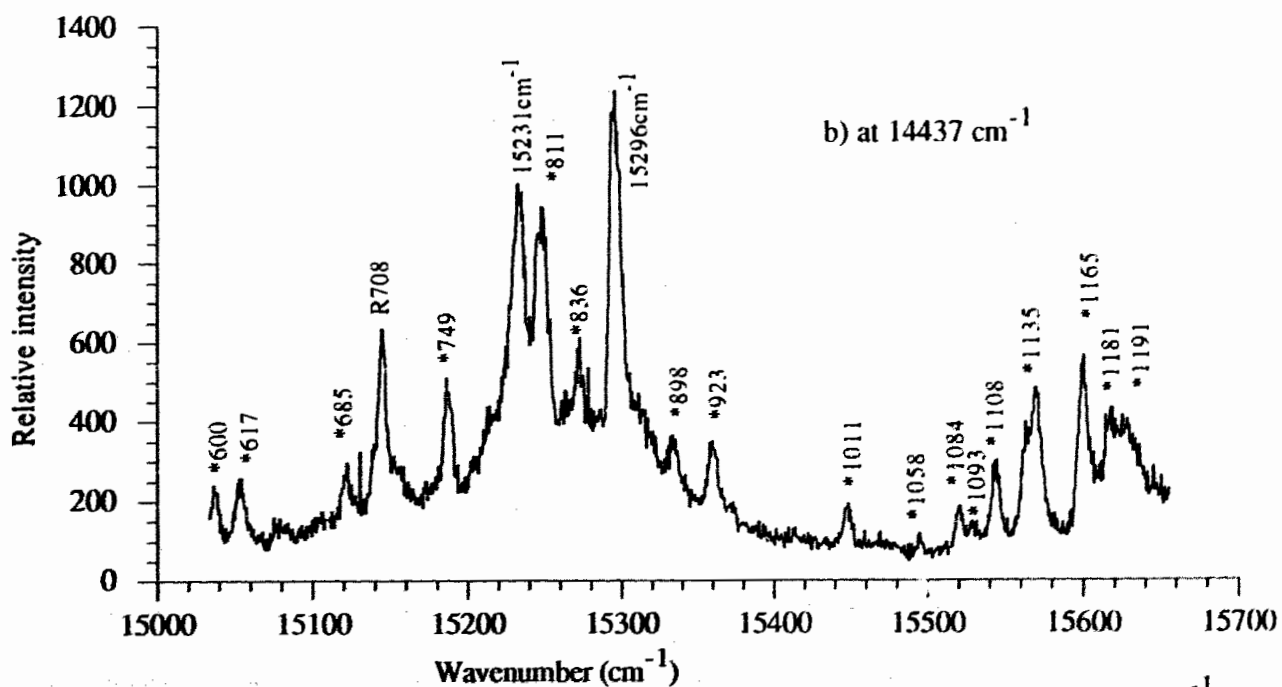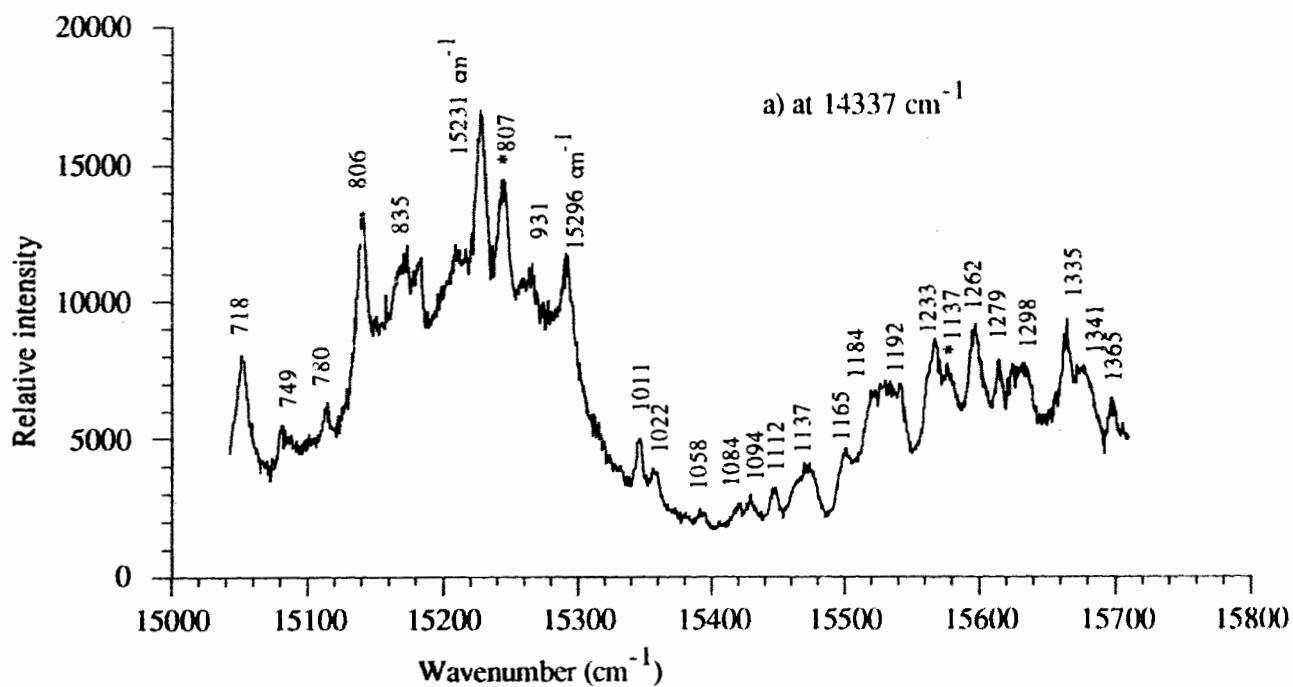
Fig. 23, (2) Fluorescence excitaton spectra of TBH$_2$Pc in C$_{18}$; a) monitored at 14337 cm^{-1},

b) at 14437 cm^{-1}. The two S$_2$ states are at 15296 cm^{-1} and 15231 cm^{-1}.
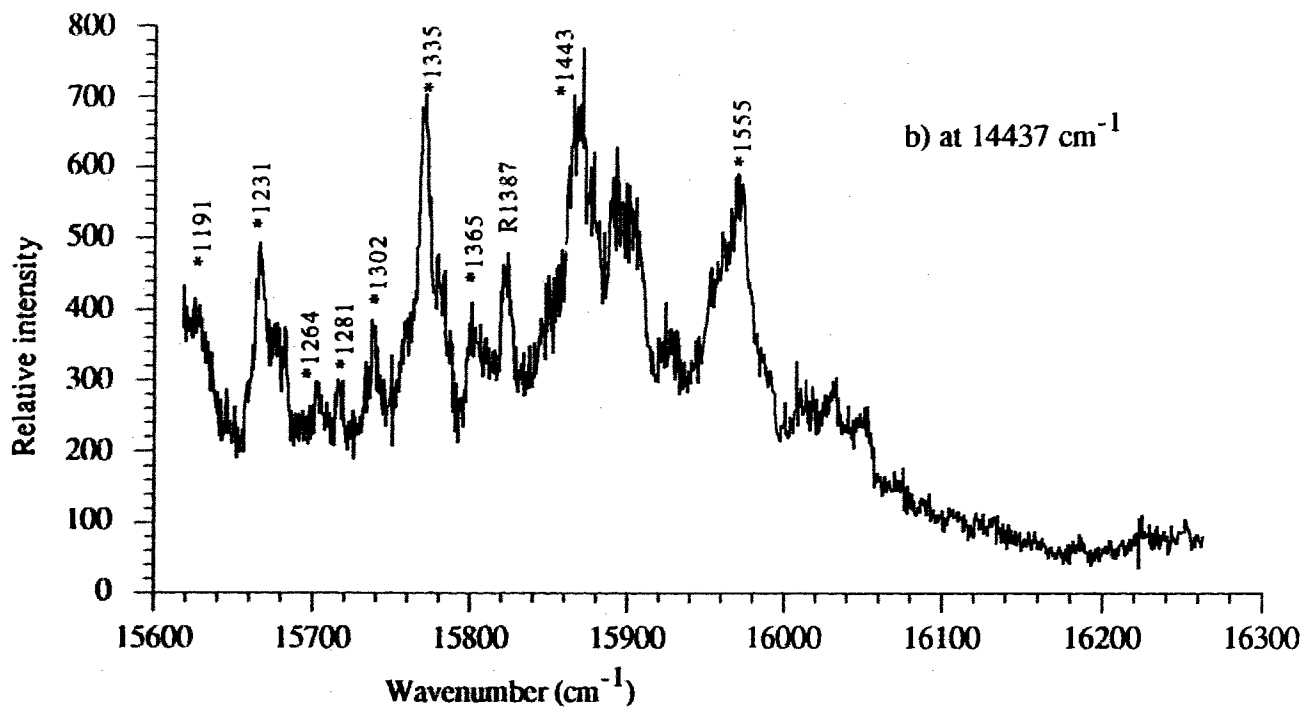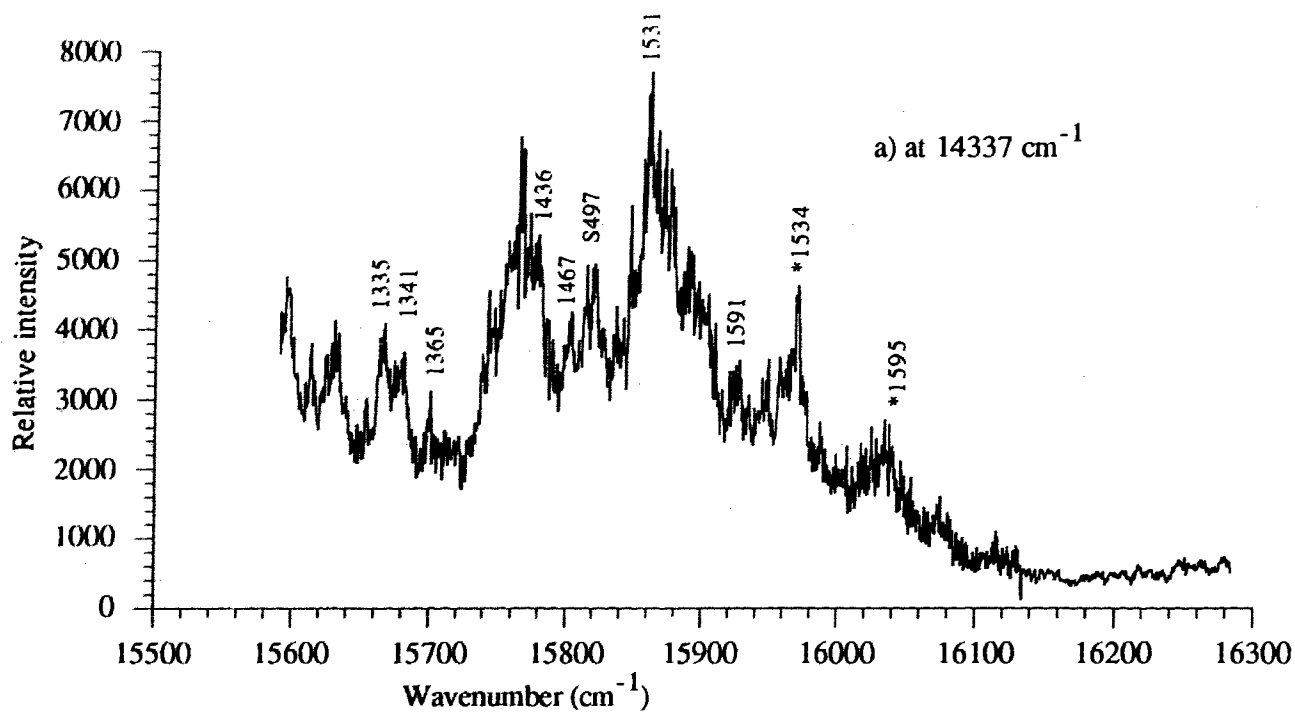
Fig. 23. (3) Fluorescence excitation spectra of TBH$_2$Pc in C$_{18}$; a) monitored at 14337 cm^{-1}, b) at14437 cm^{-1}.
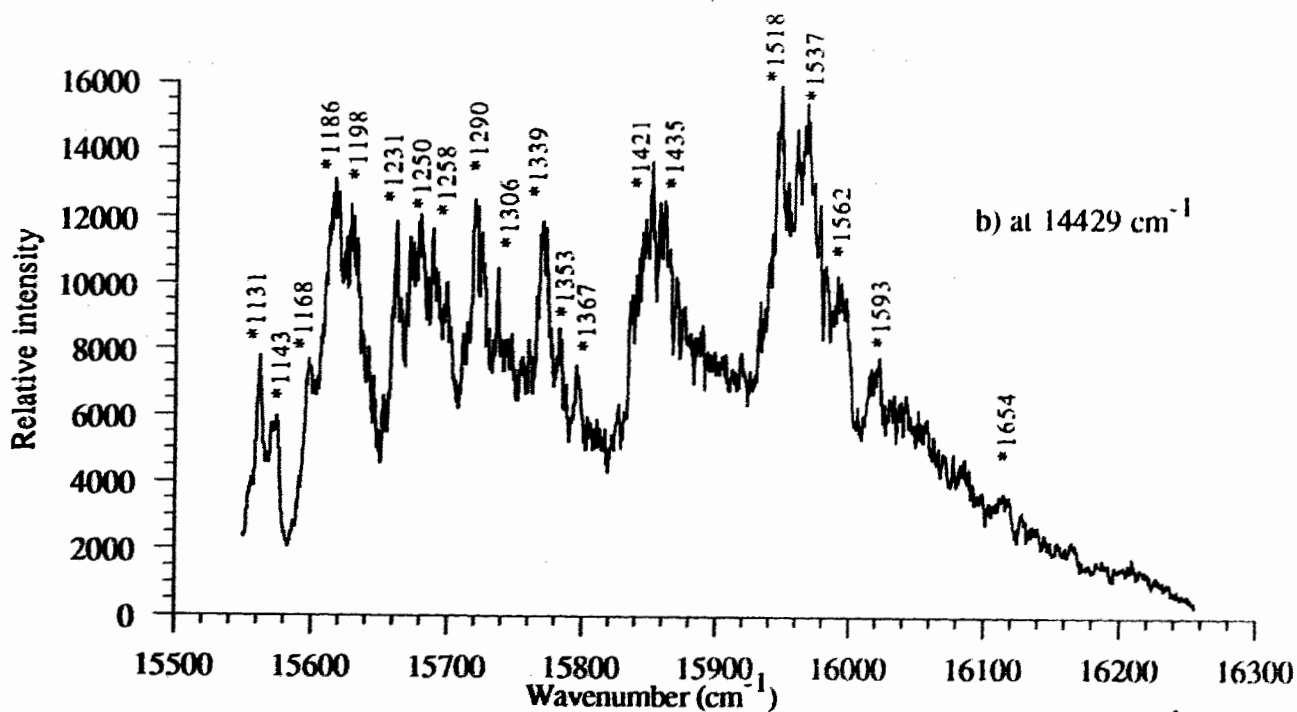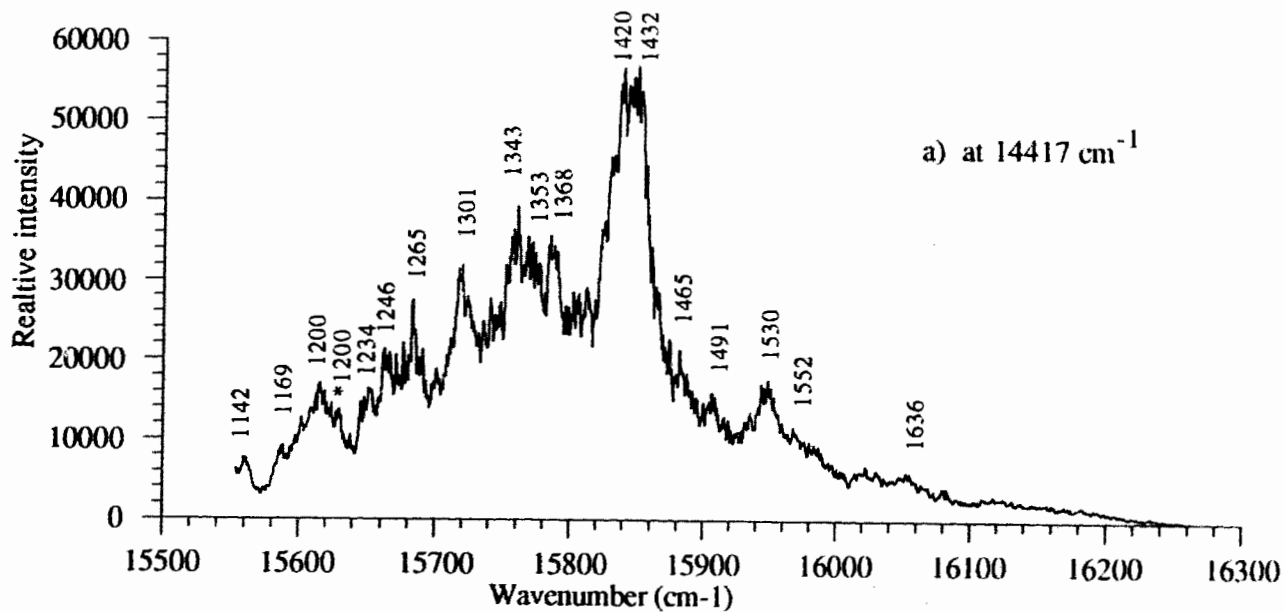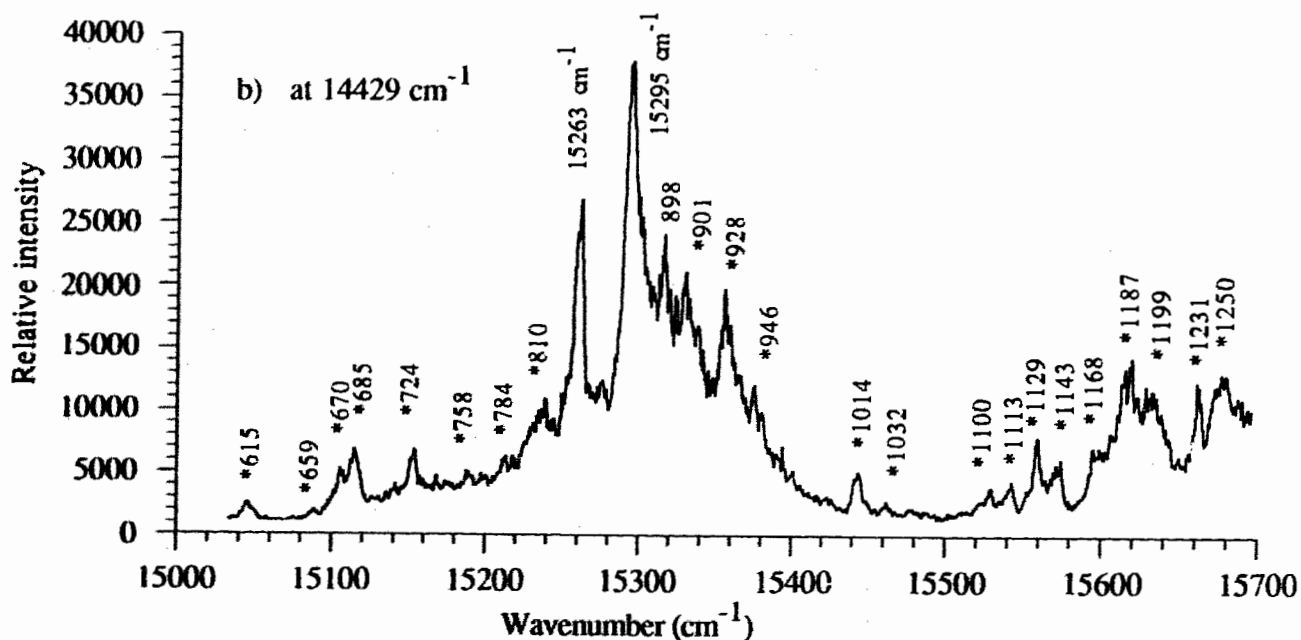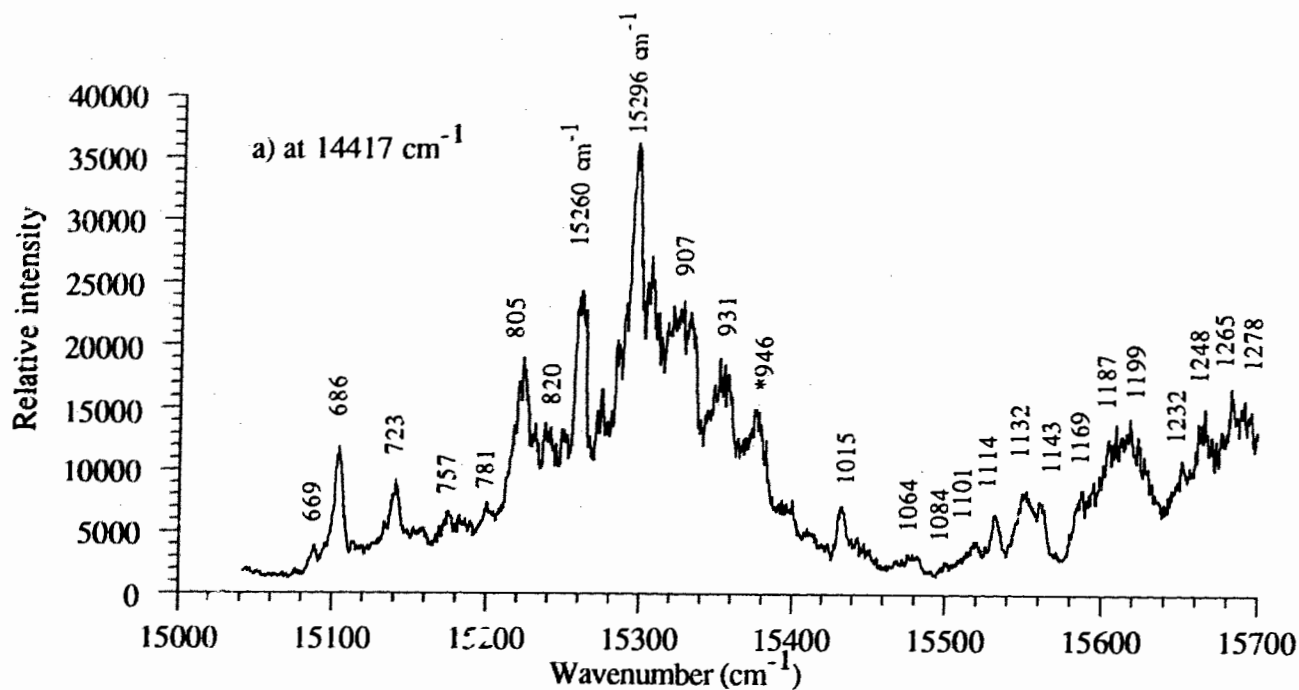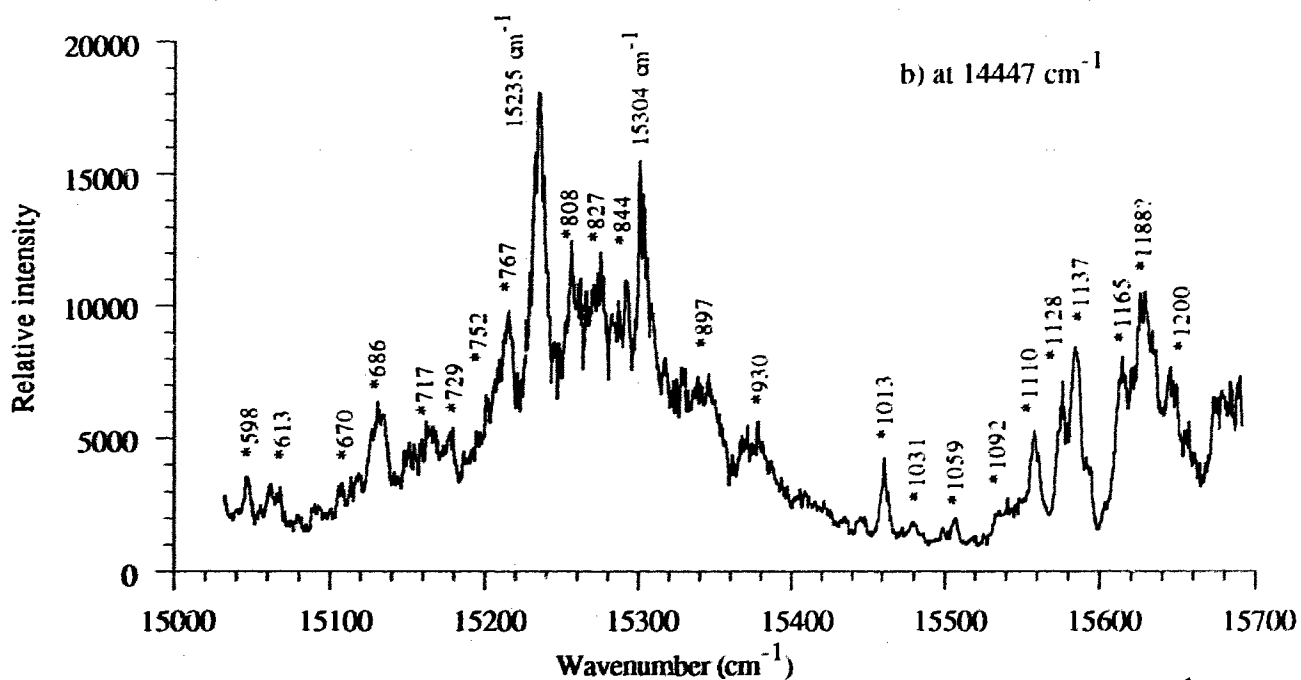
Fig. 24. (1) Fluorescence excitation spectra of TBH$_2$Pc in C$_{12}$; a) observed at 14417 cm^{-1}, b) at 14429 cm^{-1}.

Fig. 24, (2) Fluorescence excitation spectra of TBH$_2$Pc in C$_{12}$; a) observed at 14417 cm^{-1},

b) at 14429 cm^{-1}. The two S$_n$ states are at 15295 cm^{-1} and 15263 cm^{-1}.
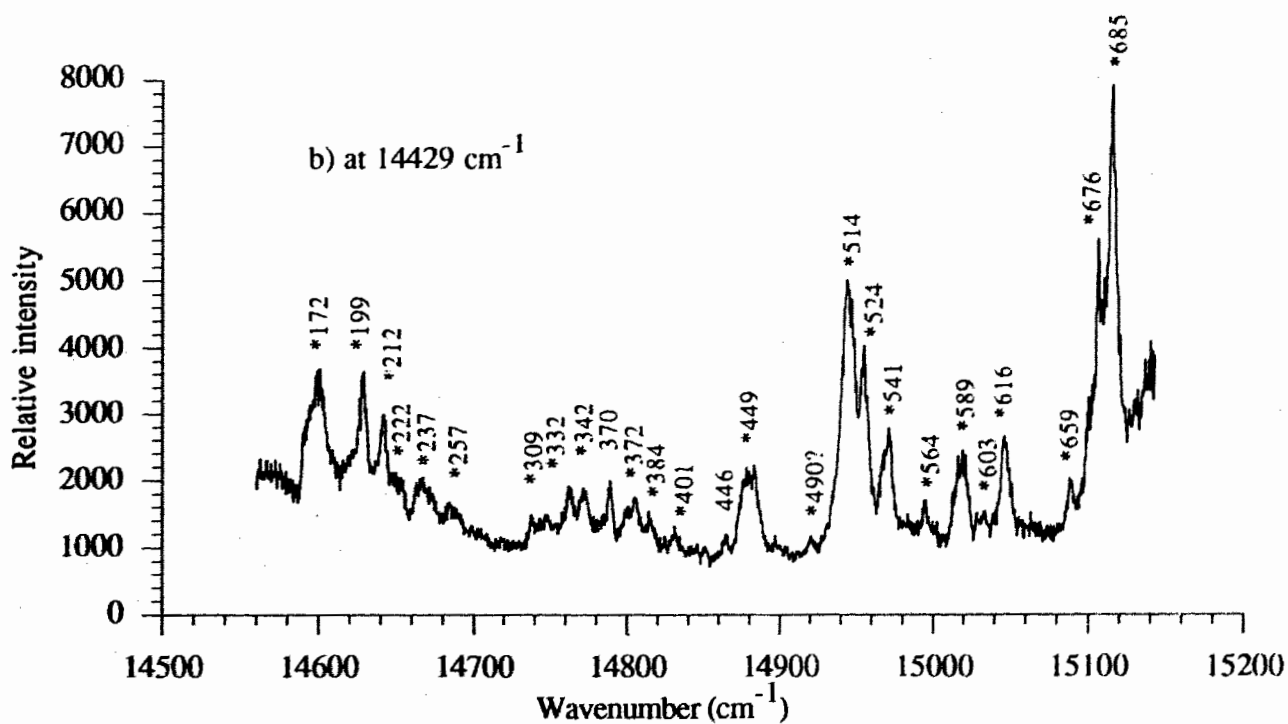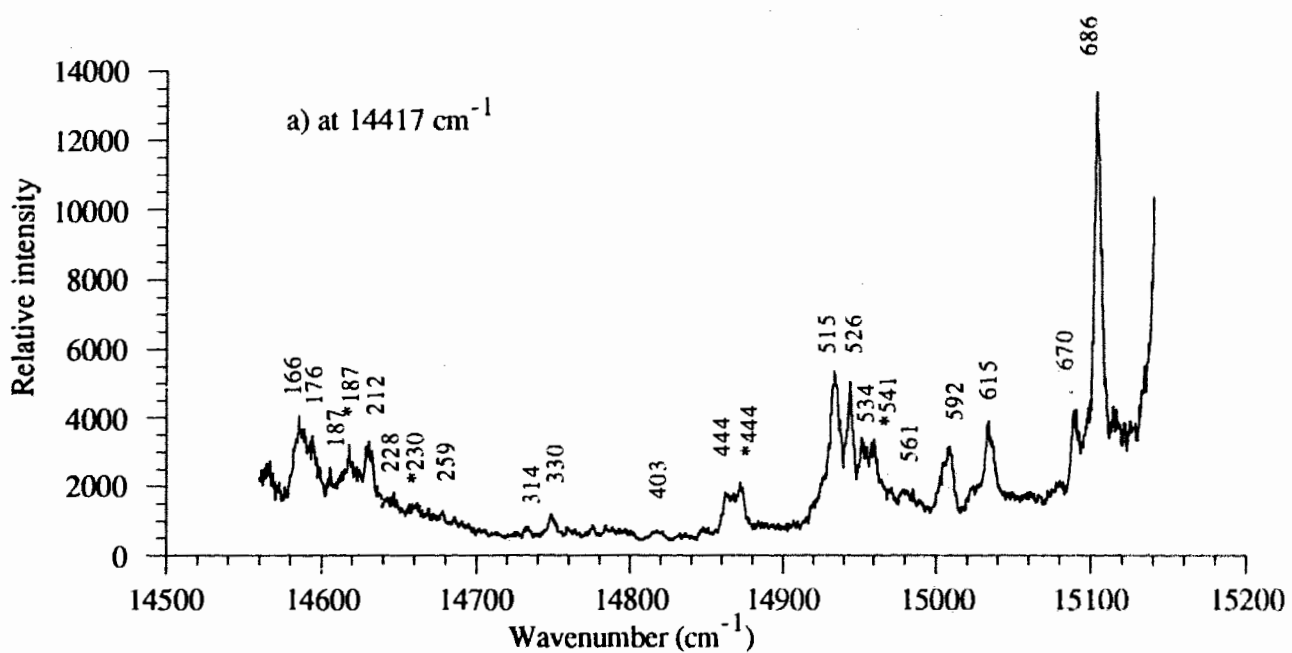
Fig. 24, (3) Fluorescence excitation spectra of TBH$_2$Pc in C$_{12}$; a) observed at 14417 cm^{-1}, b) at 14429 cm^{-1}.

77
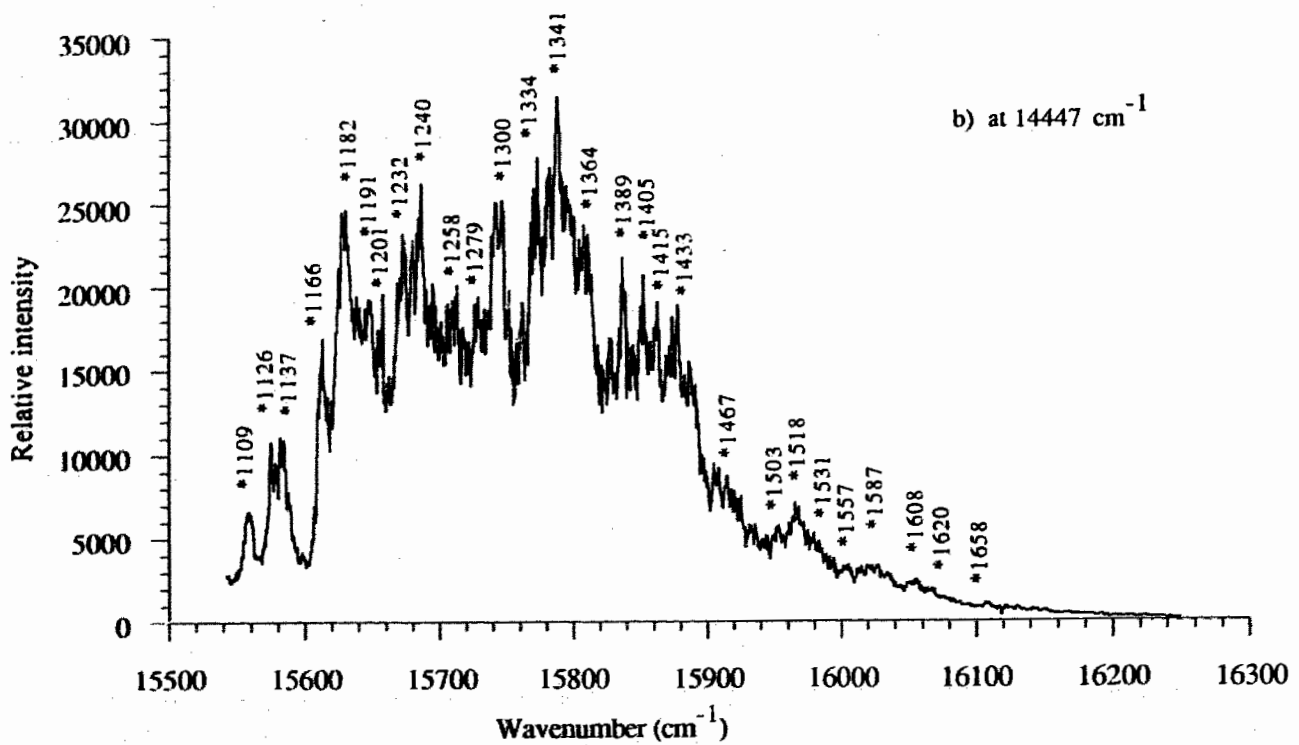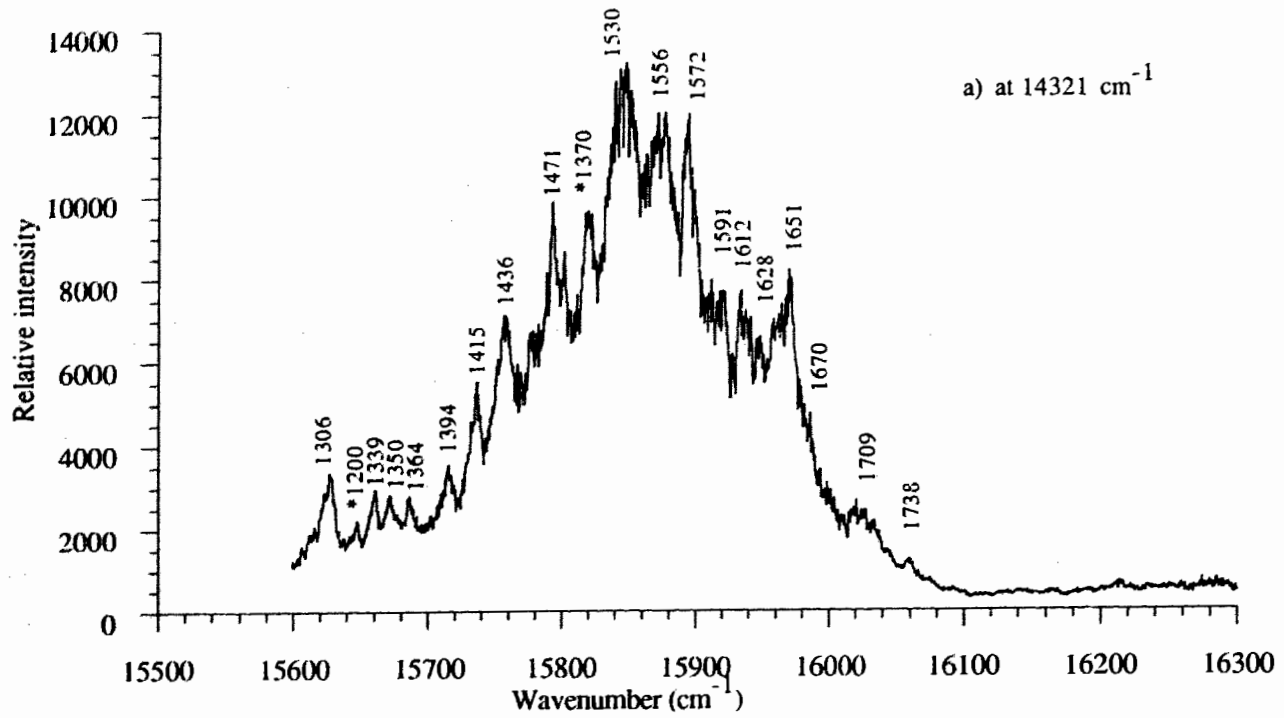
Fig. 25. (1) Excitation fluorescence spectra of TBH$_2$Pc in C$_9$; a) monitored at 14321 cm^{-1},
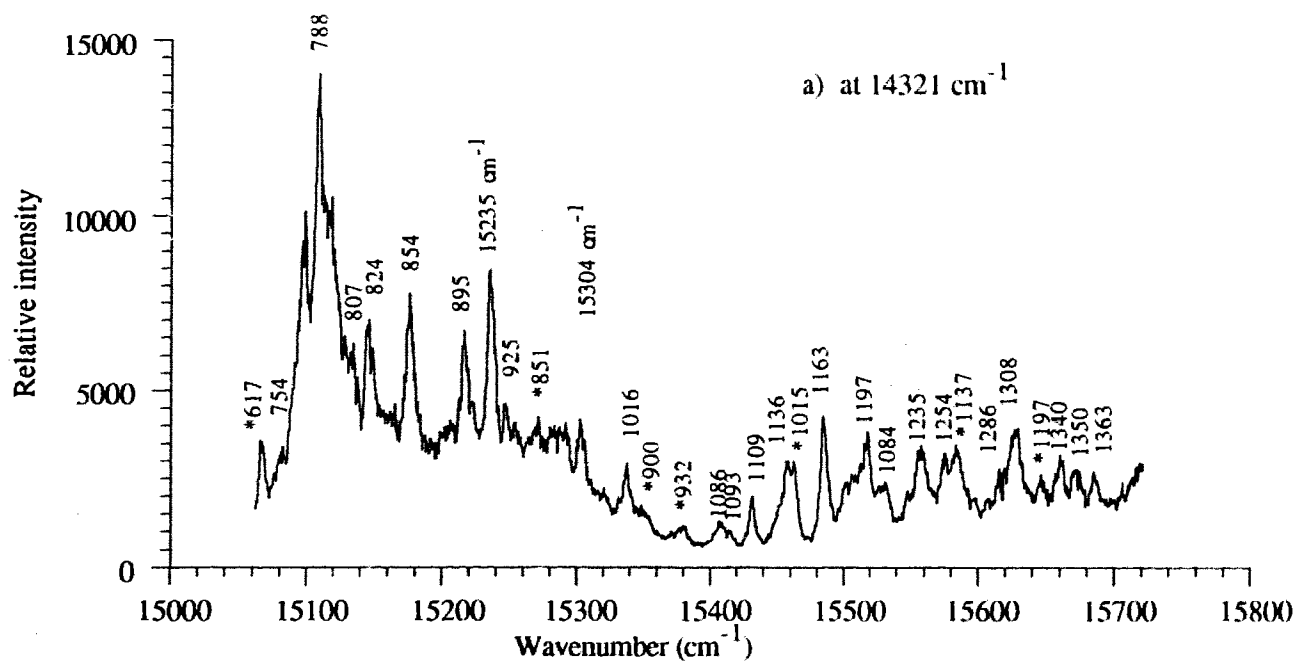
b) at 14447 cm^{-1}.

Fig. 25, (2) Fluorescence excitation spectra of TBH$_2$Pc in C$_9$. a) monitored at 14321 cm^{-1}; b) at 14447 cm^{-1}. Note two S$_2$ states are at 15304 cm^{-1} and 15235 cm^{-1}.
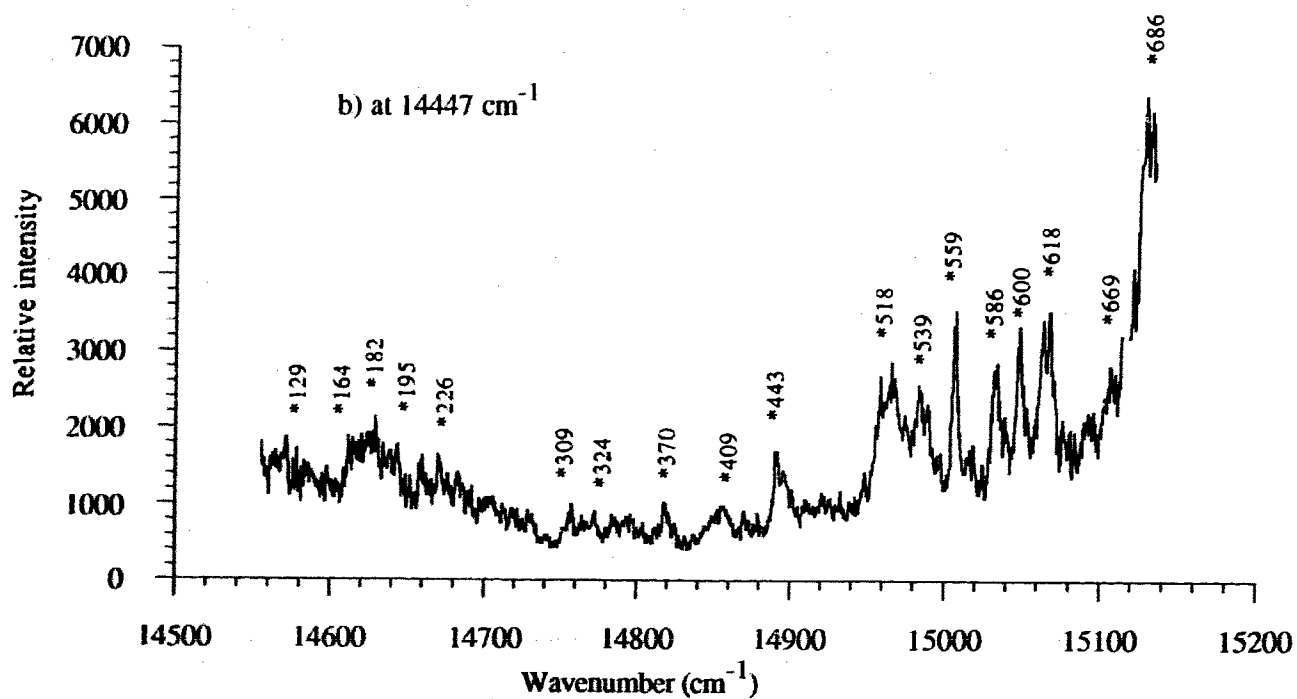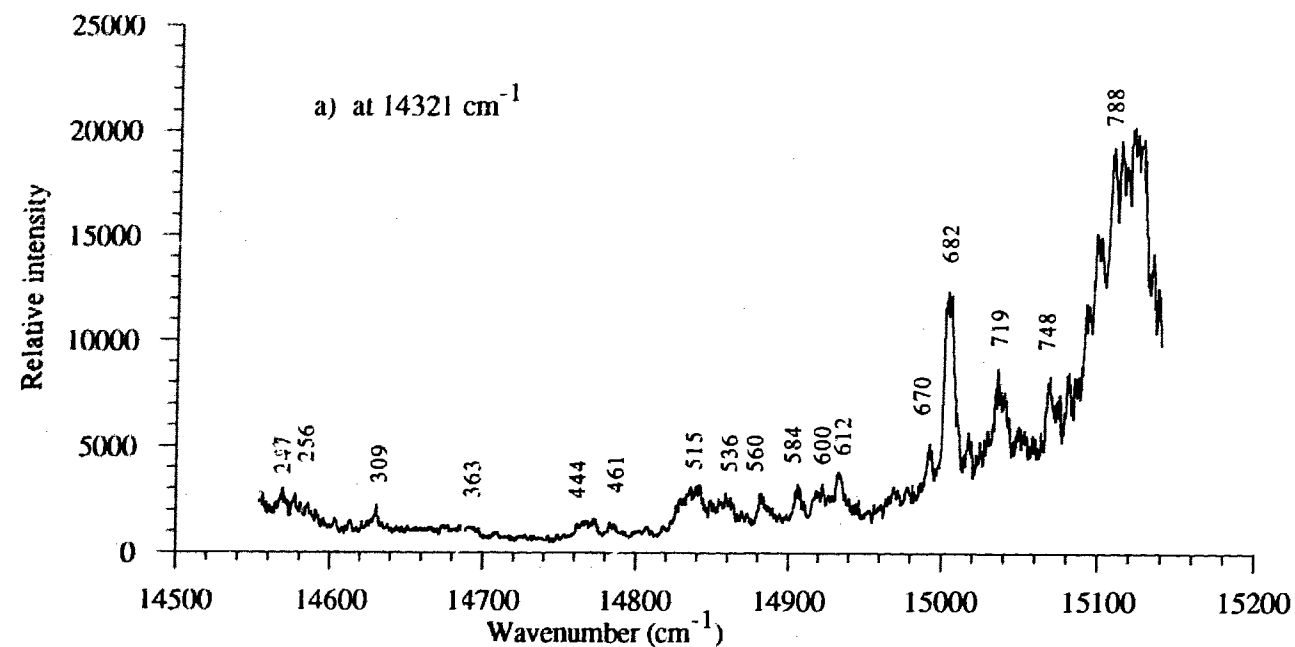
79

Fig. 25. (3) Fluorescence excitaion spectra of TBH$_2$Pc in C$_9$; a) monitored at 14321 cm^{-1}; b) at 14447 cm^{-1}.

molecules are different in position and in intensity. This is most likely the results of the combined effects of very different and complex intermolecular cage and intramolecular vibronic state interactions in these two systems.

3.5 Photochemical Transformation Dynamics

The electronic potential curves for TBH_2Pc in C_{16} have double wells in both ground and excited states (see Fig.2). The wells of the lowest excited states are separated by a barrier of about 900 cm^{-1} in height as discussed in sec. 3.2. The energy difference between double wells of the ground state is not known, but the barrier height between them has been expected from recent hole burning experiments[16]. To induce isomerisation, photon energy is used to promote one species to the excited state which then may cross over to the other state with a change to its molecular tautomer. However, even under continuous pumping of tautomer produced, this process cannot go on forever. It will slow down because some of the molecules have changed to their tautomer and eventually it will come to a halt when a steady state equilibrium between the species is established. Once this condition is reached the conversion is saturated under the given pumping intensity and no further net conversion is observed. Fig.26 shows simplified models of the phototransformation where a) has 0-0 (S_1-S_0) excitation with pre-pumping of (S_1-S_0) and the 0-1 fluorescence observation and b) shows the 0-1 excitation with pre-excitation of S_2 and the 0-0 fluorescence observation.
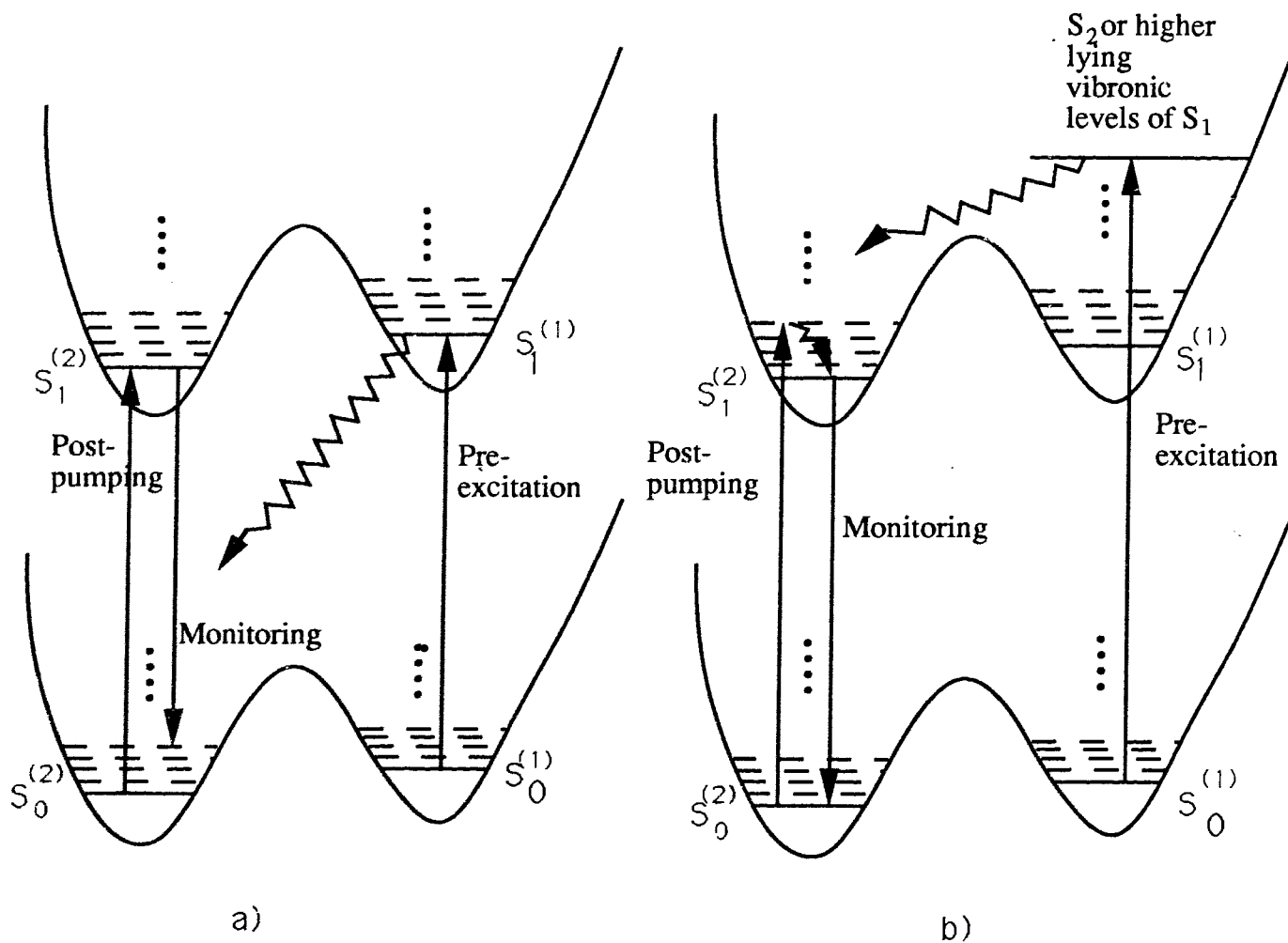
81

Fig. 26 Phototransformation mechanism diagrams; a) 0-0 pumping and 0-1 monitoring; b) 0-1 pumping and 0-0 observation.

It is worth mentioning that pre-excitation is very important in creating an excess population of one of the two molecular tautomers, otherwise phototransformation cannot be observed. Fig. 27 shows how after being pre-excitation with $\nu = 15305$ cm^{-1} and monitored at 14415 cm^{-1} ($S_1^{(2)}$), that when the sample was repeatedly excited with the lower frequency of 15102 cm^{-1}, the intensity decline occurred only on the first excitation. For the second and third periods of pumping no intensity drops are observed (see also Fig.35a in which some other situations are described), because there was no excess population left for equilibration.

For phototransformation to take place it is necessary that the initial ground state population (N) of one species exceeds its equilibrium level (N_0) which is achieved by pre-excitation. If there is only one dominant mechanism depleting one excited species to the other as shown in Fig.26, the fluorescence intensity (I) in a steady state is given by:

$$I = F \cdot \{ N_0 + (N - N_0) \cdot \exp (- t / \tau) \} \qquad (4)$$

where the coefficient F is a function of laser power, oscillator strength of the states, and all the radiative and nonradiative rates involved and τ is the characteristic time of population redistribution or transformation saturation. As the previous study of H_2Pc in $\alpha\text{--ClN+}C_8$ has shown[15], τ depends on laser power, the absorption coefficient of the pumping state and other processes involved.
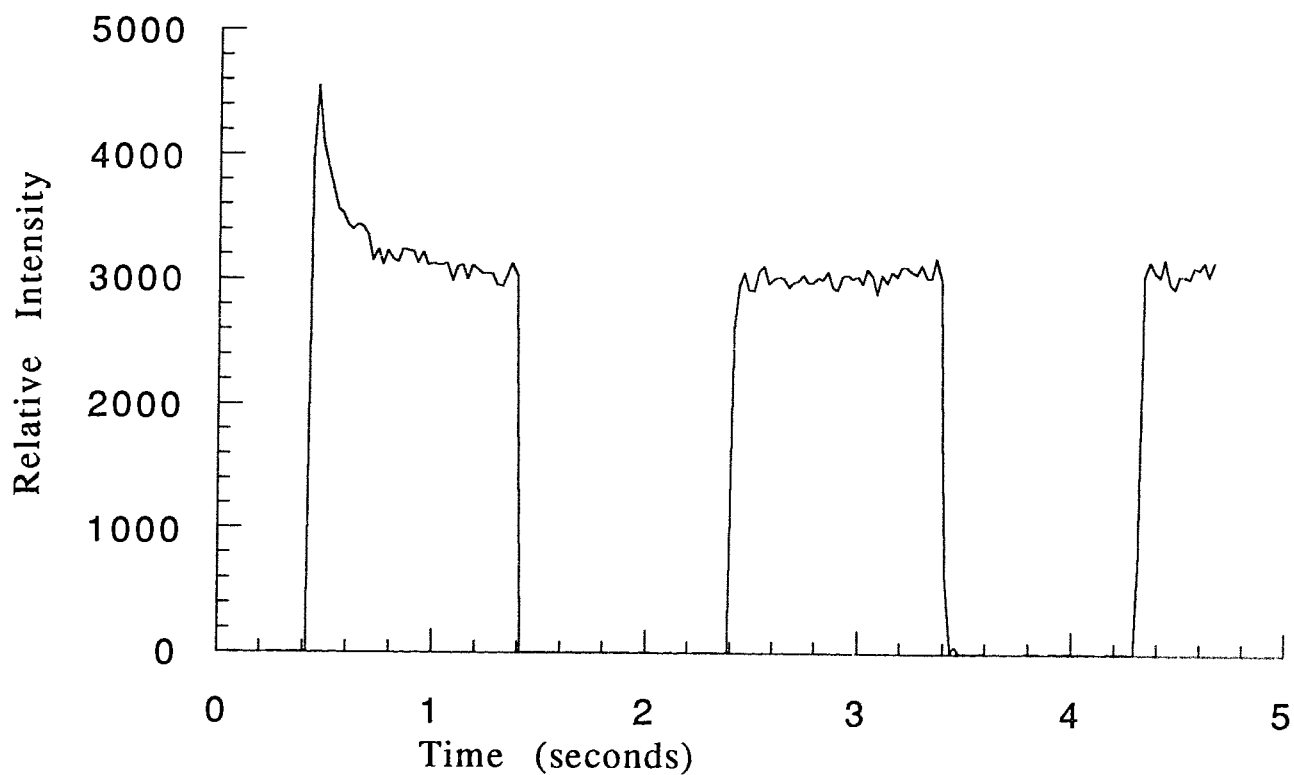
Fig. 27 Monitored at 14415 $cm^{-1}(S_1{}^{(2)})$, with pre-excitation of $\upsilon=15305$ cm^{-1}, followed by repeated pumping 15101 cm^{-1} $(S_1{}^{(2)}+$ 686 cm^{-1}): only the first excitation showed an intensity decline.

One such example was the observation of the 0-1 13729cm^{-1} ($S_0^{(2)}$ +686 cm^{-1}) fluorescence intensity as a function of time under the continuous pumping of 14415 cm^{-1} ($S_1^{(2)}$) where the equilibrium populations had been upset by a brief irradiation of 14436 cm^{-1} ($S_0^{(1)}$) prior to pumping. Fig 28 shows both the scattered data points (circles) and the fitted curve (dash line) using a single lifetime of τ=34 *ms* in Eqn. (4). However, from all the data analyzed we found none of these traces truly displayed a single lifetime decay. Further, the model given in Fig.26 is a great over-simplification since other processes, such as transformations through barrier tunneling *etc.* are likely contributors. Other fits with multiple lifetimes were tried but yielded meaningless results. Thus, we simply approximated the experimental data by considering N_0 as a linear function of time which decreases monotonically. The intensity equation then becomes:

$$I = (n_0 - a t) + [(n - (n_0 - at)] \cdot exp (-t / \tau) \qquad (5)$$

where n_0 and n are is the intensity coefficients with F being absorbed in them and a is the intensity decreasing factor (the slope). In Fig.28 the solid line is the same as the dash line, except that the solid line is fitted with Eqn. 5 and gave a better redistribution time of τ=32.4*ms*. The redistribution times τ, reported here were all calculated from the "approximate" Eqn.(5) and carried uncertainties normally in the range from 10 to 50 percent depending on experimental conditions.
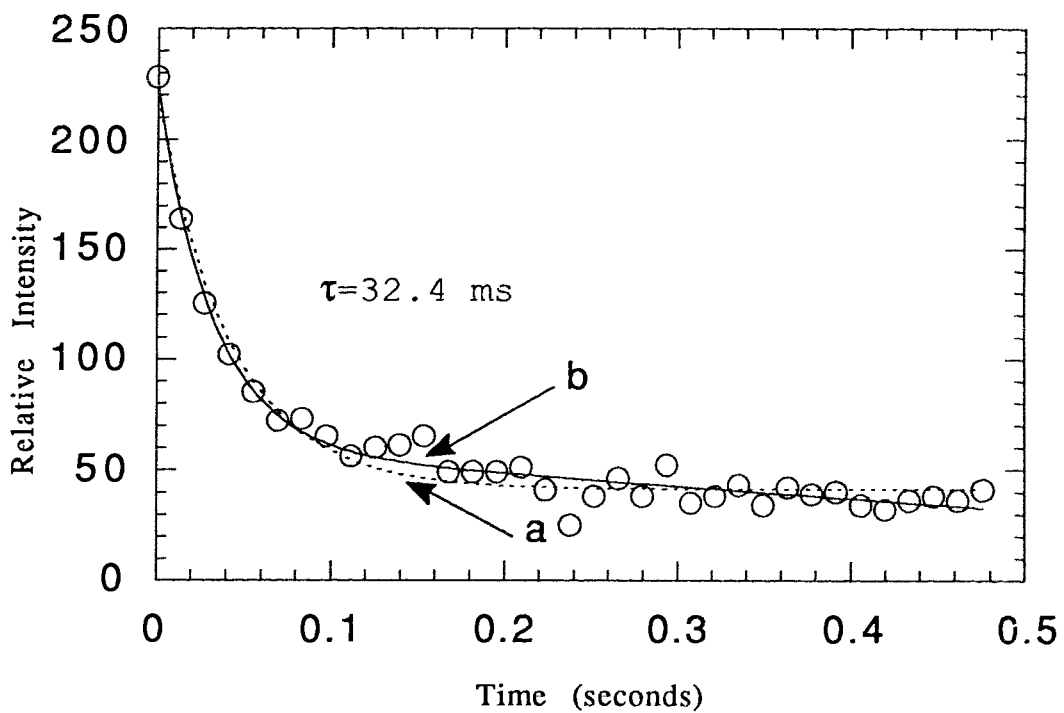
Fig.28 Phototransformation of TBH_2Pc in C_{16} by monitoring at 13729 cm^{-1}.

Pre-excitation with 14436 cm^{-1}, then pumping with 14415 cm^{-1}; The circles

represent data points. The dash line was fitted by Eqn. 4, the real line by Eqn. 5.

In general, the mechanism of phototransformation given in Fig. 26 by using 0-0 excitation could happen in several ways. For example, if we monitored at 13748 cm^{-1} ($S_0^{(1)}$+688cm^{-1}), then pre-excitation could be either by pumping with 14415 cm^{-1} ($S_1^{(2)}$) or by 14436 cm^{-1} ($S_1^{(1)}$), and post-excitation also could be at 14415 cm^{-1} or 14436 cm^{-1}. But we only observed phototransformation for pre-excitation with 14415cm^{-1} and then excitation with 14436 cm^{-1} and monitoring at $S_0^{(1)}$+688 cm^{-1}. This is clearly shown in the data presented in Fig. 29 where only for case d) a population unbalance has been achieved. Similarly, monitoring fluorescence at 13729 cm^{-1} ($S_0^{(2)}$+686cm^{-1}) and testing all the possible cases listed above, one would predict in terms of the scheme of Fig. 26 that corresponding results would be formed with monitoring at $S_0^{(1)}$+688 cm^{-1}. This was not the case as can be seen in Fig. 30 where curve c) corresponds to d) in Fig. 29 and is expected to show phototransformation. However in case b) which is under the repeat excitation at the same frequency of 14415 cm^{-1} ($S_1^{(2)}$), the intensity decline is still occurring (also see Fig.35b), which implies that phototransformation still took place. This happens also with 0-1 excitation and 0-0 observation as will be described later in Fig.35a). We believe that these phototransformations can be explained if one assumes that the $S_0^{(2)}$ ground state is lower in energy than the $S_0^{(1)}$ state (Fig. 26) and that ground state tunneling and thermally activated processes from $S_0^{(1)}$ to $S_0^{(2)}$ occur leading to the intensity decline at the beginning of later periods as in Fig.35b).
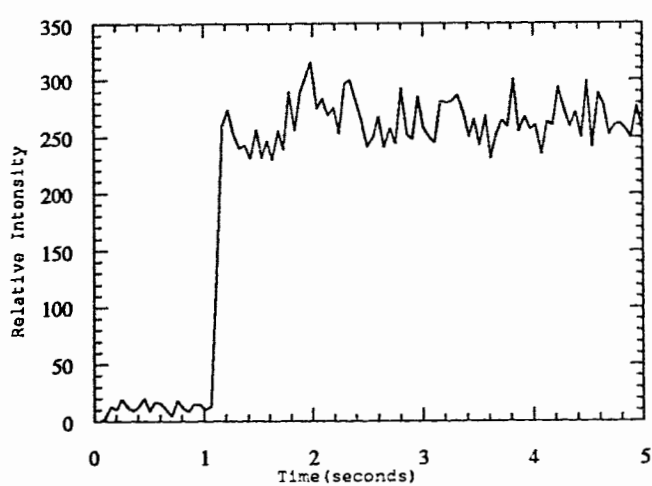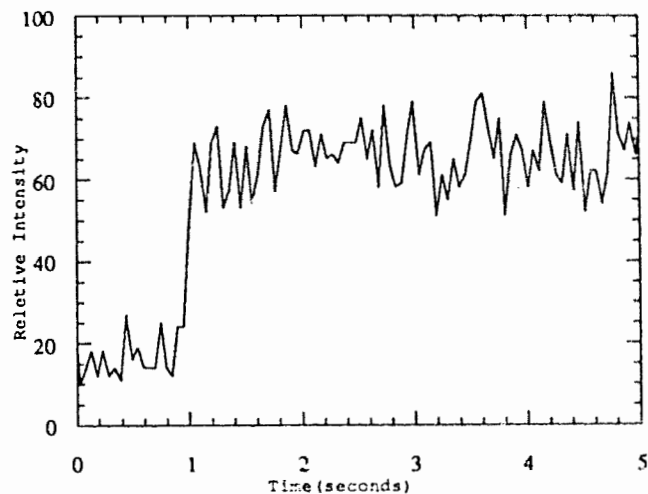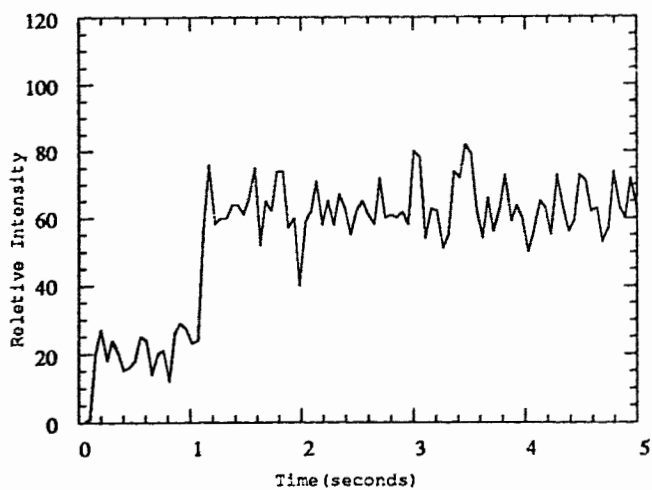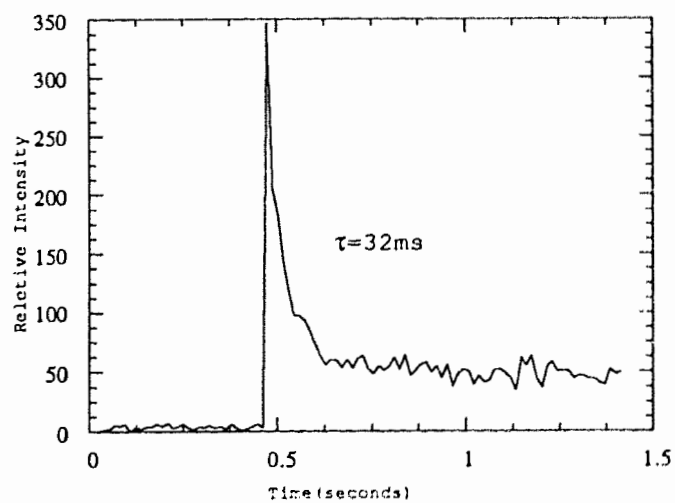
Fig. 29 Four possible 0-0 excitations with 0-1 $(S_0^{(1)}+688 cm^{-1})$ observation. a) $S_1^{(1)}$, $S_1^{(1)}$; b) $S_1^{(2)}$, $S_1^{(2)}$; c) $S_1^{(1)}$, $S_1^{(2)}$; d) $S_1^{(2)}$, $S_1^{(1)}$. Only d) has phototransformation.
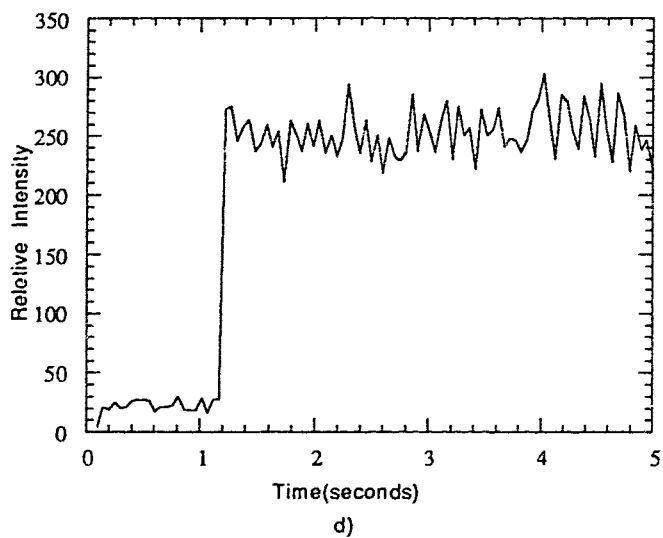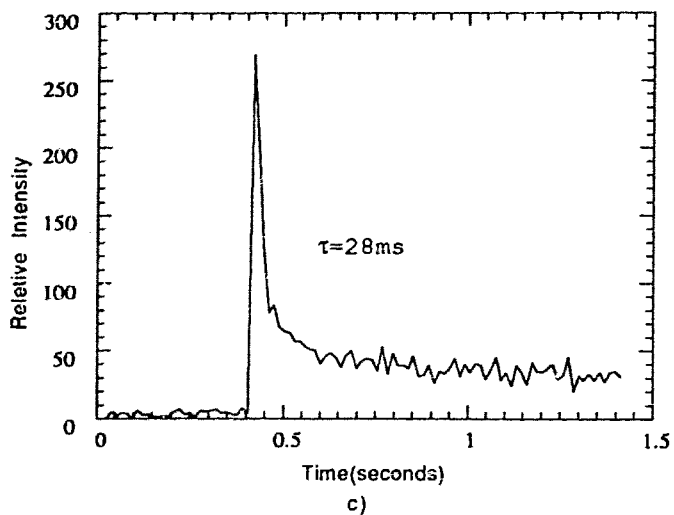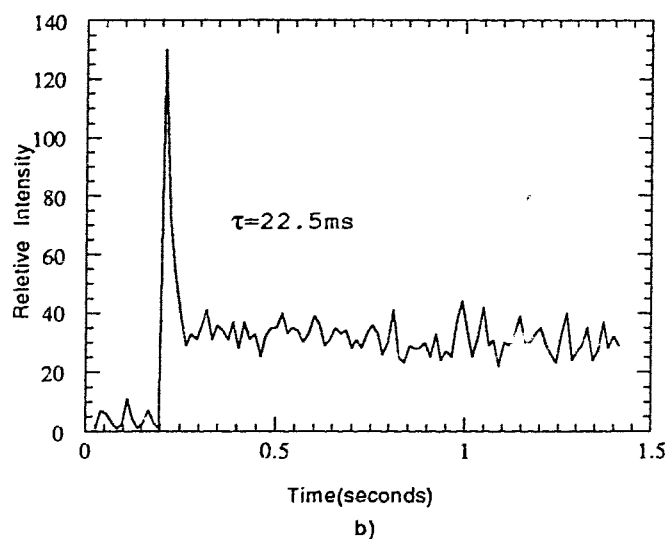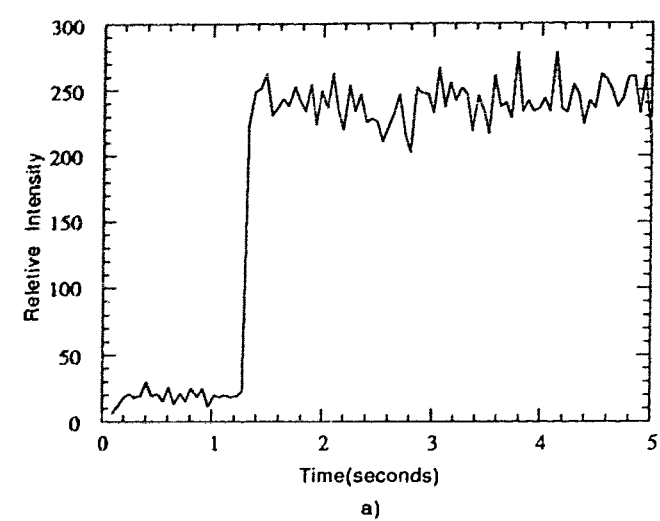
Fig. 30 Four possible 0-0 excitations with $0\text{-}1(S_0^{(2)}+686\text{cm}^{-1})$ observation. a) $S_1^{(1)}$, $S_1^{(1)}$; b) $S_1^{(2)}$, $S_1^{(2)}$; c) $S_1^{(1)}$, $S_1^{(2)}$; d) $S_1^{(2)}$, $S_1^{(1)}$. Now b) and c) have phototransformations.

This is consistent with absorption experiments conducted elsewhere in which it was found that most of the population at equilibrium is in the $S_0^{(2)}$ state at T=77K or lower[35]. Furthermore, the height of each fluorescence period depended on the length of dark time chosen which also confirmed the tunneling suggested above.

Investigation of the 0-0 transitions pumped with lower vibronics of S_1 (*i.e.* 0-1 transitions) also revealed similar time dependences. Two typical examples are given in Figs.31a and 34a: in Fig. 31a the sample was pre-excited by 15305cm^{-1} ($S_2^{(1)}$), then excited by 15101 cm^{-1} ($S_1^{(2)}$+686cm^{-1}) and monitored at 14415 cm^{-1} ($S_1^{(2)}$); in Fig. 34a, pre-excitation was 15263 cm^{-1} ($S_2^{(2)}$), then the sample was excited by 15122 cm^{-1} ($S_1^{(1)}$+686 cm^{-1}) and observed at 14436 cm^{-1} ($S_1^{(1)}$). Both show photoisomerisation clearly and their transformation redistribution times are 90 *ms* and 165 *ms* respectively. The data obtained in this study of 0-1 pumping and 0-0 observation generally departed from a single exponential function more seriously than those of 0-0 pumping and 0-1 observation. Using Eqn. 5 to compare with the data of 0-0 pumping and 0-1 observation, the error was below 1%, but for those with 0-1 pumping and 0-0 observation the errors were bigger. This indicated that perhaps more complicated photochemical transformation mechanisms occur for 0-1 pumping and 0-0 observation than for 0-0 pumping and 0-1 observation which is not surprising since for cases of 0-1 pumping and 0-0 observation more diverse relaxation channels are available.
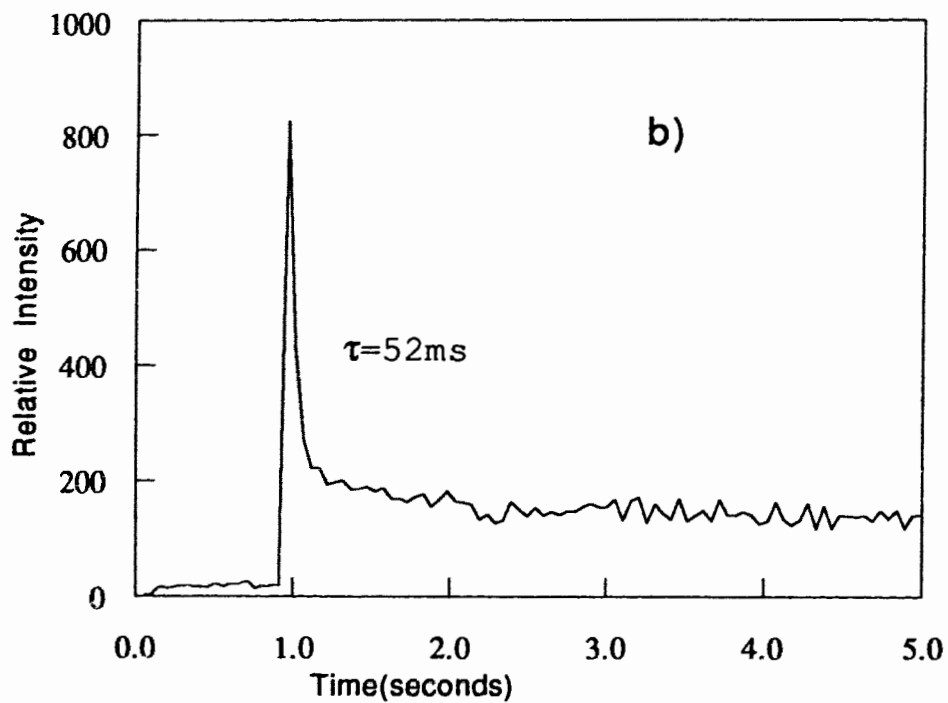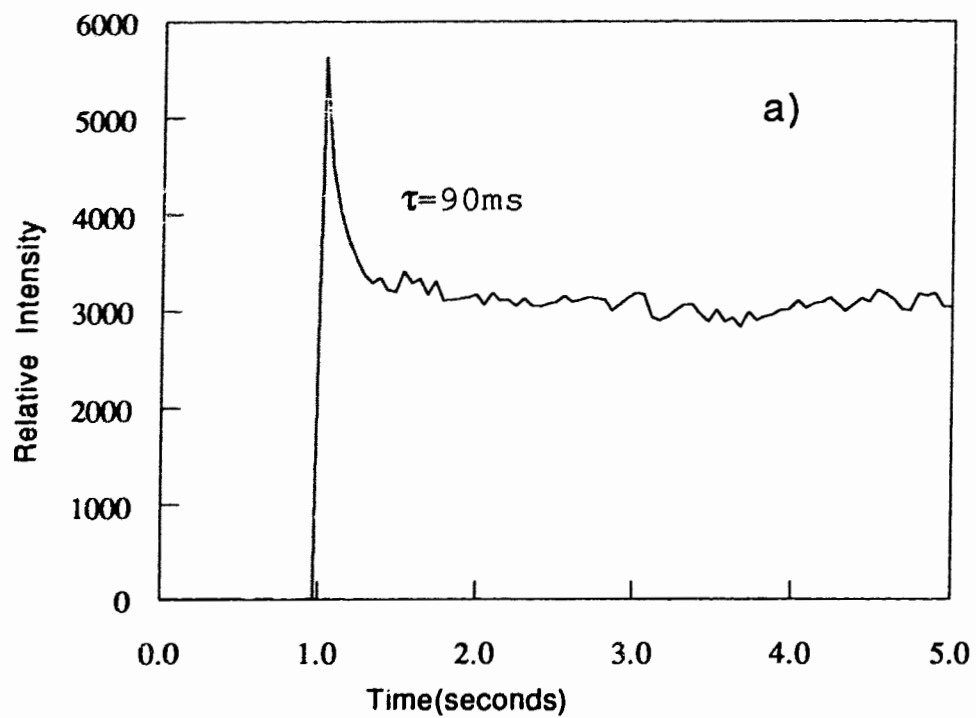
Fig. 31 Phototransformations for a) monitored at 14415 cm^{-1} ($S_1^{(2)}$) with excitation of 15101cm^{-1} ($S_1^{(2)}$+686cm-1) with τ_1=90ms. b) observed at 13729cm^{-1} ($S_0^{(2)}$+686cm^{-1}) with excitation of 14415cm^{-1} ($S_1^{(2)}$), τ_2=52ms. Both are properly pre excited. Note their time difference. $\tau_1 > \tau_2$.

Furthermore, the redistribution times measured were generally longer for 0-1 pumping and 0-0 monitoring than for those of 0-0 pumping and 0-1 observation; and the relative intensity decline of 0-0 pumping and 0-1 observation was much stronger than that in the case of 0-1 pumping and 0-0 observation. We assume that this is due to weaker absorption in the 0-1 pumping and 0-0 observations such as are shown in the two examples given in Fig.31 a), lifetime $\tau=90$ *ms* for $S_1^{(2)}+686$ cm^{-1} pumping and 14415 cm^{-1} observation and b) 0-0 pumping and observation at 13729 cm^{-1} ($S_0^{(2)}+688$ cm^{-1}), the $\tau=52$ *ms*. All the times τ were obtained using Eqn.(5).

Redistribution times monitored for the 0-0 fluorescence with different 0-1 pumping frequencies were also found to vary with the latters' absorption coefficients. Those pumped with stronger absorption bands generally resulted in a short redistribution time τ. Fig.32 shows this effect for traces obtained by pumping with a) 15101cm^{-1} ($S_1^{(2)}+686$cm^{-1}) $\tau_1=90$ *ms* and b) 14929 cm^{-1} ($S_1^{(2)}+514$ cm^{-1}) $\tau_2=136$ *ms*, using brief pre-excitation with 15305 cm^{-1}. The absorption (equivalent of fluorescence excitation peak intensity) of 15101 cm^{-1} is stronger than that of 14929 cm^{-1} from section 3.4 and we observe that $\tau_2>\tau_1$, which shows that the absorption coefficient is important in the phototransformation. On the other hand, little difference was found in τ when observing different 0-1 fluorescences using the same 0-0 pumping.
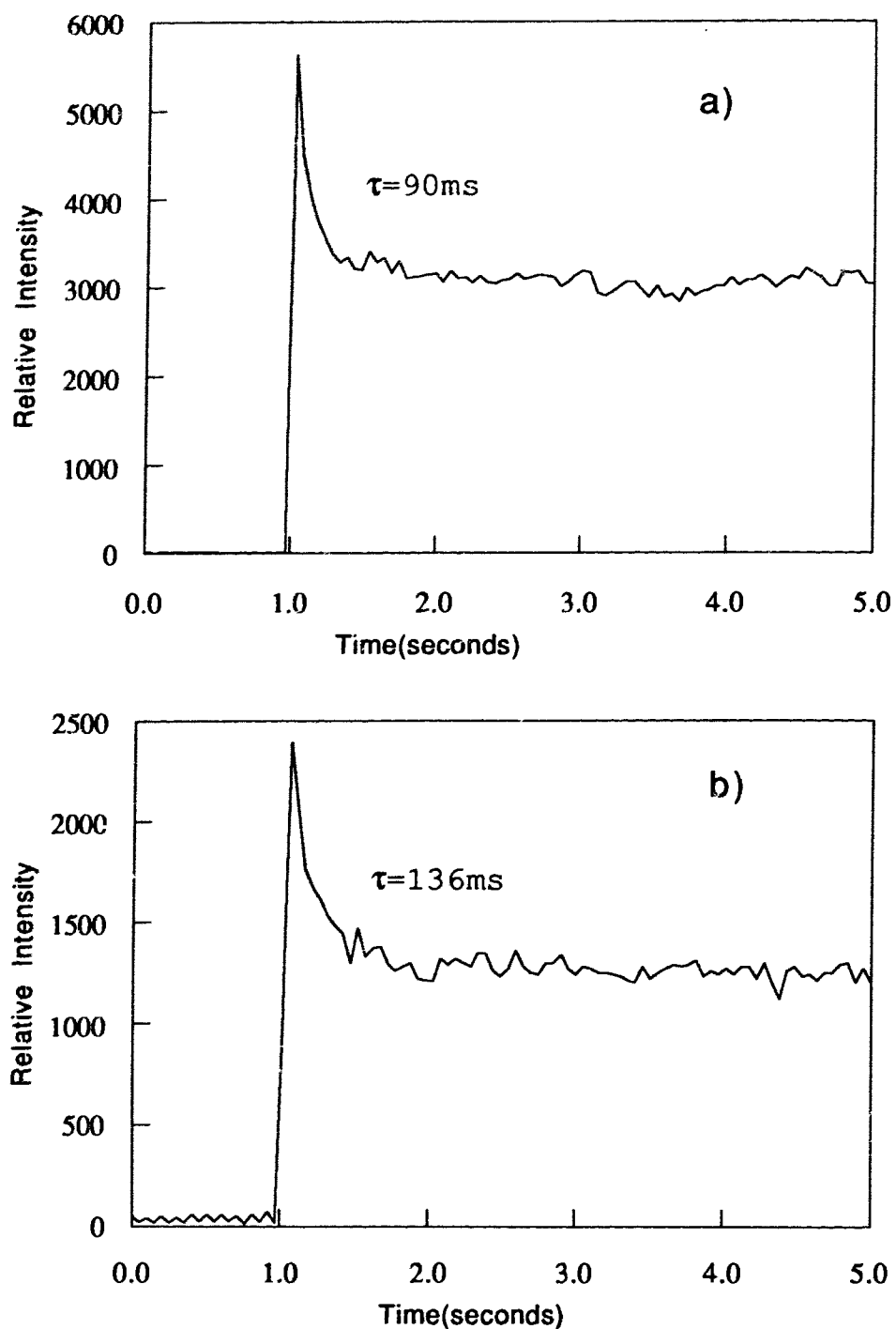
Fig.32 The relation between τ and energy state absorption coefficients. Both monitored at 14415 cm $^{-1}$ ($S_1^{(2)}$) and with same pre-excitation. a) with excitation of 15101cm^{-1}, τ_1=90ms. b) with excitation of 14929cm^{-1}, τ_2= 136ms. a) has a better absorption than b). Note $\tau_2 > \tau_1$.

We therefore conclude that τ is a function of the oscillator strength of the transition and the intensity of the pumping laser; pumping at 0-0 is more efficient than pumping at0-1 resulting in a shorter τ. A given pumping frequency observed at different monitoring positions gave approximately the same redistribution time while different pumping frequencies monitored at the same fluorescence show different decay times.

It is worth noting that the time dependence of the intensity due to photochemical transformation was most clearly seen when both pumping and observation were made for the same species, $S^{(1)}$ or $S^{(2)}$ respectively. Intensity observed for transformed species usually resulted in weak signals and ambiguous time dependence. Fig. 33 demonstrates this situation where curve a) was obtained with 14593 cm^{-1} ($S_1^{(2)}$+178 cm^{-1}) pumping and 14415 cm^{-1} ($S_1^{(2)}$) observation and a phototransformation redistribution time τ=124 ms was obtained, whereas curve b) was observed at 14436 cm^{-1} ($S_1^{(1)}$) with the same pumping. Obviously the signal from $S_1^{(2)}$ was weak and the intensity did not decline after a sharp rise. This suggested poor energy transfer from the excited $S_1^{(2)}$ species to the $S_1^{(1)}$ species even though the radiative rates of $S_1^{(1)}$ were known to be fast and comparable with nonradiative rates. It is possible that the majority of the converted population did not relax via the zero point vibration of the first excited state. The observed intensity of $S_1^{(1)}$ with the low $S_1^{(2)}$ vibronic pumping was weak therefore and showed that the intensity decline of $S_1^{(2)}$ was not offset by the intensity rise of $S_1^{(1)}$. While this
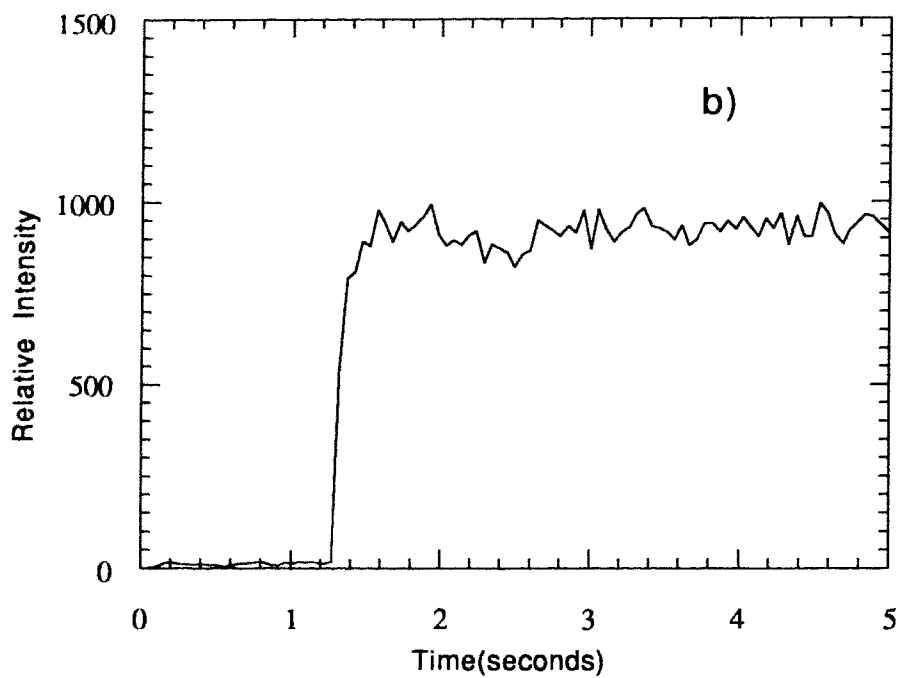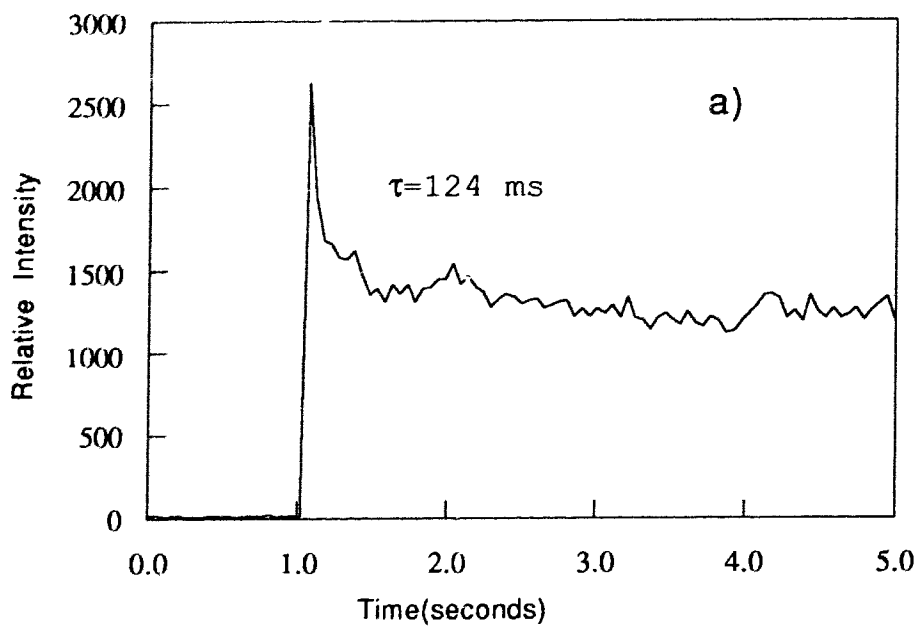
Fig. 33 Intensity responses in time with observation of 0-0 fluorescences with pumping of 14593 cm^{-1} ($S_1^{(2)}$+178cm^{-1}). a). recorded at $S_1^{(2)}$ with a redistribution time of 124 ms. b). monitored at $S_1^{(1)}$ show only a step-wise rise which means poor energy transfer from pumped $S_1^{(2)}$ vibronic to $S_1^{(1)}$.

95

Fig. 34 Intensity of 0-0 fluorescence vs time of TBH_2Pc in C_{16} ..ith $15122cm^{-1}$ ($S_1^{(1)}+686cm^{-1}$). a). recorded at $14436cm^{-1}$ ($S_1^{(1)}$) with redistribution time $\tau=165$ ms. b) recorded at 14415 cm^{-1} ($S_1^{(2)}$) with $\tau=149$ ms. Rare case where pumping was made into other species.

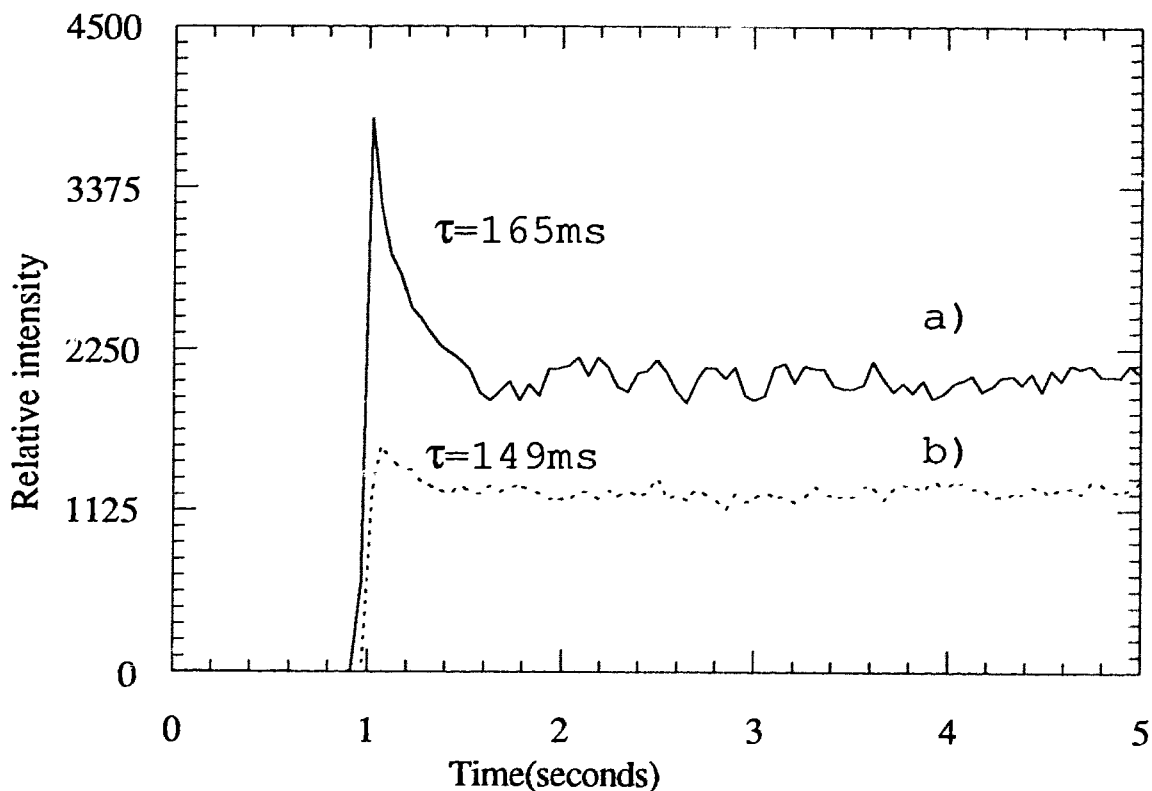is generally the case, exceptions are also observed where a state of one species is filled to some extent from the pumped species before transformation. This is shown in Fig. 34 where after pre-excitation with 15264 cm^{-1} ($S_2^{(2)}$) the intensity of $S_1^{(1)}$ recorded at 14436 cm^{-1} declines in the usual way with a redistribution time $\tau=165$ ms when excited with 15122cm^{-1} ($S_1^{(1)}+686$ cm^{-1}). However, under the same pumping in b) when observed at 14415 cm^{-1} ($S_1^{(2)}$) the intensity still declines slightly with $\tau=149$ ms. Such behaviour is found rarely when pumping into the other species and is probably due to a rather good coupling between the 686 cm^{-1} vibration of $S_1^{(1)}$ with that of $S_1^{(2)}$ or with other vibronics of $S_1^{(2)}$. Checking the fluorescence after excitation with 15122 cm^{-1}, we found a clear peak only at 14436 cm^{-1} while there was just strong background in the region around 14415 cm^{-1}. This implies that the interaction of $S_1^{(2)}+686$ cm^{-1} with other vibronics of $S_1^{(2)}$ is quite complex and that the excitation of $S_1^{(1)}+686$ cm^{-1} is served somehow by $S_1^{(2)}$.

There are also cases where 0-1 pumping is neither felt by the S_1 state of the pumped species nor by that of the other species. For these vibronic levels tautomerisation via photonic excitation and fluorescence decline cannot be observed even with proper pre-excitation. This may be due to the fact that the pumped excited state populates the ground states of both species evenly or that the pumped state has very rapid nonradiative decays which bypass the S_1 states of the species and make any variation of the intensity difficult to detect. Many of the

high-lying vibronics (>900 cm^{-1}) exhibit this behavior where no intensity decline is observed.

For 0-1 pumping and 0-0 observation of the $S^{(2)}$ isomers many vibronics belonging to $S_1^{(2)}$ show the intensity decline even without pre-excitation. One such example is given in Fig. 35 a): The first period was pre-excited by 15305cm^{-1} ($S_2^{(1)}$), then pumped with 15101cm^{-1} ($S_1^{(2)}$+686cm^{-1}) continuously. The intensity decline (phototransformation) still occurs in the later excitation periods. Recall that in Fig. 27 with the same excitation and observation, no intensity decline was observed in the later period. In this case the time interval between two excitations was only about 1 second, while in Fig. 35 the interval was about 65 seconds. Thus the height of each excitation decline depends on the dark time. Fig. 35b) describes the same phenomenon with 0-0 pumping and 0-1 observation with brief pre-excitation at 14436 cm^{-1} ($S_1^{(1)}$) followed by continuous pumping at 14415 cm^{-1} ($S_1^{(2)}$) only and monitoring at 13729 cm^{-1} ($S_0^{(2)}$+686 cm^{-1}). Note the intensity declines again in the later periods while no such behavior is observed in 0-1 pumping and 0-0 observation or 0-0 pumping and 0-1 observation of $S^{(1)}$. As pointed out before this behaviour can be explained by assuming that the $S_0^{(1)}$ electronic state is higher than the $S_0^{(2)}$ state.

Photochemical transformation of TBH_2Pc in solid C_{16} differs in two ways from that of H_2Pc in C_8[15]. One is that the saturation time τ in TBH_2Pc is slightly longer than that in H_2Pc and the other is that the extent of the intensity decline in TBH_2Pc is less than that in H_2Pc. As discussed in sections 3.2
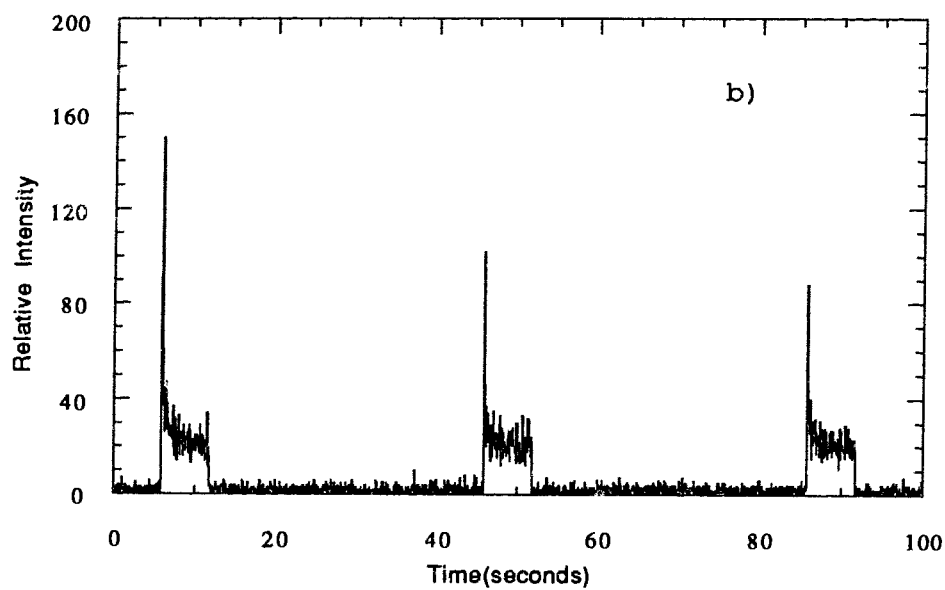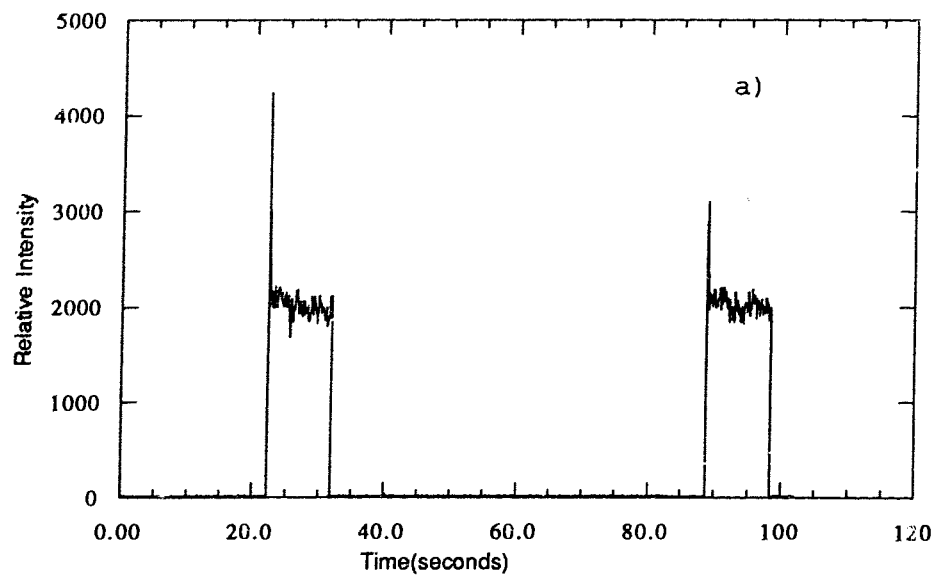
Fig. 35 a) Intensity vs time for 0-1 excitation $(S_1^{(2)}+686$

$cm^{-1})$ 0-0 observation $(14415\ cm^{-1})$. Note intensity drop occurs

in later periods. b). with 0-0 excitation $(14415\ cm^{-1})$ 0-1

observation $(13729\ cm^{-1})$; also the phototransformation
occurs in later periods.

and 3.3, stronger electron-phonon coupling for TBH_2Pc in C_{16} results in a longer redistribution time and causes shallower intensity drops than for TBH_2Pc in $C_8+\alpha ClN$.

Photochemical transformation of TBH_2Pc in C_{18} matrix was also studied with emphasis on measurements of 0-1 pumping with 0-0 observation, because one of its 0-0 transitions (14337 cm^{-1}) could not be obtained with our laser. In general, the observed phototransformation behavior is similar to that in C_{16} and a typical example is given in Fig. 36. For comparison we chose the same pumping vibronic $S_1^{(2)}+686$ cm^{-1} (in C_{16}, it was 15101 cm^{-1}; in C_{18}, it was 15022 cm^{-1}), and both were observed at $S_1^{(2)}$ (14415 cm^{-1} in C_{16}, 14337 cm^{-1} in C_{18}.) and we obtained redistribution times of $\tau=90$ ms and 168 ms for TBH_2Pc in C_{16} and C_{18} respectively. In general, since electron-phonon interaction is even stronger for TBH_2Pc in C_{18} than in C_{16}, the data show slightly longer τ's and even shallower decline in fluorescence intensity.
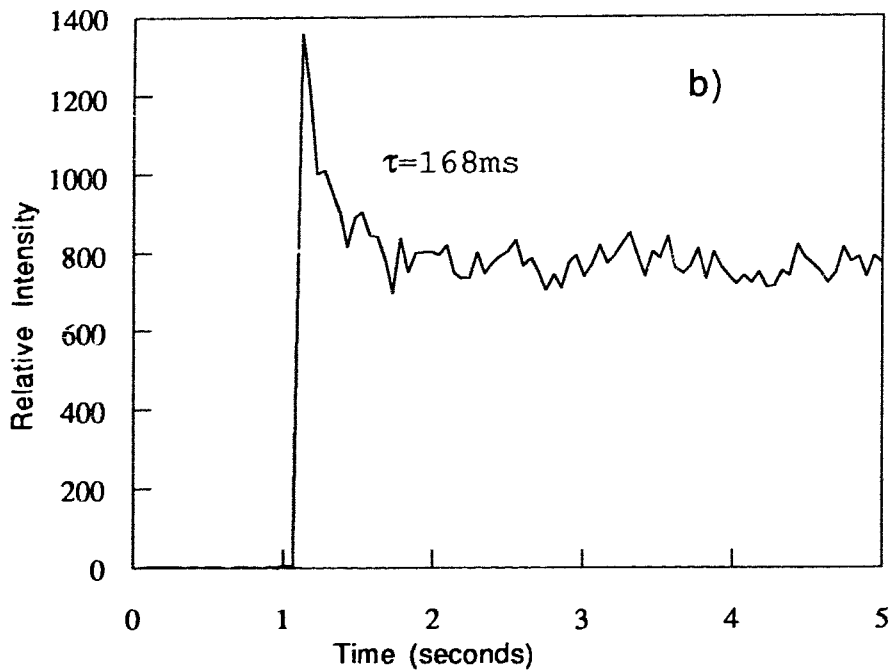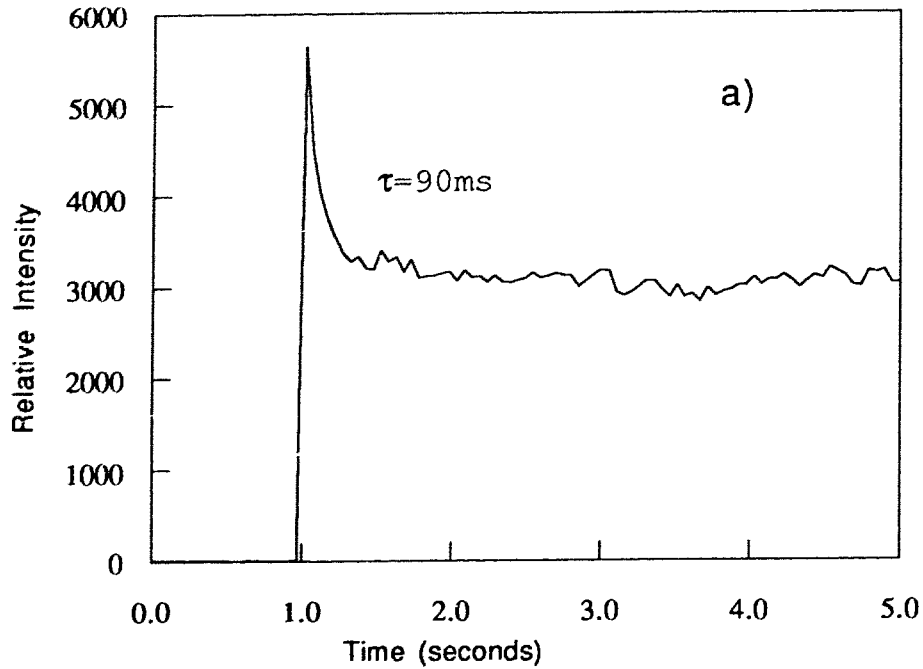
Fig. 36 The relation between time τ and Shpol'skii matrix. a) in C_{16} and b) in C_{18}, both a) and b) are properly pre-excited and observed at $S_1^{(2)}$ position a) 14415 cm^{-1} b). at 14337 cm^{-1}. Both excited with $S_1^{(2)}+686$cm^{-1}, a).15101 cm^{-1} b).15022 cm^{-1}. a). has better Shpol'skii effect than b). and $\tau_b > \tau_a$.

Chapter 4. Summary and Conclusions

1) Detailed fluorescence and fluorescence excitation spectra of TBH_2Pc in the alkanes C_8, C_9, C_{10}, C_{12}, C_{14}, C_{16}, C_{17}, and C_{18} are presented in this thesis. We identified those alkanes which at 4.2K are suitable hosts to obtain Shpol'skii spectra. C_{16} had the best spectra by having one dominant site and a relatively weak background. It was therefore the solvent of choice for comparison with previous work on H_2Pc in a mixed Shpol'skii matrix. C_{12}, C_9 and C_{18} were next best. The remaining alkanes used were found to be not suitable for detailed studies because of one or both of the following deficiencies: a) Multiple sites making identification of spectral features with a specific site difficult. b) Strong background luminescence broadened to an extent typical of an amorphous matrix, obscuring any vibronic structures. The fact that C_{17} was very poor in this respect, whereas C_{16} and C_{18} were quite suitable is deserving of further investigation that may lead to a better insight into the structural and/or dynamic properties of a host important in the formation of Shpol'skii matrices.

2) A careful comparison of the Shpol'skii spectra of TBH_2Pc in C_{16} with those of H_2Pc in C_8 showed significant differences attributable to the effect of the tertiary butyl groups on the vibronics as well as on the 0-0 transitions. Aside from a qualitatively observed reduction in the luminescence

quantum-yield – not unexpected because a higher density of vibrational levels makes an increased internal conversion rate (*i.e.* nonradiative decay from S_1 to S_0) plausible – the following differences were noted and commented on:

a) Longer vibrational progressions in the fluorescence excitation spectrum of TBH_2Pc that do not bear a 1-1 correspondence to H_2Pc.

b) Different vibrational energies in S_0 (observed in fluorescence) with the exception of some of the strongest vibronics, *i.e.* those with energies of 686, 725, 1520 and 1555 cm^{-1} in TBH_2Pc corresponding to 686, 725, 1519 and 1556 cm^{-1} in H_2Pc.

c) Fluorescence and fluorescence excitation of $S_2 \rightarrow S_0$ (*i.e.* the Q_y transition) could be observed in TBH_2Pc, which was not possible for H_2Pc in C_8. While the signals are weak they confirm S_2 (Q_y) as the high energy partner of S_1 (Q_x).

3) Through time resolved fluorescence studies under periodic square wave excitation, it was possible to observe the phototransformation between the two isomeric species of TBH_2Pc. Upon switching on the excitation, one could observe the reduction of the excited species within times of the order of tens of milliseconds (depending on pumping-power, and excitation frequency). Such transformations had previously been observed in the same manner in H_2Pc. However, whereas the population distribution between the two species remained stable in H_2Pc in the absence of excitation, for TBH_2Pc it was found that within times of the order of seconds to minutes (depending on

temperature) reequilibration to the original distribution between the isomeric species took place in the absence of excitation. This leads to the conclusion that there exists an energy difference in the ground state of the two species which is of a magnitude comparable to kT, where k is the Boltzmann constant and T the temperature of 4.2K used in most of the experiments.

In conclusion, the results reported in this thesis will provide for the first time a reference for any future spectroscopic studies of the TBH_2Pc molecule. Moreover they raise a number of intriguing questions with respect to the causes underlying the differences in the behaviour of the TBH_2Pc molecule when compared with the similar and extensively studied H_2Pc molecule, particularly with respect to the dynamics of the phototransformation between the isomers, a topic of great fundamental as well as applied interest.

References

[1]   See, for example, M. Gouterman, in *The Prophyrins*, edited
      by D. Dolphin   (Academic, New York, 1978), vol. 3, chap.
      1, and the references cited there in.

[2]   A. D. Britt and W. b. Moniz, Appl. Spectrosc. 31, 104
      (1977)

[3]   L. C. Gruen, Aust. J. Chem. 26, 1661 (1972)

[4]   N. Kawashima and K. Meguro, Bull. Chem. Soc. Jpn 48, 1857
      (1975)

[5]   K. Yoshio, K. Kaneto and Y. Inuishi, in *Energy and Charge
      Transfer in Organic Semiconductors*, edited by k. Masuda and
      M. Silver (Plenum, New York, 1974)

[6]   P. S. H. Fitch, C. A. Haynam, and D. H. Levy, J. Chem.
      Phys. 74, 6612 (1981)

[7]   P. S. H. Fitch, C. Haynam, and D. H. Levy, J. Chem. Phys.
      73, 1064 (1980)

[8]   P. S. H. Fitch, L. Wharton, and D. H. Levy, J. Chem. Phys.
      70, 2018 (1979)

[9]   T. H. Huang, K. E. Rieckhoff and E. M. Voigt, Chem. Phys.
      36, 423 (1979)

[10] T. H. Huang, K. E. Rieckhoff and E. M. Voigt, J. Chem.
      Phys. 77, 3424 (1982)

[11] T. H. Huang, W. H. Chen, K. E. Rieckhoff and E. M. Voigt,
      J. Chem. Phys. 80, 4051 (1984)

[12] W. H. Chen, T. H. Huang, K. E. Rieckhoff and E. M. Voigt, Mol. Phys. 68, 341 (1989)

[13] W. H. Chen, K. E. Rieckhoff and E. M. Voigt, Can. J. Chem. 62, 2264 (1984)

[14] T. H. Huang, K. E. Rieckhoff and E. M. Voigt, Can. J. Chem. 56, 976 (1978)

[15] W. H. Chen, K. E. Rieckhoff and E. M. Voigt, Spectrochim. Acta, 46A, 1601 (1990)

[16] J. Zollfrank and J. Friedrich, J. Chem. Phys. 93, 8586 (1990)

[17] A. A. Gorokhovskii and L. A. Rebane, Fiz. Tverd. Tela. 19, 417 (1977)

[18] A. A. Gorokhovskii and L. A. Rebane, Opt. Commun. 20, 144 (1977)

[19] L. A. Rebane, A. A. Gorokhovskii and J. V. Kikas, Appl. Phys. B29, 235 (1982)

[20] E. V, Shpol'skii, Sov. Phys. Usp. 3, 372 (1960); 5, 522 (1962); and 6, 411 (1963) (English Translation)

[21] I. E. Zalesski, V. N, Kotlo, K. N. Solov'ev and S. F. Shkirman, Soviet Phys, Soki. 17, 1183 (1973)

[22] K. N. Solov'ev, I. E. Zalesski, V. N. Kotlo and S. F. Shkirman, J. Exp. Theor. Phys. lettl 17, 332 (1973)

[23] A. A. Gorokhovski, R. K. Kaurli and L. A. Rebane, JEPT. Lett. 20, 216 (1974)

[24] S. Völker and J, H. Van der Waals, Mol. Phys. 32, 1703 (1976)

[25] R. M. MacFarlane and S. Völker, Chem. Phys. Lett. 69, 151 (1980)

[26] S. Völker and R. M. MacFarlane, J. Chem. Phys. 73, 4476 (1980)

[27] A. I. M. Dicker and S. Völker, Chem. Phys. Lett. 87, 481 (1982)

[28] P. J. Van der Zaag, J. P. Galaup and S. Völker, Chem. Phys. Lett. 166, 263 (1990)

[29] G. Herzberg, *Molecular Spectra and Molecular Structure* (Van Nostrand, Princeton, 1976), vol. 3, P50

[30] see, for example, R. M. Hochstrasser, *Molecular Aspects of Symmetry* (Benjamin, New York, 1966), Sec. 8.6

[31] Y. Mochizuki, K. kaya and M. Ito, Chem. Phys. 54, 375(1981)

[32] T. Kitagawa, M. Abe, and H. Ogoshi, J. Chem. Phys. 69, 4516 (1978)

[33] M. Abe, T. Kitagawa, and Y. Kyogoku, J. Chem. Phys. 69, 4525 (1978)

[34] D. S. Mcdonald and S. A. Rice, J. Chem. Phys. 54. 375 (1981)

[35] Dr. K. E. Rieckhoff, private communication